



Experimental Petrology Applied to Natural Diamond Growth

Robert W Luth, Yuri N Palyanov, Hélène Bureau

► To cite this version:

Robert W Luth, Yuri N Palyanov, Hélène Bureau. Experimental Petrology Applied to Natural Diamond Growth. *Reviews in Mineralogy and Geochemistry*, 2022, 88, pp.755 - 808. 10.2138/rmg.2022.88.14 . hal-03748017

HAL Id: hal-03748017

<https://hal.science/hal-03748017>

Submitted on 9 Aug 2022

HAL is a multi-disciplinary open access archive for the deposit and dissemination of scientific research documents, whether they are published or not. The documents may come from teaching and research institutions in France or abroad, or from public or private research centers.

L'archive ouverte pluridisciplinaire **HAL**, est destinée au dépôt et à la diffusion de documents scientifiques de niveau recherche, publiés ou non, émanant des établissements d'enseignement et de recherche français ou étrangers, des laboratoires publics ou privés.

Experimental Petrology Applied to Natural Diamond Growth

Robert W. Luth

*Department of Earth and Atmospheric Sciences
University of Alberta
1-26 Earth Sciences Building
Edmonton, Alberta T6G 2E3
Canada*
robert.luth@ualberta.ca

Yuri N. Palyanov

*V.S. Sobolev Institute of Geology and Mineralogy
Siberian Branch of the Russian Academy of Sciences
3, Koptyug ave., Novosibirsk 630090
Russia
and
Novosibirsk State University
2, Pirogov str., Novosibirsk 630090
Russia*
palyanov@igm.nsc.ru

Hélène Bureau

*Institut de Minéralogie de Physique de la Matière et de Cosmochimie
Sorbonne Université, UMR CNRS 7590, Muséum National d'Histoire Naturelle
Campus Jussieu boîte 115
4, place Jussieu, 75005 Paris
France*
helene.bureau@upmc.fr

INTRODUCTION

How can experiments help?

Perhaps the first point to address in this chapter is what role, or roles, experimental petrology can play in understanding the formation of natural diamond. As can be seen from the other chapters in this volume, there is a rich diversity of diamonds—even confining ourselves to terrestrial examples, there are diamonds that form in impacts, those that are found in ophiolites and in UHP metamorphic rocks, as well as those that are found in mantle-derived volcanics such as kimberlites and lamproites. Some of these—such as those found in ophiolites (e.g., Farré-de-Pablo et al. 2018 and references therein; Litasov et al. 2019a,b)—may form under P, T conditions at which diamond is metastable rather than stable, although such occurrences are controversial (Farré-de-Pablo et al. 2019; Massonne 2019; Yang et al. 2019). Others, such as mantle-derived monocrystalline, fibrous, and coated diamonds, presumably form at P, T conditions at which diamond is the stable polymorph of carbon. This diversity presents a rich P, T composition space for experimentalists to explore to provide some insights into diamond formation.

Experiments allow researchers to explore first-order questions such as

- Can diamond form from this particular composition of fluid or melt?
- Can diamond form from a specific redox reaction, such as carbonate reacting with a reduced fluid?

Experiments can also address questions such as how the diamond-forming melts or fluids originally form, and how they evolve as they interact with different lithologies in the Earth.

The vast majority of natural diamonds form in the Earth's lithospheric mantle (See Nimis 2022, this volume; Stachel et al. 2022a, this volume), and so unsurprisingly most of the experimental work to date has focused on this pressure range. There has been some work at much higher pressure and temperature conditions extending to those of the deep Earth, however, and we shall touch on those as well in this review.

CONCEPTUAL BACKGROUND

Stability of diamond

In the one-component carbon system, diamond is the high-pressure polymorph stable at pressures above the graphite—diamond transition (Kennedy and Kennedy 1976; Day 2012). Adding more components makes the situation more complex: in C–O, diamond would be stable in a region of $P, T, f\text{O}_2$ space bounded by the reactions



and

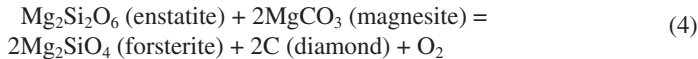


If the fluid phase contains H as well, then the relevant system is C–O–H (Fig. 1), in which the diamond saturation curve separates a two-phase field of diamond + fluid from a field of C-undersaturated fluid. It should be noted that the $f\text{O}_2$ of the fluid increases from left to right along the diamond saturation curve, and for context the value of $f\text{O}_2$ for the iron-wüstite buffer (IW), and the locations of fluids with values of $\log(f\text{O}_2)$ three and four units below the calculated (metastable) location of the fayalite-magnetite-quartz buffer (FMQ) are shown.

The situation in the Earth's mantle is more complex, given that CO_2 becomes unstable in the presence of olivine (Newton and Sharp 1975) because of the carbonation reaction



A consequence of the stability of this reaction is the well-known EMOD reaction



(Eggler and Baker 1982), which further constrains the stability of diamond. Schematically, Figure 2 shows the fields of stability for carbonate, diamond, and fluid in T – $\log(f\text{O}_2)$ space at constant pressure within the diamond P, T stability field. Under conditions where a carbonate melt rather than crystalline magnesite is stable, an analogous reaction to (3) where MgCO_3 is a component in the melt would apply, as discussed by Stagno and Frost (2010).

Under more reducing conditions such as those proposed to occur with increasing depth in the Earth's mantle (see overview by Stagno 2019), carbon can dissolve in the alloy or form carbides such as cohenite, $(\text{Fe}, \text{Ni})_3\text{C}$, or Fe_7C_3 . Another complication is the presence of sulfur—with a bulk silicate Earth estimated concentration on the same order as that for carbon

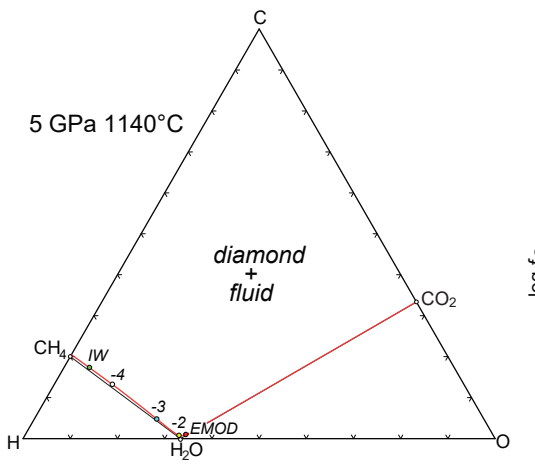


Figure 1. The system C–O–H at 5 GPa, 1140 °C. The red line denotes the composition of fluid in equilibrium with diamond as a function of composition. Numbers along the line are values of $\log f_{\text{O}_2}$ relative to that of the FMQ reference buffer. Also for reference are shown the locations of the fluids in equilibrium with the iron–wüstite reference buffer (IW) and the EMOD reaction (see text). Calculated with GFluid (Zhang and Duan 2010).

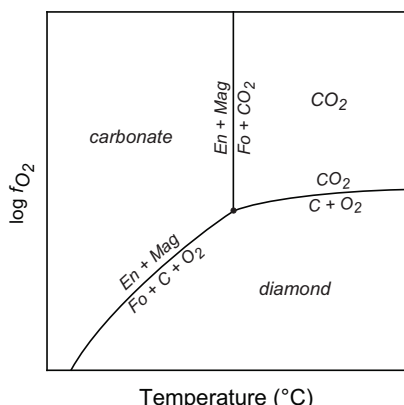


Figure 2. Schematic $\log f_{\text{O}_2}$ –temperature section at constant pressure, showing the relationship between reactions (2), (3), and (4) in the text. The fields are labeled with the stable carbon-bearing form that would coexist with forsterite and enstatite. See text for discussion.

(~250 ppmw, McDonough and Sun 1995). Although there is ongoing debate about the relative importance of alloys, carbides, and sulfide melts as hosts of carbon in the Earth's mantle, the key point for the experimentalist is that all three of these are at least potential sources of carbon that could precipitate diamond upon oxidation—a process tractable to experimental study.

Source of carbon

Considerations of the large-scale carbon cycle (e.g., Lee et al. 2019) reveal two basic categories of carbon in the Earth's mantle: primordial carbon surviving from early Earth accretion and differentiation, and carbon re-introduced into the Earth's interior via subduction. The present carbon content for the primitive mantle is ~90–130 ppm, although as outlined in the recent review by Dasgupta and Grewal (2019) estimates range from ~100 to >500 ppm. Subsequent to accretion and large-scale initial differentiation leading to core formation, it is not clear how carbon is hosted in the mantle, but it seems reasonable that this carbon would be present in its thermodynamically stable form(s) at the P, T and oxidation state of the ambient mantle. This presupposes that ferric–ferrous equilibria will serve as a sink or source for oxygen, which is reasonable at these carbon concentrations.

Subduction transports carbon down into the mantle, but the amount of carbon that survives sub-arc processing to be subducted into the mantle remains an active area of research (e.g., Kelemen and Manning 2015; Galvez and Pubellier 2019; Lee et al. 2019). Carbon would be present in both subducted sediment and altered oceanic crust (AOC) as carbonate, both biogenic and abiogenic, as well as some fraction as organic matter. The relative contribution of sediment and AOC likely depends on the specific thermal regime of a subducting slab, but a recent study by Li et al. (2019) implicates the latter as the dominant carrier of carbon as both abiogenic and biogenic carbonate into the mantle. Whether all this carbonate is reduced to graphite during subduction (Galvez et al. 2013) or survives as carbonate until partial melting ensues is unclear, so the experimentalist is faced with addressing both possibilities as carbon sources for diamond formation.

Fluids, melts, and supercritical fluids proposed to form diamond

Diamond can be formed directly from graphite in the absence of a solvent or catalyst, but this transformation requires pressures above ~10 GPa and temperatures in excess of 1800 °C (e.g., Irifune et al. 2004 and references therein). Diamond growth at lower pressures and temperatures requires some sort of solvent or growth media, and thus the first question is what that medium might be. From the examination of natural diamonds, it is well accepted that diamonds grow through metasomatic processes in C–O–H–N–S–Cl bearing mobile fluids, melts or supercritical fluids, and occurs over times and depths.

As outlined in other chapters in this volume, study of the inclusions in natural diamonds led to the identification of syngenetic inclusions, those that form as the diamond was growing (Harris 1968). The mineral inclusions enabled researchers to distinguish between diamonds that were growing in peridotitic and eclogitic lithologies, for example. Other inclusions were thought to sample the growth medium from which the diamond is precipitating. Fibrous diamonds in particular were fruitful to study in this context because they contain the so-called “HDF” (high-density fluid) inclusions. Among fibrous diamonds, the coated ones, with a monocrystalline pure core surrounded by a fibrous rim, inspired the idea that both kind of diamonds may share the same parent fluids and that a single diamond may grow in a few or several events. Chrenko et al. (1967) reported the first indication for the presence of carbonates and water in inclusions in diamond, but Navon et al. (1988) were the first to propose that coated diamonds sample mantle melts or volatile-rich fluids (enriched in H₂O, CO₃²⁻, K₂O, Cl, depleted in MgO and including several other elements) from which they grow. Numerous publications have followed (see Weiss et al. 2022, this volume), including some significant studies such as: the finding of solid carbon dioxide inclusions in fibrous diamonds (Schrauder and Navon 1993), the discovery of brine inclusions in cloudy diamonds (Izraeli et al. 2001), the chemical and isotopic connection of fluid compositions trapped in coated diamond’s inclusions from various cratons showing that fluids derived from mantle source would not be affected by local heterogeneities (Klein-BenDavid et al. 2004), the idea of miscibility/immiscibility processes linking mantle fluids of different compositions or “endmembers” during diamond growth (Klein-BenDavid et al. 2007), and many others.

In brief, the bulk compositions of these HDFs can be described in terms of four endmembers: (i) silicic HDFs that are rich in Si, Al, K, and water with some carbonate; (ii) saline HDFs that are rich in Cl, K, Na, water, and carbonate; (iii) and (iv) hydrous carbonatitic HDFs that are Mg-rich and Mg-poor, respectively.

Along with the relationship between these endmembers and their origin, a long-standing question has been whether the more common monocrystalline diamonds form from the same type of fluids. Strong evidence for this idea has been established from a variety of studies. For example: the common sinusoidal REE patterns between garnet inclusions trapped in the monocrystalline area of coated diamonds and HDFs trapped in the fibrous rims (Weiss et al. 2009); the similarity of hydrosilicic HDFs that precipitated the rims of coated diamonds with the fluids that precipitated most monocrystalline diamonds (Rege et al. 2010); the first finding of HDF micro-inclusions in a monocrystalline diamond, similar in major and trace elements compositions to those of fibrous diamonds (Weiss et al. 2014), suggesting that these HDF are involved during the growth of many monocrystalline diamonds. As a last example, Nimis et al. (2016) discovered thin “fluid” hydrous silicic films around solid mineral inclusions in gem-quality monocrystalline diamonds from peridotitic and eclogitic suites that were interpreted as potential vestiges of the original fluid present during diamond growth.

Are fibrous, coated, and monocrystalline diamonds growing by the same process? In our view, the debate was definitively closed in the affirmative—at least for lithospheric diamonds,

by the study of Jablon and Navon (2016), who found micro-inclusions of HDFs trapped in the twinning planes of twin gem diamonds (macles) together with silicate minerals. They concluded that the mechanism of diamond formation is similar for most diamonds. It is worth noting that this process also includes the growth of micro diamonds in ultra-high-pressure metamorphic rocks (e.g., Stöckert et al. 2001; Dobrzhinetskaya et al. 2007; Frezzotti et al. 2014).

Most of the studies based on fluid inclusions document the important role played by water during diamond growth, a role possibly not only limited to subduction zones where water is likely recycled from slabs, but also in the cratonic mantle. Although most of the HDFs observed in lithospheric diamonds are oxidized, some diamonds such as mixed-habit ones containing octahedral and cuboid sectors also host inclusions with reduced fluids such as CH₄ (Smit et al. 2016). Diamond growth in fluids evolving in redox state is also able to reconcile the apparent contradictory messages delivered from diamond stable isotope studies, because depending on the carbon source, CO₂ (Boyd et al. 1994) or CH₄ (Thomassot et al. 2007), the core to rim evolution of the diamond's δ¹³C signature will be reversed. Furthermore, both eclogitic and peridotitic diamonds can be derived from the same isotopically homogeneous carbon source with metasomatic growth (Cartigny 2005).

These HDFs may not be limited to the lithosphere; some evidences of volatile-bearing inclusions are found in sublithospheric diamonds, such as ice VII inclusions (Tschauner et al. 2018); CH₄ and H₂ associated with inclusions of solidified iron–nickel–carbon–sulfur melts in large gem diamonds (Smith et al. 2016); or unknown fluids in association with inclusions of iron carbides (Kaminsky and Wirth 2011). These metallic melts may take part in diamond growth in the lower mantle and transition zone, but possibly also in the lithosphere, in both cases in very reduced environments.

In this review, we will try to guide the reader into the voluminous literature on experimental studies of diamond formation. To provide some structure to this, we will look at different growth media in turn, moving from “simple” to more complex systems. In each section, we will tabulate studies chronologically, and the reader will recognize how the experimental studies have evolved as studies of natural diamonds have continued to provide insights and constraints to help ground the experiments.

C-O-H FLUIDS

Overview

There have been extensive studies over the last 30 years of diamond nucleation and growth from initially graphite-saturated C–O–H fluids. Diamond grows from a variety of these fluids, from CH₄- to CO₂-rich (Table 1). The studies tabulated here are those in which graphite was present in the starting material (or generated upon breakdown of the organic fluid source); studies examining the ability of fluids to participate in oxidation-reduction reactions, such as those in which carbonate is reduced to diamond, are discussed in a subsequent section.

In general, these studies demonstrate that diamond growth is higher in H₂O-rich systems, lowest in CH₄-rich systems, reflecting a dependence on the activity of H₂O in the fluid (which is clearly fO₂ dependent). Diamond growth is characterised by temperature-dependent induction times, certainly for nucleation of new diamond crystals, and in some cases even for growth on pre-existing seed diamonds. More recent studies such as Matjuschkin et al. (2020) have demonstrated the ability of these fluids to grow diamonds at lower temperatures (e.g., that are more realistic for lithospheric mantle geotherms). In this study, extensive efforts were devoted to improving experimental design to minimize changes in fluid composition over the course of the experiments.

Table 1. Studies of diamond nucleation and growth in C–O–H fluids.

Study	System	P (GPa)	T (°C)	Duration	Seeds	Capsule/ buffering	Results
Akaishi et al. (1990b)	H ₂ O from Mg(OH) ₂ or Ca(OH) ₂	7.7	2150	20 min	N	Mo capsule	SN; CM: {111}
Yamaoka et al. (1992)	H ₂ O	7.7	1800–2200	2 h	Y	Ta capsule	GS at 2000°, 2200°.
Onodera et al. (1992)	Hydrocarbons from camphene, adamantane (both C ₁₀ H ₁₆), and fluorene (C ₁₃ H ₁₀)	7–9	710–1325	30 min	N	Ta or Mo capsule	SN from camphene reported as low as 820°, 8 GPa or 710°, 6 GPa (in different parts of text). SN from adamantane at 8 GPa and 1325° but not at lower T. No SN from fluorene (7–9 GPa, 800–975°). These temperatures may be underestimated based on the location of their thermocouple relative to the sample (their Fig. 1)
Latourette and Holloway (1994)	CO ₂	8	950–1150	1–17 h	N	Pt	SN reported in all expts. Starting material was Fe ₃ O ₄ + Gr, NiCO ₃ + Gr, or Ni + PdO + Gr
Hong et al. (1999)	H ₂ O	7.7	1600–2200	0.5–4 h	In some	Graphite- lined Mo	SN at 2000°, 2200°; GS at 1700°, 1800°.
Yamaoka et al. (2000)	H ₂ O	5.5, 7.7	1200–1500	24 h	In some	Pt	At 5.5 GPa, No SN in unseeded expts; GS at >1300°. At 7.7 GPa, in unseeded experiments SN at ≥1400°, not below. 100% conversion at 1500°. In seeded experiments, GS at >1300°.
Sun et al. (2000)	CO ₂ from Ag ₂ CO ₃ or Ag ₂ O + Gr	7.7	1500–2000	0.5–27 h	N	Graphite	Complete conversion at ≥1800° at ≥0.5 h. Some SN at 1700°/5 h but not 1700°/2 h. Some SN at 1600°/12 h and 1500°/27 h.
Akaishi and Ya- maoka (2000)	CO ₂ –H ₂ O from OAD	7.7	1400–2000	0.5–360 h	N	Graphite- lined Mo	CM: {111}
Shaji Kumar et al. (2000)	CO ₂ –H ₂ O from OA	7.7	1300–1500	24–240 h	N	Pt	SN at 1500°, 10% at 24 h, 50% at 36 h, ~complete at 42 h; SN at 1400°, ~10% at 96 h; SN at 1300°, <10% at 240 h. CM: {111}
Akaishi et al. (2000)	CO ₂ –H ₂ O from OAD	7.7	1600	6–17 h	N	Pt	SN starting at 8 h, complete at 17 h. CM: {111}

Study	System	P (GPa)	T (°C)	Duration	Seeds	Capsule/buffering	Results
Pal'yanov et al. (2000)	CO_2 from AgOx, H_2O , $\text{CO}_2\text{-H}_2\text{O}$ from OAD, $\text{CH}_4\text{-H}_2$ from Anth ^a	5.7	1300	84 h	Y	Pt or Au	H_2O : SN in Pt; CO_2 : SN in Pt; $\text{CO}_2\text{-H}_2\text{O}$: SN in Au and Pt; $\text{CH}_4\text{-H}_2$: negligible (< 1 μm) GS in Au. No fluid; No SN, No GS, CM: {111}
Akaishi et al. (2001)	$\text{CH}_4\text{-H}_2\text{O}$ from StA and OAD	7.7	1500	1–48 h	N	Pt	No SN at 24 h, small amount of SN at 48 h. CM: {111}
Shaji Kumar et al. (2001)	$\text{CO}_2\text{-H}_2\text{O}$ from OA	7.7	1500	24 h	N	Pt	Examined effect of mixing OA and graphite and differing OA/graphite ratios. CM: {111}
Sokol et al. (2001a)	CO_2 from AgOx, H_2O , $\text{CO}_2\text{-H}_2\text{O}$ from OAD, $\text{CH}_4\text{-H}_2$ from Anth	5.7	1200–1420	42–136 h	Y	Pt or Au	CO_2 : SN at 1300°/84 h, 1420°/42 h. H_2O : SN at 1300°/84 h, 1420°/42 h, GS at 1200°/135 h. $\text{CO}_2\text{-H}_2\text{O}$: SN at 1200°/136 h, 1300°/84 h, 1420°/42 h. $\text{CH}_4\text{-H}_2$: No SN at 1200°/136 h, 1300°/84 h, 1420°/42 h. Possible GS at 1200°, negligible (< 1 μm) GS at 1300°, 1420°. CM: {111}
Sun et al. (2001)	H_2O	5.5, 7.7	1300–2200	0.25–24 h	N	Ta, Mo, or Pt	H_2O : SN at 5.5, 1400°/24 h and 7.7, 1500°/24 h in Pt; SN at higher T in Mo, Ta—capsule leakage issue.
	CO_2 from AgOx	7.7	1500–2000	0.5–27 h	N	Graphite-lined Mo	CO_2 : SN in all expts. $\text{CO}_2\text{-H}_2\text{O}$ OA: SN in Mo at 2000°/0.5, 1800°/2, 1600°/20. No SN at 1800°/0.5, 1600°/12. SN in Pt down to 1300°/240.
	$\text{CO}_2\text{-H}_2\text{O}$ from OA, $\text{CO}_2\text{-H}_2\text{O}$ from MA	7.7	1300–2000	0.5–240 h		Graphite-lined Mo, Pt	$\text{CO}_2\text{-H}_2\text{O}$ (MA): SN at 1500°/48, not 1400°/86. CM: {111}
Okada et al. (2002a,b)	H_2O from $\text{Mg}(\text{OH})_2$	7.7	1835	see Results		Mo	In situ study; SN upon heating to 1835°. CM: {111}
Yamaoka et al. (2002c)	CO_2 from C+ P_2O_5	7.7	1500	8–24 h	N	Pt	SN at 24 h, not 8 h. CM: {111}
Yamaoka et al. (2002b)	H_2O from glucose	7.7	1500	1–33 h	Y	Pt	SN starting at 10 h, 100% at 33 h GS at ≥ 1 hr. CM: {111}
Dobrzhinetskaya et al. (2004)	H_2O from $\text{Mg}(\text{OH})_2$	7.5–8	1200–1500	10 min–40 h	N	Pt	1200°: graphite only to 24 h, SN after 122 h; 1500°: SN at 5 h, 100% at 138 h
	$\text{CO}_2\text{-H}_2\text{O}$ from OAD	8.5	1500	see results			SN at 32 h (~20–25%) and ~100% at 120 h. CM: skeletal diamonds

Study	System	P (GPa)	T (°C)	Duration	Seeds	Capsule/ buffering	Results
Okada et al. (2004)	H ₂ O from Mg(OH) ₂	6.6–8.9	1400–1835	See Results		Mo	In-situ study of reaction kinetics; SN at T>1400°.
Palyanov et al. (2007a)	H ₂ O	7.5	1500–1600	15 h	Y	Pt	SN at both 1500° and 1600°. CM: {111}
Sokol et al. (2009)	Various reduced fluids from H ₂ O-to CH ₄ -rich	6.3	1400–1600	15–48 h		Pt capsule w/ Mo–Mo ₂ or Fe–FeO buffer	Focus on analysis of quench fluid phase; diamond SN in unbuffered H ₂ O expt at 1400°/42 h. GS in unbuffered H ₂ O–CH ₄ expts at 1400°/42 h. GS only in 1 buffered expt (H ₂ O-rich, 1600°/24 h). CM: {111}
Palyanov et al. (2010a)	CO ₂ from AgOx	7.5	1300–1600	2–80 h		Pt capsule, Fe ₃ O ₄ –Fe ₂ O ₃ buffer	SN at 1600°/2 h, 1600°/15 h; GS from lowest T expts (1400°/40 h at 6.3 GPa, 1300°/80 h at 7.5 GPa). CM: {111}
Zhang et al. (2011)	H ₂ O from glucose, H ₂ O–CO ₂ from OAD	9–11	1000–1400 K	1.5–50 min	DAC	Diamond-anvil cell expts. Growth reported in both expts w/ glucose, none in OAD expt	
Matjuschkin et al. (2020)	CH ₄ –H ₂ from StA	5–7	1100–1300	4–23 hr	N	Au and olivine caps, Mo–MoO ₂ buffer	Expts contain olivine and orthopyroxene. SN at 5 GPa, 1250°/15 h, 6 GPa 1100–1300°, 7 GPa 1200–1300°

Notes: All studies contained graphite in the starting composition. Gr – graphite. OAD – oxalic acid dihydrate. OA – anhydrous oxalic acid (H₂C₂O₄). AgOx – silver oxalate (Ag₂C₂O₄). StA – stearic acid (C₁₈H₃₆O₂). Anth – anthracene (C₁₄H₁₀). MA – malonic acid (C₃H₄O₄). C₆H₁₂O₆ – glucose – C₆H₁₂O₆. SN – spontaneous nucleation and growth of diamond. GS – diamond growth on seeds. CM – diamond crystal morphology (where given in article). Temperatures in *Results* column in °C.

Experimental issues

In experiments at diamond-stable conditions, C–O–H volatiles are added to the capsule as either a fluid by micro-syringe, or as solid materials that break down to fluids at the conditions of the experiment. C–O bearing materials such as oxalic acid dihydrate ($\text{H}_2\text{C}_2\text{O}_4 \cdot 2\text{H}_2\text{O}$) and silver oxalate ($\text{Ag}_2\text{C}_2\text{O}_4$) have a long history of use in experimental petrology (e.g., Holloway et al. 1968; Boettcher et al. 1973). These materials, as well as others such as anthracene ($\text{C}_{14}\text{H}_{10}$) and glucose ($\text{C}_6\text{H}_{12}\text{O}_6$), have been used to generate C–O–H fluids for diamond-synthesis experiments. A key assumption is that the solid starting material break downs to the expected fluid composition at experimental conditions; progress is being made on both *in situ* studies of these fluids (McCubbin et al. 2014) and careful characterisation of fluids following quenching of the experiment (e.g., Tiraboschi et al. 2016; Sokol et al. 2017). Other issues arise for specific compounds; for example, the elemental silver liberated by decomposition of silver oxalate can alloy with the sample capsule, which can lead to melting, capsule rupture, and loss of fluid (e.g., Brey et al. 1991).

Because of the potential for hydrogen diffusion across the capsule wall during the experiment, evolution of the composition of the fluid phase during the experiment is an issue relevant to these experiments (see discussions in Sokol et al. 2004, for example; Palyanov et al. 2010a). This long-standing experimental issue has led to various approaches to buffer the fluid composition (see overviews by Rubie 1999; Stagno 2019), and Table 1 notes studies in which buffering of the fluid phase by an external hydrogen buffer was employed.

Possible future directions

Continued focus on experiments with well-constrained redox conditions to maximize experimental run durations and to maintain constant fluid compositions will undoubtedly improve our understanding of the dependence of diamond growth rate on fluid composition. Given the solubility of silicates in C–O–H fluids at high P and T , continued study of diamond growth in fluids saturated with peridotitic or eclogitic mineral assemblages would seem to be the most fruitful in terms of direct relevance to diamond growth in the Earth's mantle. Finally, studies of diamond growth in C–O–H fluids will benefit from continued efforts to improve thermodynamic models of fluids at high P, T . As an example, the solubility of carbon in CO_2 fluid at 6.3 GPa and 1250–1400°C measured by Palyanov et al. (2010a) is ~1 order of magnitude larger than that predicted by the GFluid thermodynamic model (Zhang and Duan 2010). Furthermore, fluid models such as GFluid are restricted to fluid constituents in the C–O–H system. Extending these models to quantitatively model the effects of the solubility of silicates and oxides is sorely needed—and will require an enormous amount of experimental data to calibrate.

CARBONATES

Overview

Like C–O–H fluids, carbonate melts have attracted significant attention of experimentalists as potential growth media for diamond over the past three decades. A rich variety of alkali- and alkaline earth carbonates have been explored in these studies (Table 2), including those most likely to be relevant to diamond growth in the Earth's mantle, such as those in the Na_2CO_3 – K_2CO_3 – CaCO_3 – MgCO_3 – FeCO_3 system. All studies in Table 2 have graphite present in the starting material (or likely formed by breakdown of oxalate or other solid sources in the initial stages of the experiment) and use carbonate melts as media for graphite transformation into diamond. Experiments that explore diamond nucleation and growth as a result of redox reactions involving carbonates are described in another section.

Table 2. Studies of diamond nucleation and growth in carbonate systems.

Study	System	P (GPa)	T (C)	Duration	Seeds	Capsule/ buffering	Results
Akaishi et al. (1990a)	$\text{Li}_2\text{CO}_3\text{-Gr}$, $\text{Na}_2\text{CO}_3\text{-Gr}$, $\text{SrCO}_3\text{-Gr}$, $\text{CaCO}_3\text{-Gr}$, $\text{MgCO}_3\text{-Gr}$	7.7	2150	20 min	N	Mo	All had SN at 2150°. Expts with $\text{CaCO}_3\text{-Gr}$: No SN at 1800°, ~50% conversion at 2000°. CM: rounded shape
Akaishi et al. (1996)	$\text{MgCO}_3\text{-Gr}$, $\text{K}_2\text{Mg}(\text{CO}_3)_2\text{-Gr}$	7.7	1800–2450	5, 30 min	Y	Ta	Sintering of diamond powder at >2000°
Taniguchi et al. (1996)	$\text{MgCO}_3\text{-Gr}$, $\text{K}_2\text{Mg}(\text{CO}_3)_2\text{-Gr}$	9–10	1300–1700	20 min	N	Gr	$\text{MgCO}_3\text{-Gr}$: SN at 9.5 and 10 GPa at ≥1600°; none observed at 9 GPa 1400–1750°. $\text{K}_2\text{Mg}(\text{CO}_3)_2\text{-Gr}$: SN above 1650° at 9–10 GPa. CM: {111}>{100}
Litvin et al. (1997)	$\text{K}_2\text{Mg}(\text{CO}_3)_2\text{-Gr}$	8–11	1700	5–10 min	N	MgO-BN	SN at 9–11 GPa, 1700°, 10 min, 8–9 GPa, 1700°, 5 min recrystallized Gr only. CM: {111}, {100}
Srikarhan et al. (1997)	$\text{MnCO}_3\text{-Gr}$	6.5–7.7	1700–2100	20 min	N	Mo	No SN at 6.5 GPa, 1700° or 1800°, or at 7.7 GPa below 2000°. SN at 7.7 GPa, 2000° and 2100°. CM: {111}>{100}
Litvin et al. (1998a,b,c)	$\text{Na}_2\text{Mg}(\text{CO}_3)_2\text{-K}_2\text{Mg}(\text{CO}_3)_2\text{-Gr}$, $\text{NaKMg}(\text{CO}_3)_2\text{-Gr}$	8–10	1700–1800	?	Y	Gr	SN and GS.
Sokol et al. (1998)	$\text{Na}_2\text{CO}_3\text{-Gr}$	6.8	1700	10 min, 16 h	Y	Gr	SN, CM: {111}
Pal'yanov et al. (1998a)	$\text{Li}_2\text{CO}_3\text{-Gr}$, $\text{Na}_2\text{CO}_3\text{-Gr}$, $\text{K}_2\text{CO}_3\text{-Gr}$, $\text{Cs}_2\text{CO}_3\text{-Gr}$, $\text{CaCO}_3\text{-Gr}$, $\text{MgCO}_3\text{-Gr}$, $\text{SrCO}_3\text{-Gr}$, $\text{CaMg}(\text{CO}_3)_2\text{-Gr}$	7	1700–1750	18.5 h			Ranked carbonates in terms of diamond growth efficacy as $\text{Li}_2\text{CO}_3 > \text{Na}_2\text{CO}_3 > \text{K}_2\text{CO}_3 > \text{Cs}_2\text{CO}_3$ and $\text{CaMg}(\text{CO}_3)_2 > \text{CaCO}_3 >$ $\text{MgCO}_3 > \text{SrCO}_3$. CM: Na_2CO_3 {111}>{100}; K_2CO_3 {111}, {111}>{100}; Li_2CO_3 {100}, {111}; Cs_2CO_3 {111}; alkaline-earth carbonates {111}, {hhk}, {hll}
Borzsov et al. (1999)	$\text{K}_2\text{CO}_3\text{-Gr}$	7	1700–1750	2–11.5 h	Y	Pt	SN at 2 h, 100% diamond at 11.5 h. CM: {111}, {111}>{100}
Litvin et al. (1999a)	$\text{K}_2\text{Ca}(\text{CO}_3)_2\text{-Gr}$, $\text{Na}_2\text{Ca}(\text{CO}_3)_2\text{-Gr}$	8.5, 9.5	1680–1800	40–65 min	Y	Gr	$\text{K}_2\text{Ca}(\text{CO}_3)_2\text{-Gr}$: 100% diamond at 9.5 GPa, 1750°, 40 min. $\text{Na}_2\text{Ca}(\text{CO}_3)_2\text{-Gr}$: GS at 8.5 GPa, 1750° and 9.5 GPa, 1800°. CM: {111}
Litvin et al. (1999b)	$\text{Na}_2\text{Mg}(\text{CO}_3)_2\text{-Gr}$, $\text{NaKMg}(\text{CO}_3)_2\text{-Gr}$	8–10	1700–1800	~30 min?	Y	Gr or MgO	GS reported. Figure shows SN down to ~1550° at 8.5 and 9 GPa. CM: {111}
Litvin and Zharkov (1999)	$\text{K}_2\text{Fe}(\text{CO}_3)_2\text{-Gr}$, Mixed K-Na-Ca-Mg-Fe carbon- ate + Gr	7–9	1650–1800	20–60 min	Y	Gr	$\text{K}_2\text{Fe}(\text{CO}_3)_2\text{-Gr}$: SN at 9 GPa, 1800°. Mixed carbonate: GS reported at 7–9 GPa, 1650–1800°. CM: {111}
Pal'yanov et al. (1999b)	$\text{Li}_2\text{CO}_3\text{-Gr}$, $\text{Na}_2\text{CO}_3\text{-Gr}$, $\text{K}_2\text{CO}_3\text{-Gr}$, $\text{Cs}_2\text{CO}_3\text{-Gr}$	7	1700–1750	10 min–18.5 h	Y	Pt	SN in all systems at 2 h; not at 20 min for Na_2CO_3 and K_2CO_3 or at 30 min for Cs_2CO_3 . Catalytic activity trend seen: $\text{Li}_2\text{CO}_3 \gg \text{Na}_2\text{CO}_3 > \text{K}_2\text{CO}_3 > \text{Cs}_2\text{CO}_3$. CM: Li_2CO_3 {111}>{100}, {hk}, {Na}_2\text{CO}_3 {111}>{100}; K_2CO_3 {111}, {111}>{100}; Cs_2CO_3 {111}

Study	System	P (GPa)	T (°C)	Duration	Seeds	Capsule/buffering	Results
Pal'yanov et al. (1999a)	Na_2CO_3 -Gr, $\text{Na}_2\text{CO}_3\text{-CO}_2\text{-H}_2\text{O}$ (OAD)-Gr, K_2CO_3 -Gr, $\text{K}_2\text{CO}_3\text{-CO}_2\text{-H}_2\text{O}$ (OAD)-Gr	5.7	1150–1420	20–120 h	Y	Pt	Na_2CO_3 -Gr; No SN at 1360°/40 h; SN at 30 h at 1420°, GS but no SN at 20 h. K_2CO_3 -Gr; No GS at 1250°/40 h, GS but no SN at 1300–1420°. $\text{Na}_2\text{CO}_3\text{-CO}_2\text{-H}_2\text{O}$ (OAD)-Gr; SN at 1150/120 h, GS but no SN at 1250/40 h; SN at 1360/40 h and 1420°/20 h. $\text{K}_2\text{CO}_3\text{-CO}_2\text{-H}_2\text{O}$ (OAD)-Gr; SN at 1150/120 h, GS but no SN at 1250°/40 h and 1420°/20 h.
Sato et al. (1999)	CaCO_3 -Gr, MgCO_3 -Gr; $\text{Ca}_{0.4}\text{Mg}_{0.6}\text{CO}_3$ -Gr	7.7	1600–2000	1–12.5 h	N	Mo with Gr liner, two in Pt	CM: Na_2CO_3 {111}, {100}; K_2CO_3 and $\text{Na}_2\text{CO}_3\text{-CO}_2\text{-H}_2\text{O}$ {111} Caco ₃ -Gr; SN at 1800°/6 h, not at 1 h; SN 1 h at 2000° but not 1900°. MgCO_3 -Gr; SN at 2000°/1 h, not at 1900°/1 h or 1800°/6 h. $\text{Ca}_{0.4}\text{Mg}_{0.6}\text{CO}_3$ -Gr; No SN at 1600°/12.5 h or 1600°/1 h; SN at 1700° at 11 h, not at 9 or 6 h; SN at 1800° at 6 h, not at 1 h; SN at 1900°/1 h and 2000°/1 h. CM: {111}
Sumiya and Satoh (1999)	CaCO_3 -Gr, MgCO_3 -Gr; CoCO_3 -Gr	7.7	2000–2100	15 min	N	Mo	SN at 2000°, complete at 2100° in CaCO_3 and MgCO_3 , SN at 1850° in CoCO_3 , CM: {111}
Sokol et al. (2000)	Li_2CO_3 -Gr, Na_2CO_3 -Gr, K_2CO_3 -Gr, Cs_2CO_3 -Gr, CaCO_3 -Gr, $\text{CaMg}(\text{CO}_3)_2$ -Gr	7	1700–1750	4–19 h	Y	Pt	SN reported for all expts; focus of study was analysis of quenched fluid phase.
Liu et al. (2001)	MnCO_3	6–12	>2000	?	DAC		Laser-heated DAC; reported formation of diamond by breakdown of carbonite at $P \sim 12$ GPa
Sokol et al. (2001b)	$\text{CaMg}(\text{CO}_3)_2$ -Gr, $\text{CaMg}(\text{CO}_3)_2\text{-H}_2\text{O}$ -Gr, $\text{CaMg}(\text{CO}_3)_2\text{-CO}_2\text{+H}_2\text{O}$ (OAD)-Gr, $\text{CaMg}(\text{CO}_3)_2\text{-Na}_2\text{C}_2\text{O}_4$ -Gr	5.7, 7	1300–1700	2–42 h	Y	Pt	CMg(CO_3) ₂ -Gr; SN at 7 GPa, 1700° at ≥ 4 h; Gr at 2 h, No SN at 5.7 GPa, 1420°/42 h. CaMg(CO_3) ₂ - H_2O -Gr; SN at 5.7 GPa, 1420°/42 h. CaMg(CO_3) ₂ - CO_2 + H_2O -Gr; SN at 5.7 GPa, 1420°/42 h; GS only at 1300°/42 h. CaMg(CO_3) ₂ - $\text{Na}_2\text{C}_2\text{O}_4$ -Gr; GS only at 5.7 GPa, 1300°/42 h
Pal'yanov et al. (2002a)	Na_2CO_3 -Gr, K_2CO_3 -Gr, $\text{Na}_2\text{CO}_3\text{-H}_2\text{O}$ -Gr, $\text{K}_2\text{CO}_3\text{-H}_2\text{O}$ -Gr, $\text{Na}_2\text{CO}_3\text{-CO}_2$ -Gr, $\text{K}_2\text{CO}_3\text{-CO}_2$ -Gr, $\text{Na}_2\text{CO}_3\text{-H}_2\text{O+CO}_2$ (OAD)-Gr, $\text{Na}_2\text{CO}_3\text{-H}_2\text{O+CO}_2$ (OAD)-Gr, $\text{K}_2\text{CO}_3\text{-H}_2\text{O+CO}_2$ (OAD)-Gr	5.7	1150–1420	5–136 h	Y	Mostly Pt, 1 in Gr, 2 in Au	Study focused on how the induction period changes with P , T , and presence of fluids. Found reactivity much higher in fluid-bearing expts. Na_2CO_3 -Gr; At 7 GPa, and 1700°, SN at 2 h, not 0.3 h; at 5.7 GPa 1420°, SN at 30 h, not 20 h; No SN at lower T (1250–1360°) at 40 h. K_2CO_3 -Gr; SN at 7 GPa, 1700/2 h. No SN at 5.7, 1250°/84 h, 1300°/40 h, 1420°/40 h. For both with CO_2 or H_2O , have SN at 5.7 GPa, 1420°/40 h. With H_2O -CO ₂ , had SN at 1150°/120 h, and with decreasing time with increasing T to 20 h at 1420° (for Na_2CO_3). CM: Na_2CO_3 {111}>{100}; K_2CO_3 {111}; $\text{Na}_2\text{CO}_3\text{-CO}_2\text{-H}_2\text{O}$ {111}; $\text{Na}_2\text{CO}_3\text{-CO}_2\text{-H}_2\text{O}$ {111}; $\text{K}_2\text{CO}_3\text{-CO}_2\text{-H}_2\text{O}$ {111}
Shatsky et al. (2002)	K_2CO_3 -Gr	6.3	1650	40 h	Y	Gr	SN (~25–29% transformation). CM: {111}

Study	System	P (GPa)	T (C)	Duration	Seeds	Capsule/ buffering	Results
Litvin and Spivak (2003)	Mixed K–Na–Ca–Mg–Fe carbonatite + Gr, Natural limestone + Gr	7.5–8.5	1500–2000	< 1 h	N	Gr	SN at >7.5 GPa, > 1500° in 45–50 min expts reported for both starting materials. CM: {111}
Sokol and Pal'yanov (2004)	Review of fluid, carbonate+fluid results	5.7–7.7	1150–2000				Review of previous work; discusses induction period preceding spontaneous SN of diamond, which increases with decreasing T . Report increasing intensity of diamond formation in the order: $K_2CO_3(Na_2CO_3) \rightarrow H_2O-CO_2-C \rightarrow CO_2-C \approx H_2O-CO_2-C \approx H_2O-C \approx CaMg(CO_3)_2H_2O-C \Rightarrow CH_4-H_2O-C \gg CH_4-H_2-C$
Spivak and Litvin (2004)	Mixed K–Na–Ca–Mg–Fe carbonatite + Gr	5.5–8.5	~1200–2250	?	?	?	Updated and expanded on Litvin and Zharkov (1999). Few expt'l details. Photos of diamonds formed at 7.8 GPa 1990°, 8 GPa 1500°. Figure has diamond growth down to ~1200° at ~6 GPa. CM: {111}
Palyanov et al. (2007a)	$K_2CO_3 + Gr$, H_2O-Gr , $K_2CO_3 + H_2O + Gr$	7.5	1400–1600	15 h	Y	Pt	K_2CO_3-Gr : SN at ≥1500°, none at 1400°. H_2O-Gr : SN at 1500° and 1600°. $K_2CO_3 + H_2O + Gr$: SN at 1500° and 1600°, increasing amt of diamond formation as H_2O content increases. CM: K_2CO_3 {111}, {100}; $K_2CO_3 + H_2O$ {111}
Spivak et al. (2008)	Mixed K–Na–Ca–Mg–Fe carbonatite + Gr	7–8.1	1500–1600	1–24 min	N	Gr	SN reported in 3 expts (7 GPa 1500°/8 min, 7 GPa 1600°/1 min, 8.1 GPa 1530°/24 min). CM: {111}
Tomlinson et al. (2011)	$MgCO_3 + Gr$	10–20	1900–2100	15 min	N	Re	Diamond formation reported at 1900° at 10 GPa and 2000° at 15 and 20 GPa. CM: {111} + {100}
Spivak et al. (2012)	$CaCO_3$	11–43	1600–3900 K	5 min	N	DAC (Be gasket + Ne) and MAP	Laser-heated DAC. Diamond formation from breakdown of $CaCO_3$ melt at ~3500 K, ~16 and ~43 GPa. CM: {111}
Solopova et al. (2013)	Mixed K–Na–Ca–Mg carbonate + Gr	7–8.5	1500–1800	5–60 min	N	?	SN at 7.5 GPa 1600° to 8.5 GPa 1800°. CM: {111}
Palyanov et al. (2016)	$Na_2CO_3-Gr, Na_2C_2O_4$	6.3, 7.5	1250–1700	10–66 h	Some exps	Pt	$Na_2C_2O_4$ w/o graphite added: Breaks down via $2Na_2C_2O_4 = 2Na_2CO_3 + C + CO_2$. Formed diamond at 6.3 GPa, ≥1300°, 7.5 GPa, ≥1350° from $Na_2CO_3-CO_2$ melt. Control expts with Na_2CO_3-C grew diamond at 6.3 GPa, 1400–1570°. CM: $Na_2CO_3 + CO_2$ {111}, {100} with convex faces and fibrous structure
Khokhryakov et al. (2016)	$Na_2C_2O_4-CaCN_2$	6.3	1500	2, 30 h	Y	Pt	Some GS at 2 h, no SN. SN at 30 h. Observed nitrogen conc up to 1100 ppm, depending on growth sector. CM: Hexaoctahedron with {100}, fibrous structure

Notes: DAC – diamond-anvil cell. MAP – multi-anvil press. Gr – Graphite. OAD – oxalic acid dihydrate. SN – spontaneous nucleation and growth of diamond. GS – diamond growth on seeds. CM – diamond crystal morphology (where given in article). Temperatures in Results column in °C.

Review of Table 2 reveals that the early experiments were conducted at temperatures well above those reasonable for diamond growth in the mantle for two reasons: (1) diamond nucleation and growth require temperatures significantly overstepping of the graphite–diamond transition and (2) diamond growth requires the carbonate to be partially molten in order to serve as a viable growth medium. The solidus temperatures of alkaline-earth carbonates are in excess of ~1400–1600 °C at ≥ 6 GPa for successful growth of diamond. Alkali carbonates, with their lower melting temperatures, allow melt-present experiments at lower temperatures, which facilitates crystallization of diamond at lower temperatures. The addition of volatiles such as water and CO₂ to the systems further encourages diamond crystallization to proceed at lower temperatures.

Experimental issues

Carbonate melts are characterised by low viscosity at least to pressures of ~6 GPa (c.f. Jones et al. 2013 and references therein) although their viscosity may increase at higher pressures (Wilding et al. 2019). In the experiments, possible escape of the liquid through a graphite or MgO capsules must be considered—most of the experiments use Pt or Au in part for this reason.

Oxygen (hydrogen) fugacity control is also a consideration; hydrogen diffusion through the capsule wall can drive carbon precipitation via $2\text{H}_2 + \text{CO}_2(\text{melt}) = \text{C} + 2\text{H}_2\text{O}$, which also introduces H₂O in the system (e.g., see discussion in Palyanov et al. 2016). However, it is worth emphasizing that use of an external oxygen buffer in a double-capsule configuration with hydrogen diffusion across the capsule wall equalizes the chemical potential of hydrogen, not the fO₂ (e.g., Whitney 1972), and these buffers are best used as hydrogen sinks unless there is a fluid coexisting with the carbonate melt in the experimental charge.

Alkali carbonates, particularly K₂CO₃, are notoriously hygroscopic and special care must be taken in experiments with these carbonates. Figure 7 of Shatskiy et al. (2015a) illustrates the effect of adsorbed H₂O on phase relationships: the lowest-*T* eutectic in the K₂CO₃–CaCO₃(–H₂O) drops from ~1200 °C to ~1000 °C at 6 GPa when the samples were dried at 100 °C rather than 300 °C. Some of the differences in the results of the studies involving alkali carbonates may result from this issue. Parenthetically, the temperature effect Shatskiy et al. (2015a) observed also implies high solubility of H₂O in carbonate melts at high pressures—a field relatively unexplored except at much lower pressures (0.025–0.225 GPa; Keppler 2003).

Possible future directions

Further studies of diamond growth in carbonate melts could focus on exploring more of the composition space relevant to natural melts. These studies will benefit from insights provided by recent experimental studies of phase relationships in carbonate systems at mantle pressures (see review by Shatskiy et al. 2015b, for example). The study of systems such as K₂CO₃–CaCO₃–MgCO₃ (Arefiev et al. 2019) and Na₂CO₃–CaCO₃–MgCO₃ (Podborodnikov et al. 2019) hold particular promise in this regard.

Given that it has been firmly established that diamond can indeed grow in carbonate melts, another fruitful line of research is to take advantage of these melts to grow diamond to continue to address issues such as nitrogen incorporation into diamond (e.g., Khokhryakov et al. 2016) and isotopic fractionation between diamond and coexisting melts or fluids (Reutsky et al. 2015a,c, 2018; Bureau et al. 2018) (see later sections).

On another front, there remains another unresolved question: How does carbon dissolve in carbonate melts? Can it dissolve as a neutral carbon species, or does it dissolve as carbonate? A key challenge in resolving this question is the fact that almost all carbonate liquids do not quench to glass, with the intriguing exceptions of some K–Mg carbonates and some more complex melts in the BaSO₄–La(OH)₃–Ca(OH)₂–CaF₂–CaCO₃ system (see *Carbonate glasses* in Jones et al. 2013 and references therein). This issue naturally complicates both measurements of solubility and solution mechanisms. The available data on C solubility in

carbonate melts show low solubility: <0.3 wt.% at 6.8 GPa and 1700 °C in Na₂CO₃ melt (Sokol et al. 1998). On the other hand, CO₂ appears to dissolve readily in carbonate melts: Palyanov et al. (2016) observed a solidus depression of ~100 °C at 6.3 and 7.5 GPa in the system Na₂CO₃-CO₂-C compared to Na₂CO₃, and argued that the 16.4 wt.% of CO₂ produced upon decomposition of sodium oxalate (Na₂C₂O₄) dissolved completely in the melt at these conditions. This solubility is higher than the 11.5 wt.% and 6.5 wt.% CO₂ dissolved in CaCO₃ and MgCO₃ melts, respectively, at liquidus conditions at 2.7 GPa (Huang and Wyllie 1976). To our knowledge, there are no spectroscopic data on solution mechanisms of either C or CO₂ in carbonate melts at diamond-stable *P, T*. This topic would of course be an ideal *in situ* study, such as those done at lower pressures (~700 MPa e.g., Mysen 2018), when technology has evolved sufficiently to make measurements at these conditions possible.

SILICATE MELTS

Overview

The existing experimental data indicate that volatile-free silicate melts cannot provide either diamond nucleation or growth on seeds in the range of *P, T*-parameters that are of interest for natural diamond formation. Silicate and oxide systems become diamond-forming only when H₂O is added (Table 3). Clearly, part of this effect is a result of water lowering the solidus and liquidus temperatures to stabilize the melt to lower temperatures more representative of conditions of natural diamond formation. In most systems, however, we lack basic information about the solubility of H₂O in the melt as a function of *P* and *T*—or indeed the basic phase equilibria—needed to differentiate the effects of melt fraction and melt composition on diamond growth. Nevertheless, the studies in Table 3 show that the nucleation and growth of diamond on seeds was established at temperatures of 1500–1600 °C in water-bearing silicate melts and silicate-bearing aqueous fluids. An increase in the H₂O content in such systems results in a significant increase in the degree of graphite into diamond transformation and is accompanied by a reduction in the induction period preceding diamond nucleation and an increase in carbon mass transfer. As a result, the most favorable conditions for nucleation and growth of diamond occur in the water-rich fluid phase, containing small amounts of silicate or oxide solute. A decrease in temperature leads to a decrease in the diamond-forming ability of silicate–aqueous media, which is usually attributed to more sluggish kinetics at lower temperature. The minimum nucleation temperature for diamond was 1500 °C at 6.3 and 7.5 GPa. The minimum temperature for diamond growth on seeds is 1400 °C at 6.3 GPa (Table 3).

Experimental issues

The overwhelming majority of experiments in the silicate–water systems were carried out in Pt ampoules without special buffering. The presence of graphite and water among the initial reagents due to H₂ diffusion through the walls of Pt ampoules, in the absence of buffering, can lead to the formation of an uncontrolled amount of CO₂ in a predominantly aqueous fluid.

Future directions

One of the unsolved problems is the determination of the solubility of carbon depending on temperature and on the content of H₂O. Experimental studies in this direction will make it possible to evaluate the real scale of diamond formation in the processes of evolution of the system composition and with a decrease in the *P, T*-parameters.

As seen in Table 3, most experiments in the silicate–water systems were carried out without the participation of alkalis. The addition of alkaline components can change the pH of the medium and bring the model system closer to the eclogitic fluid and, possibly, allow to reduce the minimum *P, T*-parameters.

Table 3. Studies of diamond nucleation and growth in silicate melts.

Study	System	P (GPa)	T(°C)	Duration	Seeds	Capsule/ buffering	Results
Borzdov et al. (1999)	KAlSi ₂ O ₈ -Gr	7.0	1700–1750	2–18 h	Y	Gr	No SN
Sokol et al. (1999)	CaMgSi ₂ O ₆ -OAD (20 wt.%)–Gr, NaAlSi ₂ O ₆ -OAD (20 wt.%)–Gr	7.0	1700–1750	4 h	Y	Pt	SN in silicate–H ₂ O–CO ₂ –C systems. CM: {111}
Palyanov et al. (2005a)	SiO ₂ –H ₂ O (4–74 wt.%)–Gr, Mg ₂ SiO ₄ –H ₂ O (4–74 wt.%)–Gr	7.5	1600	40 h	Y	Pt	SN of diamond. With an increase in the H ₂ O content, the degree of graphitic into diamond transformation significantly increases. CM: {111}
Dobrzhinetskaya and Green (2007)	Gr–SiO ₂ ± muscovite ± albite– H ₂ O (6–15 wt.%)	7.0–8.5	1500	1–43 h	Y/N	Pt/Ni–NiO	No diamonds found
Sokol and Palyanov (2008)	Gr–SiO ₂ –H ₂ SiO ₃ (10 wt.%) ± Al ₂ O ₃	7.0–8.5	1500	2–62 h	Y/N	Pt/Fe–FeO	SN of diamond occurred in all experiments with a duration more than 2 hours, mainly in assemblage with SiC and coesite
Palyanov and Sokol (2009)	SiO ₂ –H ₂ O–Gr w/H ₂ O/(H ₂ O + SiO ₂) = 1 – 0.05, Mg ₂ SiO ₄ –Gr w/H ₂ O/(H ₂ O + Mg ₂ SiO ₄) = 1 – 0.08	7.5	1600	15, 40 h	Y	Pt	SN of diamond occurred in the entire composition range. The degree of graphite to diamond transformation is a function of the H ₂ O content, which controls both the kinetics of diamond nucleation and the intensity of carbon mass transfer. Decreasing H ₂ O content decreases degree of transformation. CM: {111}
Sokol et al. (2010)	Mg ₂ SiO ₄ –H ₂ O (13–86 wt.%)–Gr	7.5	1500–1600	15 h	Y	Pt	SN of diamond occurred in all expts. A decrease in temperature results in a decrease in the intensity of diamond forming processes and the formation of metastable graphite. CM: {111}
Fagan and Luth (2011)	Mg ₂ SiO ₄ (72 wt.%)–H ₂ O (8 wt.%)–Gr (20 wt.%)	6.3	1200–1600	16–40 h	Y	Pt	No SN of diamond at 1200°/40h. Only GS at 1400°/40h. SN of diamond at 1600°/16h, 40h. CM: {111}
	SiO ₂ ·0.36H ₂ O + 1.5 Mg(OH) ₂ (16.7 wt.%H ₂ O)	5.5–7.0	1300–1600	4–24 h	Y	Pt	No SN at 1300°/24h ($P = 6$ and 7 GPa) and at 1500°/4h ($P = 6$ GPa). GS at 1500–1600°/4h ($P = 7$ GPa). CM: {111}

Notes: Gr – Graphite. OAD – oxalic acid dihydrate. SN – spontaneous nucleation and growth of diamond. GS – diamond growth on seeds. CM – diamond crystal morphology (where given in article). Temperatures in *Results* column in °C.

BRINES

Early studies showed that diamond can grow in anhydrous alkali halides (Wang and Kanda 1998; Litvin 2003), but such studies are unlikely to be directly relevant to diamond growth in the Earth because of the absence of H₂O. Brines, or hydrous solutions of alkali halides, on the other hand, do form one of the “endmembers” of HDF inclusions in natural diamonds. Remarkably few studies address diamond growth in such systems. The two studies in Table 4 demonstrate that both KCl + H₂O and NaCl + H₂O fluids can nucleate and grow diamonds at 7.5 GPa and high temperatures (1500–1600 °C). The more extensive work in the former system documents a composition-dependence on the degree of transformation of graphite to diamond (see Table 4). Subsequent work in brine-containing systems has shifted to systems coexisting with silicates or carbonates (see subsequent sections).

CARBONATE-CHLORIDE SYSTEMS

There has been limited study of chloride-carbonate systems (Table 5). From these results, it is clear that diamond nucleation and growth can proceed in either anhydrous or hydrous carbonate-chloride melts. An unresolved issue is the minimum temperature at which this occurs: Tomlinson et al. (2004) observed growth as low as 1050 °C at 7 GPa, whereas Palyanov et al. (2007a) did not see diamond growth at 1400 °C at 7.5 GPa. Given the limited data, it is impossible to say whether the presence of H₂O in the system allows diamond nucleation and/ or growth at lower temperatures.

MODEL CARBONATE-SILICATE SYSTEMS

Overview

These studies explore the efficacy of carbonate-silicate melts as a medium for diamond nucleation and growth. In effect, these studies can be considered extensions of carbonate-melt studies that explore the effect of dissolution of silicate constituents into the melt. At the same time, these studies mark a significant step towards simulating systems representative of those potentially present in the Earth’s mantle. Examination of Table 6 shows that these melts are effective growth media for diamond, particularly at higher temperatures, which in part reflects the temperatures required for melt to be present, but also the temperature-dependence of diamond nucleation and growth as seen in the previous systems.

Future directions

Unresolved questions in these systems include whether the effect of adding carbonate is strictly a result of stabilising a melt to lower temperatures, a compositional effect of the presence of carbonate, or a result of decreasing viscosity of the melt with increasing carbonate content. Systematic studies to tease out these possibilities may be warranted if such systems are viewed to be useful models for natural diamond growth.

Table 4. Diamond growth in brines.

Study	System	P (GPa)	T (°C)	Duration	Seeds	Capsule	Results
Palyanov et al. (2007a)	KCl + H ₂ O + Gr	7.5	1500, 1600	15 h	Y	Pt	1500°: No SN at 19 wt.% H ₂ O, SN from 35–91 wt.% H ₂ O with increasing % diam, slight decrease in total % diam in 100% H ₂ O. 1600°: SN from 17–100 wt. % H ₂ O, maximum trans-formation at 66–69 wt. % H ₂ O CM: {111} Growth and entrapment of graphite inclusions. CM: {111}
Khokhryakov et al. (2009)	NaCl + H ₂ O + Gr	7.5	1600	40 h	Y	Pt	

Notes: Gr – graphite. SN – spontaneous nucleation and growth of diamond. GS – diamond growth on seeds. CM – diamond crystal morphology. Temperatures in *Results* column in °C

Table 5. Studies of diamond nucleation and growth in carbonate–chloride (\pm H₂O) systems.

Study	System	P (GPa)	T (°C)	Duration	Seeds	Capsule	Results
Tomlinson et al. (2004)	KCl + K ₂ CO ₃ + Gr	7–7.7	1050–1420	5–60 min	Y	Pt	GS at 1050°/60 min, 1260°/60 min, 1420°/≤5 min. CM: {1111}
Palyanov et al. (2007a)	KCl + K ₂ CO ₃ + Gr	7.5	1400–1600	15 h	Y	Pt	No SN at 1400°, SN at 1500° (more in K ₂ CO ₃ -rich) and 100% diam at 1600° w/KCl varying from 25–80 wt.%. CM: {1111}, {100}
Palyanov et al. (2007a)	KCl + K ₂ CO ₃ + H ₂ O + Gr	7.5	1500	15 h	Y	Pt	SN in three compositions with variable KCl:K ₂ CO ₃ :H ₂ O. CM: {1111}

Notes: Gr – graphite. SN – spontaneous nucleation and growth of diamond. GS – diamond growth on seeds. CM – diamond crystal morphology. Temperatures in *Results* column in °C.

Table 6. Studies of diamond nucleation and growth in model carbonate–silicate systems.

Study	System	P (GPa)	T (°C)	Duration	Seeds	Capsule	Results
Borzdov et al. (1999)	66.6 wt.% K ₂ CO ₃ + 33.4 wt.% SiO ₂ + Gr; 80 wt.% K ₂ CO ₃ + 11.4 wt.% MgO + 8.6 wt.% SiO ₂ + Gr;	7	1700–1750	1–17.5 h	Y	Pt	K ₂ CO ₃ –SiO ₂ + Gr; SN in 1 h K ₂ CO ₃ –MgO–SiO ₂ + Gr; SN in 17.5 h. K ₂ CO ₃ –MgO–Al ₂ O ₃ –SiO ₂ + Gr; SN in 17 h. Contrasts w/ no SN or GS in 2–18 h exps with KAlSi ₃ O ₈ + Gr. Carbonate– or carbonate ± silicate ± oxide melts fluxed diamond growth. CM: {111}, {111}→{100}
Shatsky et al. (2002)	K ₂ CO ₃ + K ₂ CO ₃ (5–75 wt. % SiO ₂) + Gr K ₂ CO ₃ + Gr, K ₂ CO ₃ + Mg ₂ SiO ₄ (Fo) (5–95 wt.% Fo) + Gr	6.3	1650	40 h	Y	Gr	K ₂ CO ₃ + SiO ₂ + Gr; SN up to 25 wt. % SiO ₂ ; GS only at higher SiO ₂ ; K ₂ CO ₃ + Fo + Gr; SN up to 50 wt.% Fo; GS only in 50–90 wt.% Fo; no GS at 95 wt.% Fo. In both series, maximum intensity of diamond growth at ~10 wt.% silicate. All exps contained K-bearing carbonatite–silicate melt. CM: {111}, {100}
Litvin et al. (2008a)	NaAlSi ₃ O ₈ + K ₂ CO ₃ (50–90 wt.% Ab) + Gr, Mg ₂ SiO ₄ + K ₂ CO ₃ (60–80 wt. % Fo) + Gr, SiO ₂ + K ₂ CO ₃ (30–50 wt.% SiO ₂) + Gr	7.6–8.5	1620–1800	4–40 min	Y	Gr	GS in all exps in presence of carbonate–silicate melt. SN reported in exps except for Mg ₂ SiO ₄ –K ₂ CO ₃ at <40 wt.% carbonate and SiO ₂ –K ₂ CO ₃ at <60 wt.% carbonate. CM: {111}
Spivak et al. (2008)	NaAlSi ₃ O ₈ + K ₂ CO ₃ (60–80 wt.% Ab) + Gr	8.5	1730, 1800	6 min 30 min	N	Gr	SN reported in presence of melt in both experiments. CM: {111}
Bataleva et al. (2012)	(Ca,Mg)[CO ₃ –SiO ₂ –Al ₂ O ₃ –(Mg,Fe)(Cr,Fe,Ti)O ₃] (16.1 wt.% CO ₂)	6.3	1350–1650	20 h	Y	Pt, Pt + Gr	GS at 1550° and 1650° in Pt capsules (not at 1350° or 1450°), at 1350° and 1450° in Pt–Gr capsules. Melt present in all exps, amount increased from <10 wt.% at 1350–1450° to >20 wt.% at 1550° and 1650°. Observed dissolution of diamond seeds in exps w/ Pt capsules but not in Pt–Gr capsules (fO ₂ dependent). CM: growth {111}, regeneration of {100}→{111}

Notes: Gr – graphite. SN – spontaneous nucleation and growth of diamond. GS – diamond growth on seeds. CM – diamond crystal morphology. Temperatures in *Results* column in °C.

MULTICOMPONENT CARBONATE–SILICATE MEDIA AND “DIAMOND-BEARING” ROCKS

Overview

The main regularities in diamond crystallization, as revealed in simple model systems (above), are also valid for multicomponent media and are as follows:

- Silicate melts do not facilitate nucleation and diamond growth; it is the addition of water makes the silicate + H₂O systems diamond-forming. The silicate component acts as a diamond formation inhibitor (e.g., Sokol and Pal’yanov 2008), with all other parameters being constant.
- In carbonate–silicate environments, the silicate component also inhibits diamond formation.
- The most effective diamond-forming media are alkaline carbonate melts as well as H₂O- and CO₂-bearing fluids; nucleation and growth of diamond in these media are realized at the lowest P, T , probably reflecting their stability as melts or fluids at these conditions.
- The induction period preceding the nucleation and growth of diamond depends on P, T and the composition of the crystallization medium.
- With an increase in P and T , the diamond-forming ability of all media increases. A decrease in P and T in all media leads to crystallization of metastable graphite.
- An increase in pressure from 5.7 to 12 GPa and above allows the reduction of the minimum diamond nucleation temperature in all systems, including multicomponent carbonate–silicate media.
- All other parameters being equal, the nucleation of a diamond requires higher temperatures than the growth of a diamond on seeds.
- Crystallization of diamond or graphite in a carbonated eclogite at 9–23 GPa was suggested to result from oxidation of Fe²⁺ to Fe³⁺ in coexisting garnet (Kiseeva et al. 2013).

Experimental issues

Experiments in multicomponent carbonate–silicate systems and using the “diamond-bearing” rocks were carried out mainly in Pt ampoules (Table 7). The effect of the ampoule material (for example, Pt and Au) on the diamond nucleation process in non-metallic solvents has been studied insufficiently. For example, in long-term experiments (tens of hours), the dissolution of Au and its crystallization on diamond in the C–O–H fluid were shown (Sokol et al. 2001a). The effect of Pt on diamond nucleation was established in long-term experiments in the kimberlite–graphite system (Palyanov et al. 2015); however, the real scale of the effect of Pt is not clear. It can be most significant at high P and T , especially when using small diameter Pt ampoules.

Future directions

New experimental studies need to be performed in these fields:

- Despite a large number of experiments carried out in a wide range of P, T -parameters and in various media, there is still no clarity and experimental confirmation of how diamond is formed in eclogites and peridotites in the pressure range of 4–7 GPa and 900–1400 °C,

characteristic of formation of most natural diamonds (Stachel and Harris 2008).

- There is still insufficient experimental data to assess the effect of various components of the C–O–H–N–S system fluid on the crystallization of diamond in multicomponent media. The data on the defect-impurity composition of diamonds synthesized in various model media are still scarce, which does not allow us to fully assess the overall picture of the effect of the composition of diamond-forming media on the real structure of diamond.

SULFIDE MELTS

The studies in this section (Table 8) document that diamond can nucleate and grow in iron-sulfide melts, but typically at temperatures higher than those appropriate for corresponding pressures in the mantle. From these studies, sulfide melts appear to be less effective at mediating diamond growth than either H₂O-rich fluids or carbonate melts.

CARBONATE REDUCTION

To this point, all of the studies had graphite in the starting materials, and the primary focus was on whether a particular melt or fluid would mediate the transformation of graphite to diamond at conditions approaching those appropriate for the Earth. In contrast, the studies in this section all contain carbonate as a carbon source and use different reducing agents to produce diamond by reduction (Table 9). The early studies demonstrated the viability of this mechanism, using metal, metal carbides, or metal hydrides as reducing agents. Subsequent studies looked at the possible role of C–H fluids, sulfides and oxides. Overall, reduction of carbonate has been shown to be a viable mechanism for formation of diamond; the key question in terms of applicability to the Earth is what the appropriate reducing agent might be in different environments, particularly in the lithospheric mantle at depths shallower than those at which iron metal or carbide are stabilized.

DIAMOND-ANVIL CELL EXPERIMENTS

Overview

Whereas they are not designed for that purpose for most of the cases, laser heated diamond anvil cells (LHDAC) experiments may give significant information about the formation of superdeep diamonds, and demonstrate progress towards multiphase mantle petrology at conditions of the lowermost mantle.

Most of these studies (Table 10) are looking at high *T*- and *P*-dependent breakdown of carbonates like CaCO₃ = CaO + C + O₂ in the context of subduction recycling, or to characterize the formation of new mineralogical species of carbonates in the deep Earth. For example, Dorfman et al. (2018) show that CaCO₃ is preserved at pressure and temperature conditions reaching those of the deep lower mantle, supporting its relative stability in carbonate-rich lithologies under reducing lower mantle conditions. Boulard et al. (2011) provide evidence for the presence of both diamonds and an oxidized C-bearing phase, suggesting that oxidized and reduced forms of carbon might coexist in the deep mantle.

Litvin et al. (2014) took the benefit of these HPHT tools to study the diamond-forming lower mantle systems, by investigating melting phase relations of simple carbonates of Ca, Mg, Na and multicomponent Mg–Fe–Na–carbonate up to 60 GPa and 3500–4000 K (LHDAC and multi-anvil presses). They grew diamonds that showed that ‘Super-deep’ diamonds can crystallize in the system carbonate-magnesiowüstite-Mg-perovskite-carbon.

Table 7. Studies of diamond nucleation and growth in multicomponent carbonate–silicate media and diamond-forming rocks.

Study	System	P (GPa)	T (C)	Duration	Seeds	Capsule/ buffering	Results
Arima et al. (1993)	Kimberlite–Gr	7–7.7	1800–2200	20–900 min	Y/N	Gr (Mo, Ta) Pt	SN of diamond in both expts w/ this composition. Contrasts with garnet–pyroxene rock at 5.7, 1420° that did not produce diamond. Analysis of gas phase after expt showed $H_2O \gg CO_2$
Palyanov et al. (2001b)	Natural pyroxene–carbonate (~22 wt.% SiO_2)–Gr	5.7 7	1420 1700	41 h 3 h	Y		SN reported for all four compositions. Melt present in all expts
Litvin et al. (2001)	Natural calcio–carbonates (~12–~22 wt.% SiO_2) + Gr	7	1450–1550	10–40 m	Y	Gr	
Litvin et al. (2003)	Natural garnet–cpx–carb rock	5.5–7.5	1420–1720	1–31 min (in some)	Y	Gr	Reported GS at T as low as 1420° (6.5 GPa) in presence of melt. SN in expts from 1420–1720°; dissolution of seeds in other expts from 1450° at 6.1 GPa to 1660° at 5.5 GPa SN at 1500° and 8.1 GPa/34 h
Dobrzhinets– kaya et al. (2004)	Carbonate–talc–Gr	7.5–8.5	1200–1500	1–138 h	N	Pt	
Bobrov et al. (2004)	Natural carbonate–silicate rock	4–7	1200–1700	20–125 min	Y	Pt ₆₀ Rh ₄₀	Reported diamond formation from carbonatitic melt
Litvin et al. (2005a)	Natural carbonatite	7–8.5	1500–2000	40 min	N	Gr	Liquidus reported to be at ~1700–1730°.
Litvin et al. (2008b)	Eclogite + dolomite, eclogite + K_2CO_3 , eclogite + K–Na–Mg– Ca–Fe carbonate	8.5	1570–1800	4–42 min	Y	Gr	Diamondite formed at 7–8.5 GPa, 1800° in carbonate–silicate melt GS in all expts. SN reported in carbonate–silicate melt at low % (~30–40 wt.%) eclogite
Litvin and Bobrov (2008)	Peridotite + K–Na–Mg–Ca–Fe carbonate	8.5	1750–1780	12–15 min	Y	Gr	SN in carbonate–silicate melt up to ~30 wt. % peridotite in starting material
Litvin et al. (2008a)	Eclogite + dolomite, eclogite + K_2CO_3 , eclogite + K–Na–Mg– Ca–Fe carbonate	7–8.5	1000–1800	2–45 min	Y	Gr	GS except one expt at 1000° (rest $\geq 1500^\circ$). Reported barrier to nucleation of diamond in the melts that varied depending on the carbonate composition
Spivak et al. (2008)	cpx–gt + K_2CO_3 + Gr, Eclogite + dolomite	7.3–8.5	1650–1800	6–40 min	N	Gr	SN reported in presence of melt in all 5 expts (7.3 GPa 1650°/40 min, 8.5 GPa 1720–1800°)
Bobrov and Litvin (2009, 2011)	Peridotite + carbonate, eclogite + carbonate. Carbonates: K_2CO_3 , $CaMg(CO_3)_2$, K–Na–Mg–Ca–Fe carbonate	7–8.5	1750–1820	10–15 min	Y	Gr	GS in all expts at 8.5 GPa, 1750–1820°. Reported barrier to nucleation of diamond in the melts that varied depending on the carbonate and silicate composition of the melt

Study	System	P (GPa)	T (C)	Duration	Seeds	Capsule/ buffering	Results
Bureau et al. (2012)	MELD-SiO ₂ -Al ₂ O ₃ -TiO ₂ - (Ca,Mg)Na ₂ K ₂ CO ₃ -H ₂ O-Gr ± D	7-9	1200-1700	10 min- 144 h	In most Pt		MELD = average inclusion composition from Navon et al. (1988). Observed SN in unseeded expts at 1500°-5 h but not 1450°/10 min at 7 GPa. In seeded expts, observed GS at 7 GPa as low as 1200° (144 h expt), SN in most other expts at higher P and T
Spivak and Litvin (2012)	Calcio-carbonatite w/~28 wt.% SiO ₂ + Gr	8.5	1320-1750	30 min	Y	Gr	Sample previously studied by Litvin et al. (2001) at 7 GPa. Varied C content in SM. Melt present in expts at >1325°. Diamond reported in expts at 20 and 40 wt.% C, not in 0 or 10 wt.% C expts. Diamond reported in subsolidus expt at 1320°, 40 wt.% C
Kiseeva et al. (2013)	Natural eclogites	9-21	1100-1800	12-80 h	N	Au ₇₅ Pd ₂₅ capsules	Report diamond SN as accessory minerals in experiments on one of their eclogite compositions at 9-23 GPa; attributed to reduction of carbonate concomitant with Fe ²⁺ oxidation in coexisting garnet SN at T ≥ 1400° and 12 GPa/12 h. SN at T ≥ 1200° and 16 GPa/24 h
Litasov et al. (2014)	Peridotite + Fe (3 wt.%) + C ₁₈ H ₃₆ O ₂ Eudialyte + Fe (3 wt.%) + C ₁₈ H ₃₆ O ₂	3-16	1200-1600	1-24 h	N	AuPd or Pt/Mo/ MoO ₂ or Fe/FeO	
Litvin et al. (2014)	CaCO ₃ Na ₂ CO ₃ MgCO ₃ FeCO ₃ Gr, MgCO ₃ -Gr, CaCO ₃ -Gr, Na ₂ CO ₃ -Gr and Mg-Fe-Na-carbonate-magnesiowüstite-Mg-perovskite-Gr Kimberlite-Gr	10-60	1100-4000 K	About 5 min	N	DAC (in Ne) and MAP	SN of nano diamonds
Palyanov et al. (2015)	Na-gloss + Gr with 6 wt.% CO ₂ and 7 wt.% H ₂ O	6.3	1300-1570	40 h	Y	Pt	GS of diamond at T ≥ 1520°. SN at T ≥ 1520° (Pt). No SN in volume
Brey et al. (2015)	K-gloss + Gr	7.5	1450-1570	40 h	Y	Pt	GS at T ≥ 1400°. SN at T ≥ 1450° (Pt). SN at T ≥ 1570° (in volume)
		7.5	900-1300	18-73 h	?	Pt with Re	No SN of diamond
		9.5	1000,1300	26-72 h			No SN at 1000°/72 h. SN at 1300°/26 h
		12	1200,1400,1600	2-48 h			No SN at 1200°/48 h. SN at 1400°/27 h and 1600°/2 h
		7.5	800-1300	24-100 h	Pt with Re		No SN at 800-1300°/48 h. SN at 1300°/25 h
		8.5-9.5	900-1300	25-101 h			No SN at 900-1200°. SN at 1300°/25 h
		10.5	900-1300	4-98 h			No SN at 900°, 1200°/4-15 h. SN at 1200°/27 h, 1300°/25 h
		12	800-1400	24-100 h			No SN at 800°/100 h. SN at 1200°/24 h at 1400°/27.5 h

Study	System	P (GPa)	T (C)	Duration	Seeds	Capsule/ buffering	Results
Bureau et al. (2016)	MORB + Pelagic sediments + $H_2O + NaCl + Gr$	6–7	1300–1400	6–10 h	Y	Pt	No SN, GS only at 1350° and 7 GPa
Gittins et al. (2018)	H_2O - and CO_2 -bearing model sediment + garnet harzburgite +Gr (+T gradient)	7.5–10.5	1300–1500	6–119 h	N	Pt(Re)	SN above 1300° at 7.5 GPa and 1200° at 10.5 GPa
	H_2O - and CO_2 -bearing model sediment + garnet harzburgite + Dm + Gr (No T gradient)	7.5	1100–1400	2–210 h	Y	Pt(Re)	SN observed above 1200° at 7.5 GPa
Palyanov et al. (2021b)	$Mg_2Si_4O_{10}(OH)_2$ (Talc) + mag- nesite or dolomite or dolomitic + $Al_2O_3 + SiO_2$	6.3–7.5	1300–1600	6–40 h	N	Pt, Pt loop (cathode) field of 0.4–1 V	SN (in the cathode zone) from carbon of carbonates under electric

Notes: Gr – graphite, DAC – Diamond-anvil cell, MAP – Multi-anvil press, SN – spontaneous nucleation and growth of diamond, GS – diamond growth on seeds. Temperatures in *Results* column in °C.

Table 8. Studies of diamond nucleation and growth in sulfide melts.

Study	System	P (GPa)	T (C)	Duration	Seeds	Capsule/ buffering	Results
Litvin et al. (2002)	$CuFeS_2-(Fe,Ni)_9S_8 + Gr$, $CuFeS_2-Fe_{1-x}S + Gr$, $CuS + Gr, Ag_2S + Gr$	7–7.5	1450–1500	40–80 min	Y	Gr	SN reported in all compositions
Pal'yanov et al. (2003)	$(Fe,Ni)_9S_8 + Gr$	6.3, 7, 7.5	1450–1800	8.5–65 h	Y	Gr	SN at ≥ 1600° at 7.5 GPa, GS at 1450° at 6.3 GPa, ≥ 1550° at 7 GPa. CM: {111}
Litvin and Butvina (2004)	$CuFeS_2-(Fe,Ni)_9S_8 + Gr$, $CuFeS_2-Fe_{1-x}S + Gr, Ag_2S$ + Gr	7–8	1650–1800	10–180 min	Y	Gr	SN reported in all sulfide + Gr expts; unclear which SM mix used in each expt
Palyanov et al. (2006)	$(Fe,Ni)_9S_8 + Gr, FeS + Gr$	6.3–7.5	1450–2200	2–40 h	Y	Gr	$(Fe,Ni)_9S_8 + Gr$: SN at ≥ 1900° at 7 GPa, ≥ 1600° at 7.5 GPa; GS at 1450° at 6.3 GPa, ≥ 1550° at 7 and 7.5 GPa. FeS + Gr: No SN at 6.3 GPa, 1500°, 7 GPa 1550–1800°. SN at ≥ 1600° at 7.5 GPa; GS in all expts (6.3 GPa, 1500°, 7 GPa 1550–1800°; 7.5 GPa 1550–2200°)
Litvin et al. (2005b)	$Fe_{1-x}S + Gr$	7.5–8.9	1800–2100	5–60 min	N	Gr	SN reported at these conditions; photo of diam formed at 8.2 GPa, 1910°/30 min
Shushkanova and Litvin (2006)	$Fe_{1-x}S + Gr$	6.7	1660	4 min	N	Gr	SN of polycrystalline diamond

Study	System	P (GPa)	T (C)	Duration	Seeds	Capsule/ buffering	Results
Shushkanova and Litvin (2008a,b)	Fe _{1-x} S + Gr	6–7.1	1409–1695	?	Y	Gr	Determined P, T range of SN and GS in sulfide melt
Spivak et al. (2008)	FeS	6.7	1660	4 min	N	Gr	SN observed
Chepurov et al. (2009a)	Fe–Co–S + Gr	5.5	1300	5–48 h	Y	?	Variied Fe:Co:S ratios; SN reported in most expts. Used Ti in sample as nitrogen sink
Zhimulev et al. (2012)	Fe–Co–S + Gr, Fe–Ni–S + Gr	5.5	1300	5–51 h	Y	MgO	Observed SN in metal-rich, S-poor melts: up to 14 wt.% S in Fe–Co–S; up to 9.9 wt.% S in Fe–Ni–S
Zhimulev et al. (2013)	Fe–S + Gr	5.5	1350	21–25 h	Y	MgO	Observed SN in 4/5 expts with ~5 wt.% S
Zhimulev et al. (2016a)	Fe–S + Gr	5.3–5.5	1300–1370	1–25 h	Y	MgO	SN in 4 wt.% S at 5.5 GPa, $\geq 1350^\circ$ but no SN at 5.3 GPa, 1300° in 4 wt.% S.
Palyanov et al. (2020a)	Fe ₃ Ni ₁ +Gr + FeS ₂ , S from 0 to 20 wt %	6	1400	20 h	Y	MgO	GS observed at 5.3 GPa, 1300° at 0.8–3.2 wt.% S. With an increase in the S content from 0 to 20 wt%, it was established a decrease in the degree of transformation Gr to Diam from 100 to 0, the formation of metastable graphite, a decrease in the solubility of carbon from 6.6 to 0.8 wt% and a decrease in the nitrogen content in diamonds from 50–100 ppm.

Notes: Pn – pentlandite; Gr – graphite. SN – spontaneous nucleation and growth of diamond. GS – diamond growth on seeds. CM – diamond crystal morphology (where given in article). Temperatures in *Results* column in °C.

Table 9. Studies of diamond nucleation and growth by reduction of carbonate.

Study	System	P (GPa)	T (C)	Duration	Seeds	Capsule/ buffering	Results
Arima et al. (2002)	CaMg(CO ₃) ₂ –Si CaMg(CO ₃) ₂ –SiC	7.7	1500–1800	1–24 h	In some	Pt	CaMg(CO ₃) ₂ ; No SN at 1800°. CaMg(CO ₃) ₂ –Si; SN at 1600°/4 h, 1800°/1 h. GS at 1800° except in expt w/ lowest Si content.
Pal'yanov et al. (2002b)	MgCO ₃ + SiO ₂ , MgCO ₃ + Na ₂ CO ₃ + SiO ₂ , No Gr. High [H ₂] from TiH _{1.9} in sample assembly.	6–7	1350–1800	10–43 h	Y (in most) from TiH _{1.9} in sample	Pt, high fH ₂ from TiH _{1.9}	CaMg(CO ₃) ₂ –SiO ₂ ; GS at 1400°. SN at 1450° at 6 GPa; At 7 GPa, no SN or GS at 1500°, 1600°; SN at 1750, 1800°. MgCO ₃ +Na ₂ CO ₃ +SiO ₂ ; SN at 1400°, 1500° at 6 GPa and 1800° at 7 GPa. MgCO ₃ present in all expts.
Yamaoka et al. (2002a)	CaCO ₃ + stearic acid (C ₁₈ H ₃₆ O ₂)	7.7	1500	0.5–48 h	N	Pt	Proposed diamond-forming reactions: MgCO ₃ + SiO ₂ = MgSiO ₃ + CO ₂ and MgCO ₃ + MgSiO ₃ = Mg ₂ SiO ₄ + CO ₂ , then CO ₂ + 2H ₂ = C + 2H ₂ O. CM: {111} and fibrous patterns on the {100} face of seed crystals
Pal'yanov et al. (2005b)	MgCO ₃ + SiO ₂ , CaMg(CO ₃) ₂ + SiO ₂ , MgCO ₃ + Al ₂ O ₃ + SiO ₂	5.2–7	1200–1800	10–91 h	Y	Pt, most expts had high fH ₂ from TiH _{1.9} in sample	Two capsule configurations. Single capsule w/ CaCO ₃ + SiA pro- duced Gr in short runs, diamond at ≥24 h. In double capsule expts (CaCO ₃ in IC, SiA in OC), found Gr in IC in 2 h expt, Gr + Diam in 12 h expt, Diam in 24 and 48 h expts. CM: {111}
Siebert et al. (2005)	FeCO ₃ + Si, FeCO ₃ + FeSi	10–25	1700–1800	1–7 min	N	Gr or MgO	More diamond growth in MgCO ₃ –SiO ₂ –Al ₂ O ₃ than in MgCO ₃ –SiO ₂ . Diamond growth from either subsolids fluid or carbonate–silicate melt, depending on conditions.
Gunn and Luth (2006)	MgCO ₃ + (Mg,Fe)SiO ₃ + Fe–S–O mix	6–7.5	1300	6–8 h	N	MgO	Analysis of quench fluid phase documented high X(H ₂ O) in TiH _{1.9} – present expts.
Palyanov et al. (2007b)	MgCO ₃ –SiO ₂ –Al ₂ O ₃ –FeS	6.3	1250–1800	8–44 h	Y	MgO+Pt, MgO+BN, MgO+Gr Pt	CM: {111} and fibrous patterns on the {100} face of seed crystals Gr reported in expt
Chepurov et al. (2011)	CaCO ₃ + Ca(OH) ₂ + Fe	4	1350	5 h	Y		
Martin and Hammoda (2011)	CaMg(CO ₃) ₂ + SiO ₂	4.25–6	800–1300	~2–94 h	N	AuPd or Mo-lined Pt	AuPd expts: Gr produced at 800° at 4.25, 5.5, 6 GPa and at 1000° at 6 GPa. Mo–Pt expts: Gr produced at 950–1150° at 4.25 GPa, 1150° and 1300° at 5.5, and 900°, 1050°, 1150°, 1250° at 6 GPa

Study	System	P (GPa)	T (C)	Duration	Seeds	Capsule/buffering	Results
Bataleva et al. (2012)	(Ca,Mg)CO ₃ -SiO ₂ -Al ₂ O ₃ -(Mg,Fe)(Cr,Fe,Ti)O ₃	6.3	1350-1650	20 h	Y	Pt, Pt + Gr	GS at 1550° and 1650° in Pt capsules (not at 1350° or 1450°), at 1350° and 1450° in Pt-Gr capsules. Observed dissolution of diamond seeds in expts w/ Pt capsules, not in those w/ Pt-Gr capsules.
Palyanov et al. (2013b)	Fe-(Mg,Ca)CO ₃	6.5, 7.5	1000-1650	8-60 h	Y	Pt	Diamond formation in Pt capsules attributed to decarbonation of carbonate; in Pt-Gr capsules, recrystallization of Gr from capsule. CM: Growth form {111}, regeneration of {100} → {111}
Bataleva et al. (2016b)	Fe-(Mg,Ca)CO ₃ -S	6.3	900-1400	18-20 h	N	Gr, talc	Graphite produced in all expts. Diam SN at 1350-1600° at 6.5 GPa, at ≥1300° at 7.5 GPa. GS at 1200-1400° at 7.5 GPa. CM: {111} in metal melt and in carbonate-oxide melt
Bataleva et al. (2016d)	(Mg,Ca)CO ₃ -Al ₂ O ₃ -SiO ₂ -FeO	6.3	1150-1650	20 h	Y	Pt	Graphite produced in all expts (900-1400°). Carbonate seen only at 900°.
Bataleva et al. (2019)	Fe-(Mg,Ca)CO ₃ -S	6.3	1500, 1600	18 h	Y	Gr	Diamond growth at 1150° and 1250°, diamond dissolution at 1350-1650°. Gr reported at 1150-1450°.
Zdrokov et al. (2019)	olivine-ankerite-S, olivine-ankerite-FeS ₂	6.3	1050-1550	20-60 h	Y	Gr	CM: Growth form {111}, regeneration of {100} → {111} Gr present in both expts; Diam SN in both.
<i>Notes:</i> SN – spontaneous nucleation and growth of diamond; GS – diamond growth on seeds. CM – diamond crystal morphology. Temperatures in Results column in °C.							
Study	System	P (GPa)	T	Duration	Seeds	Capsule/buffering	Results
Liu et al. (2001)	MnCO ₃	6-12	>2000 °C	?	DAC		Laser-heated DAC; reported formation of diamond by breakdown of carbonate at P ~12 GPa
Tschäuner et al. (2001)	CO ₂	30-80	1500-3000 K	?	DAC	DAC	Laser-heated DAC; reported formation of diamond by breakdown of CO ₂ , Raman peaks attributed to new diamond observed between 36 and 72 GPa
Seto et al. (2008)	MORB + CaCO ₃ , SiO ₂ + MgCO ₃ , MgCO ₃	31-80	1700-3300 K	1-2 h	DAC	DAC	Laser-heated DAC expts. Reported diamond formation at >3000 K at 33-80 GPa in MORB + CaCO ₃ , at 3300 K at 31, 44 GPa and at 2500 K at 73 GPa in SiO ₂ + MgCO ₃

Table 10. Studies of diamond formation at very high pressures–diamond anvil cell experiments.

Study	System	P (GPa)	T	Duration	Seeds	Capsule/ buffering	Results
Bayarjargal et al. (2010)	CaCO_3 in NaCl pressure medium	9–21	1000–4000 K	?	DAC	DAC	Formed graphite by decomposition of CaCO_3 , Annealing of sample produced diamond
Boulard et al. (2011)	MgCO_3 , $(\text{Fe}_{0.75}\text{Mg}_{0.25})\text{CO}_3$, $\text{MgO} + \text{CO}_2$, $(\text{Mg}_{0.6}\text{Fe}_{0.4})\text{O} + \text{CO}_2$	80–105	2400–2805 K RT	?	DAC	DAC	Reported diamond formation (nanodiamonds)
Litasov et al. (2011)	CO_2	40–70	1800–2000 K		DAC	DAC	Diamond formation from CO_2 at 40–70 GPa
Zhang et al. (2011)	H_2O from glucose, $\text{H}_2\text{O}-\text{CO}_2$ from OAD	9–11	1000–1400 K	15–50 min	DAC	DAC	Growth reported in both expts w/ glucose, none in OAD expt
Boulard et al. (2012)	$\text{FeO} + \text{CO}_2$, $\text{FeO(OH)} + \text{CO}_2$, $\text{Fe}_2\text{O}_3 + \text{CO}_2$, $(\text{Mg}_{0.6}\text{Fe}_{0.4})\text{O} + \text{CO}_2$	40–105	1460–3650 K	About 2 h	DAC	DAC	Reported diamond formation (nanodiamonds) in all expts except with Fe_2O_3
Spivak et al. (2012)	CaCO_3	11–43	1600–3900 K	5 min	N	DAC (Re gasket + MAP (in Ne) and MAP)	Laser-heated DAC. Diamond formation from breakdown of CaCO_3 melt at ~3500 K, ~16 and ~43 GPa
Litvin et al. (2014)	CaCO_3 , Na_2CO_3 , MgCO_3 , FeCO_3 , Gr, MgCO_3 -Gr, CaCO_3 -Gr, Na_2CO_3 -Gr and Mg–Fe–Na–carbonate–magnesio-wüstite–Mg–perovskite–Gr	10–60	1100–4000 K	About 5 min	N	DAC (in Ne) and MAP	SN of nano diamonds
Solopova et al. (2015)	MgCO_3	12–84	1600–3300 K	1 min	DAC	DAC (and MAP at 23 GPa)	Reported MgO + diamond in MAP at 23 GPa, 2700 K, inferred diamond formation in DAC at >2700 K by presence of MgO
Thomson et al. (2016)	Peridotite + Fe + carbonate	20	1590 °C	124 min	DAC	DAC	Reduction of carbonate melt by Fe metal to diamond reported
Maeda et al. (2017)	$\text{MgCO}_3 + \text{SiO}_2 + \text{Pt}$ (in NaCl or SiO_2 pressure media)	~30–152	300–3100 K	10–120 min	N	DAC	Laser-heated diamond anvil cell. Diamond nucleation at 70 GPa
Litvin et al. (2017)	$\text{MgO-FeO-SiO}_2 + \text{Mg-Fe-Na-K}$ carbonate + Gr	26	?	?	DAC	DAC	Reported diamond formation at 26 GPa coexisting with oxide + silicates
Dorfman et al. (2018)	$\text{CaMg}(\text{CO}_3)_2 + \text{Fe}$	51–113	1800–2500 K	10–20 min	DAC	DAC	Reported diamond formation in all 4 expts (51, 66, 77, 113 GPa)
Drewitt et al. (2019)	$\text{FeO-MgO-SiO}_2-\text{CO}_2$ and $\text{CaO-MgO-SiO}_2-\text{CO}_2$ systems	48–89	1580–2160 K	24–61 min	DAC	DAC	Report formation of diamond in higher-T expts (1745–2160 K at 54–88 GPa in FMSC, 1905–2160 K at 40–84 GPa in CMS) by decarbonation of carbonate
Martirosyan et al. (2019)	Natural MgCO_3 –Fe	70–150	800–2600 K	10–20 min	DAC	DAC	Reported diamond formation in part of the experiments

Notes: DAC – Diamond anvil cell. MAP – Multi-anvil press. SN – Spontaneous nucleation and growth of diamond.

Recently, Martirosyan et al. (2019) performed LHDAC experiments in the $\text{MgCO}_3\text{-Fe}$ system combined with *in situ* synchrotron X-ray diffraction and *ex situ* transmission electron microscopy. Based on the results they suggest that the interaction of carbonates with Fe^0 or Fe^{0+} -bearing rocks can produce Fe-carbide and diamond, which can accumulate in the D'' region (the lowermost portion of the mantle that sits just above the molten iron-rich outer core).

Future Directions

Because of the pressure limitation of large volume presses, DAC experiments may be precious tools to understand the growth of superdeep diamonds in the lower mantle. Another potentially interesting approach is the use of dynamic compression experiments (i.e., laser-compressed materials), to generate diamonds at ultrahigh pressures and temperatures in order to study impact diamonds or the formation of diamonds in planetary interiors conditions (Kraus et al. 2017).

CARBIDES: SOURCES OF CARBON AND REDUCING AGENTS

There has been significant interest in exploring the possibility for iron carbides to act as both carbon sources and reducing agents since the general acceptance of the idea that depth-driven reduction in the Earth's mantle stabilizes Fe–Ni metal and carbide in C-bearing mantle regimes. Studies have examined interaction of carbides, particularly cohenite (Fe_3C), with oxides, silicates, carbonates, and sulfides, as can be seen in Table 11 below. Cohenite has proved to be an effective source of carbon upon reaction, usually forming metastable graphite. Growth of diamond is not typically observed in the absence of a melt. In many of the studies in Table 11, it is notable that the presence of melt in itself is insufficient, and diamond growth is inhibited until a sufficiently high temperature is achieved. In carbonate-bearing experiments, elemental carbon is produced by both breakdown of cohenite as well as reduction of CO_2 produced by decarbonation reactions involving the carbonate.

INCLUSIONS IN DIAMOND: EXPERIMENTAL CONSTRAINTS

Inclusions trapped during growth of synthetic diamonds at high pressure and temperature have been observed since the first syntheses in metallic melt solvents. In one of the early reports from the G.E. group, Bovenkerk (1961) stated "It has not been possible so far to grow diamond without trace inclusions." For industrial purposes, of course, inclusions are something to avoid or minimize (e.g., discussion in Sumiya et al. 2002). On the other hand, given that inclusions in natural diamonds provide valuable clues to the nature of the growth medium, it is of interest to deliberately try to grow diamonds with inclusions to see, for example, if the inclusions provide an accurate picture of the fluid or melt from which the diamond is growing. Early studies of synthetic diamond documented metal inclusions inferred to be from the growth medium (Lonsdale et al. 1959), and, intriguingly, coesite (Milledge 1961). The possibility of formation of single fluid inclusions during diamond crystallization in metal–carbon system was shown by Osorgin et al. (1987). Later work documented the presence of a rich diversity of inclusions (taenite, wüstite, spinel, silicate, diamond, and fluid) in synthetic diamond grown in the Fe–Ni–C system (e.g., Pal'yanov et al. 1997). In this study, the oxide and silicate inclusions resulted from diffusion of elements from the container materials and from impurities in the initial reagents. These examples suggested that detailed study of inclusions in diamond growing in other systems would be fruitful in exploring how representative these inclusions are of the growth medium.

As shown in Table 12, many studies report the presence of inclusions in passing, such as graphite (e.g., Pal'yanov et al. 1999b) and quenched melt, either reduced or oxidized—sometimes in the same experiment (Palyanov et al. 2013b), but there have been also some studies designed specifically to synthesize inclusion-bearing diamonds (e.g., Khokhryakov et

al. 2009; Bureau et al. 2012, 2016; Bataleva et al. 2016c). The first of these documented the rich variety of ways in which graphite inclusions in diamond can be formed; importantly it showed that graphite inclusions could form during growth of the diamond crystal from a carbonate melt—in the stability field of diamond. The others showed a good fidelity between the materials trapped as inclusions and those present in the environment in which the diamonds were growing. These studies provide a foundation for further studies on inclusion formation and trapping in a variety of media. For example, Bataleva et al. (2016c) suggested that slower growth rates would decrease the relative proportion of fluid or melt inclusions in the growing diamond, as had been previously documented for inclusions in magmatic minerals (Roedder 1984). Applying these methodologies to other growth media—such as the saline-rich endmember seen in natural fibrous diamonds—would be of considerable interest, as another example.

NITROGEN AND BORON STUDIES

Overview

Natural diamonds are known to contain impurities, the most common being nitrogen. The concentrations of nitrogen depend on the paragenesis and vary from below 10 ppm to > 3500 ppm (see Stachel et al. 2022b, this volume). Boron and hydrogen are also naturally present in the diamond lattice (Green et al. 2022, this volume).

Synthesis of commercial HPHT diamonds in, for example Fe–Co melts under standard synthesis conditions, contain ~100–300 ppm N in {111} growth sectors, and usually about half that in {100} growth sectors when grown under “standard conditions” (i.e., 1300–1400 °C, 5.5 GPa, Burns et al. 1999); lower growth temperatures can reverse this difference, and increase N contents up ~1000 ppm because of the decreased solubility of N in the melt at lower temperatures. In these syntheses, nitrogen is introduced as a contaminant in the starting materials, and its concentration in the diamond can be reduced by addition of so-called nitrogen “getters” such as Al, Ti, or Zr, which form nitrides at the experimental conditions.

In general, non-metallic solvents—carbonate, carbonate–silicate, sulfide, and sulfur—tend to crystallize diamond with higher (500–1500 ppm) N contents. Use of N-bearing compounds such as BN, NaN₃, Ba(N₃)₂, CaCN₂, Fe₃N, P₃N₅, or C₃H₆N₆ can produce diamond with >3000 ppm N (Table 13).

With the methodology for growing diamond with specific amounts of N, the next frontier is to use modern ion probe methods to examine N concentrations and isotopic compositions across diamond crystals, as pioneered by Reutsky et al. (2008b, 2017), for example. An attempt to find the interconnection between morphology and defect-impurity composition of diamond with its formation conditions was performed by Palyanov et al. (2021a).

Boron is another significant impurity found in diamonds, which gives them a blue color. Defined as Type IIb diamonds, they are very rare <0.1% of the worldwide extracted diamonds and naturally contain almost no N and up to 10 ppm B (Gailiou et al. 2012). Blue diamonds are synthesized for industry because B gives diamonds semi-conductive properties, given that significant amounts of boron (> 1000 at.ppm) can be incorporated in synthetic CVD diamonds (Polyakov et al. 2001). Synthetic boron-doped diamonds are also used as heaters either in large volume presses or in diamond anvil cells for HPHT experimentation (Shatskiy et al. 2009).

Table 11. Studies of diamond nucleation and growth in carbide-bearing systems.

Study	System	P (GPa)	T (C)	Duration	Seeds	Capsule/ buffering	Results
Palyanov et al. (2013b)	(Mg,Ca)CO ₃ -Fe ₃ C	7.5	1000–1400	60 h	Y	Pt	Graphite formed in all expts. GS at $\geq 1200^\circ$, SN at 1400° . Carb + oxide melt present in all diamond-forming expts. CM: {111} in carbonate-oxide melt
Bataleva et al. (2015b)	Fe ₃ C-S	6.3	900–1600	18–20 h	Y	Gr (mostly), Talc, MgO	Graphite formed in all expts. Al/T < 1200° , reaction 2Fe ₃ C + 3S ₂ \rightarrow 6FeS + 2C. At $\geq 1200^\circ$, formed melt + C. GS at 1400 – 1600° . Expts in talc and MgO capsules confirmed C production by breakdown of Fe ₃ C.
Bataleva et al. (2015a)	(Mg,Ca)CO ₃ -Al ₂ O ₃ - SiO ₂ -Fe	6.3, 7.5	1150–1650	8–20 h	N	Pt	CM: Growth form [111] on seed crystals. Formed Fe ₃ C and graphite in all expts. Subsolidus at 6.3 GPa 1150 – 1450° . At 7.5 GPa formed carb-silicate melt + graphite at 1450 – 1650° . No diamond SN reported, but no diamond seeds in expts. See paper for full phase assemblages
Bataleva et al. (2016a)	Fe ₃ C + Fe _{0.7} Ni _{0.3} S	6.3	1100–1500	20 h	Y	Gr	Graphite formed in all experiments. Cob + 2 liquids at 1100 – 1200° . One liquid + Gr at 1300 – 1500° with GS of diamond.
Bataleva et al. (2016e)	Fe ₃ C-Fe ₂ O ₃ , Fe ₃ C-Fe ₂ O ₃ -MgO-SiO ₂	6.3	900–1600	18–20 h	Y	Gr (mostly), Talc, MgO	CM: Growth form [111], regeneration of {100} \rightarrow {111} on seed crystals. Graphite formed in all expts in both systems, including those in talc or MgO capsules. Both systems subsolidus at 900 – 1300° . GS in presence of Fe-C liquid at 400 – 1600° in Fe ₃ C-Fe ₂ O ₃ , GS in presence of a Fe-C liquid at 1400° and two liquids (Fe-C and silicate-oxide) at 1500° and 1600° in Fe ₃ C-Fe ₂ O ₃ -MgO-SiO ₂ .
Bataleva et al. (2017)	Fe ₃ C-S, Fe ₃ C-FeS ₂ , Fe ₃ C-S-MgO-SiO ₂	6.3	900–1600	18–40 h	Y	Gr (mostly), Talc, MgO	CM: Growth form [111], regeneration of {100} \rightarrow {111} on seed crystals. Graphite formed in all experiments, including those in talc and MgO systems (Fe ₃ C-S, Fe ₃ C-S-MgO-SiO ₂ systems). GS at $\geq 1300^\circ$ in all three systems in presence of liquid(s), but no GS at 1200° despite presence of liquid(s).
Bataleva et al. (2018a)	Fe ₃ C-SiO ₂ -Al ₂ O ₃ -(Mg,Ca) CO ₃	6.3, 7.5	1100–1650	8–40 h	Y	Pt	CM: Growth form [111], regeneration of {100} \rightarrow {111} on seed crystals. Graphite formed in all expts. No Cob or carb at 6.3 GPa 1100 – 1500° , and diamond GS only at 1500° at 6.3 GPa where melt was seen in inclusions in garnet. At 7.5 GPa, GS seen in all expts (1250 – 1650°). Liquid present at $\geq 1450^\circ$. C formed from both carbide and decarbonation-produced CO ₂ . CM: {111} and {100}
Bataleva et al. (2018b)	Fe ₃ C-SiO ₂ -(Mg,Ca)CO ₃	6.3	1100–1500	20–40 h	Y	Gr	Graphite formed in all expts. Diamond GS only at 1500° , not at 1100 – 1400° . Fe-C melt present at $\geq 1300^\circ$. C formed from both carbide and decarbonation-produced CO ₂ . CM: {111} and {100}
Bataleva et al. (2018c)	Fe ₃ C-SiO ₂ -(Mg,Ca)CO ₃ , Fe ₃ C-SiO ₂ -Al ₂ O ₃ -(Mg,Ca) CO ₃	6.3	1300–1500	20 h	Y	Gr	Graphite formed in all expts. Diamond GS reported at 1400° (both systems) and at 1500° in the Al ₂ O ₃ -bearing system. Fe-C melt in all expts at least as inclusions in silicates. CM: {111} and {100}
Bataleva et al. (2018d)	Fe ₃ C-SiO ₂ -MgO	6.3	1100–1500	20–40 h	Y	Gr	Graphite formed in all expts; Fe-C melt present at $\geq 1300^\circ$. Diamond GS at 1500° . CM: {111} and {100}
Bataleva et al. (2019)	Fe ₃ C-(Mg,Ca)CO ₃ -S	6.3	900–1400	18–20 h	Y	Gr (mostly), Talc, MgO	Graphite formed in all expts; two immiscible liquids at $\geq 1100^\circ$. Diamond GS at $\geq 1400^\circ$ (including in MgO capsule). SN at $\geq 1400^\circ$ in Gr capsules. CM: {111} in both melts

Notes: SN – spontaneous nucleation and growth of diamond. GS – diamond growth on seeds. CM – diamond crystal morphology. Temperatures in Results column in °C.

Table 12. Studies of inclusion formation.

Study	System	P (GPa)	T (C)	Duration	Seeds	Capsule/ buffering	Results
Lonsdale et al. (1959)	G.E. synthetic diamonds						XRD identification of Ni inclusions in synthetic diamonds;
Milledge (1961)	G.E. synthetic						observation of other inclusions but were not able to identify
Osorgin et al. (1987)	Ni-Mn-C	5–6	1300–1400	2–8 h	No	talc	XRD identification of coesite inclusions in synthetic diamonds from GE
Pal'yanov et al. (1994, 1997)	Ni-Mn-C, Fe-Ni-C	5–6	1300–1600	1–150 h	Y		Fluid and metal-fluid inclusions (CO, H ₂ , N ₂)
Tonilenko et al. (1998)	Ni-Mn-C and Ni-Fe-C	5–6	1350–1550				Inclusions of taenite, wüstite, spinel, garnet, diamond, and hydrocarbon fluid
Pal'yanov et al. (1999b)	Li ₂ CO ₃ -Gr, Na ₂ CO ₃ -Gr, K ₂ CO ₃ -Gr, Cs ₂ CO ₃ -Gr	7	1700–1750	10 min–18.5 h	Y	Pt	Hydrocarbon fluid inclusions
Burns et al. (1999)							Graphite inclusions observed
Kanda (2000)	Metal solvent (Ni, Co, Fe)-catalyst (Cu, Mg) + Gr + NaCl	5	1500–1800	1–3 mg/h	Y		Summary of DeBeers syntheses. Discusses inclusion formation as function of solvent/catalyst composition, growth rates, synthesis <i>P, T</i> .
Pal'yanov et al. (2002a)	Na ₂ CO ₃ -Gr, K ₂ CO ₃ -Gr, Na ₂ CO ₃ -H ₂ O-Gr, K ₂ CO ₃ -H ₂ O-Gr, Na ₂ CO ₃ -CO ₂ -Gr, K ₂ CO ₃ -CO ₂ -Gr, Na ₂ CO ₃ -H ₂ O+CO ₂ (OAD)-Gr, K ₂ CO ₃ -H ₂ O+CO ₂ (OAD)-Gr	5.7	1150–1420	5–136 h	Y	Mostly Pt, 1 in Gr, 2 in Au	Notes use of Ti as N “getter” produces abundant TiC inclusions
Sumiya et al. (2002)	Fe-Ni + Gr	5.5	1300	12 min	?	?	Inclusions identified graphite, (FeNi) ₂₃ C ₆
Yin et al. (2002)	Ni _{0.7} Fe _{0.3} + Gr + Ti + B ₂ O ₃	5.5–6	1350–1450	80–120 h	N		Diamond nucleation and growth with inclusions of metallic solvent
Chepurov et al. (2007)	NaCl + H ₂ O + Gr, KCl + K ₂ CO ₃ + H ₂ O + Gr, Mg ₂ SiO ₄ + H ₂ O + Gr,	7.5	1500–1600	15–40 h			Examine formation of graphite inclusions. Found they formed by three mechanisms: 1) protogenetic (pre-existing graphite incorporated into growing diamond) in NaCl + C and Na ₂ CO ₃ + C systems.
Khokhryakov et al. (2009)	(Ca,Mg)CO ₃ + SiO ₂ + H ₂ O + CO ₂ + Gr, kimberlite + H ₂ O + CO ₂ + Gr						2) Syngenetic, forming during joint crystallization of diamond + graphite. Seen only in H ₂ O-bearing systems.
							3) Post-grown inclusions resulting from graphitization

Study	System	P (GPa)	T (C)	Duration	Seeds	Capsule/ buffering	Results
Palyanov et al. (2009)	S + Gr	6.3–7.5	1550–2000				Observed red and black inclusions, suggested to form from trapping of CS ₂ melt during growth
Palyanov et al. (2010b)	Ni _{0.7} Fe _{0.3} + Gr + Fe ₃ N and CaCN ₂	5.5	1400	65 h	N	MgO	Diamond growth with metallic inclusions
Tomlinson et al. (2011)	Fe _{0.9} Ni _{0.1} + Gr	15	2000	15 min	N	Re–Gr	Noted common occurrence of metal inclusions
Bureau et al. (2012)	MELD (SiO ₂ –Al ₂ O ₃ –TiO ₂ –(Ca,Mg,NB ₂ K ₂)CO ₃) + H ₂ O + Gr	7–9	1250–1700	10 min–144 h most	In Pt		Observed inclusions containing phengite or glass, sometimes with empty void in inclusion, and discrete empty inclusions. Voids and empty inclusions interpreted to have been fluid-filled before breach of inclusion wall during sample prep
Palyanov et al. (2012)	Ni _{0.7} Fe _{0.3} + Mg(OH) ₂ + SiO ₂ + Gr	6	1370	15 h	Y	Pt	Nucleation and growth on seeds, Observed inclusions of metallic solvent
Palyanov et al. (2013a)	Ni _{0.7} Fe _{0.3} + Gr + Mg(OH) ₂ + SiO ₂	6	1300–1370	15 h	N	Pt?	Diamond nucleation and growth inclusions of metal–carbon melt and metal-free fluids of hydrocarbon composition
Palyanov et al. (2013b)	Fe–(Mg, Ca)CO ₃	6.5, 7.5	1000–1400	8–60 h	Y	Pt	Diamonds in reduced part of sample contained inclusions of quenched Fe–C melt, those that grew in the carbonate melt contained carbonate inclusions
Zhimulev et al. (2013)	Fe–S + Gr	5.5	1350	21–25 h	Y	MgO	Metal–sulfide inclusions in diamonds led to fracture of the crystals
Palyanov et al. (2015)	Gp I kimberlite (Udachnaya–East), synthetic Gp. II kimberlite	6.3, 7.5	1300–1570	40 h	Y	Pt w/Gr liner	Alkaline carbonate–silicate melt and silicate (olivine and pyroxene) inclusions observed in polycrystalline diamond aggregates
Bataleva et al. (2016c)	SiO ₂ –(Ca,Mg)CO ₃ –(Fe,Ni)S	6.3	1650–1750	2–24 h	Y	Gr	Study designed to trap inclusions during diamond growth. Inclusions of gr, carb–silicate liquid and sulfide liquid, opx, diamond, and CO ₂ -rich fluid. Inclusions characterised by Raman spectroscopy. Abundant inclusions of melt and fluid attributed to high growth rate of diamond
Bureau et al. (2016)	MELD + H ₂ O + NaCl + Gr, MELD + FeCO ₃ + H ₂ O ± NaCl + Gr	7	1300–1400	6–30 h	Y	Pt or Au/Pd	Observed both monocrystalline, pure fluid, and multi-phase inclusions of same mineralogy as found in matrix: diam, carbonate, phengite, coesite, rutile in MELD expts, olivine + carbonate in MELD + FeCO ₃ expts
Khokhryakov et al. (2016)	Na ₂ C ₂ O ₄ –CaCN ₂	6.3	1500	2, 30 h	Y	Pt	Carbonate inclusions inferred from IR spectra
Palyanov et al. (2016)	Na ₂ C ₂ O ₄ ± Gr	6.3, 7.5	1250–1700	10–66 h	Y	Pt	Inclusions of Na–carbonate melt identified by Raman.
Smith and Wang (2016)	HPHT diamonds						Peaks for CO ₂ interpreted as having exolved from melt on cooling
Bataleva et al. (2019)	Fe–(Mg,Ca)CO ₃ –S	6.3	1500, 1600	18 h	Y	Gr	Found CH ₄ and H ₂ coexisting with metallic inclusions in commercially grown HPHT diamonds
							Reported inclusions of magnesiostilbite, graphite, sulfide, and carbonate

Notes: MELD – average inclusion composition from Navon et al. (1988).

Table 13. Studies of nitrogen and boron incorporation into diamond.

Study	System	P (GPa)	T (C)	Duration	Seeds	Capsule/ buffering	Results
Kanda and Yamaoka (1993)	Co + Gr	6	~1500	12–18 h	?	?	Grew diamond w/ ~200 ppm N, found heterogeneous distribution of A and C centres
Sumiya and Satoh (1996)	Ni + Gr, Ni–Fe + Gr, Co–Fe + Gr						Review paper of diamond growth in metallic melts. Discusses nitrogen getters to reduce N to <0.1 ppm and techniques for minimizing B
Fisher and Lawson (1998)							N concentrations from ~170–455 ppm. Examined effect of Ni concentration on N aggregation in synthetic diamonds, mostly in {111} growth sectors
Burns et al. (1999)	Co–Ti, Fe–Al, Fe–Co, Fe–Al–B						Review of DeBeers research; N contents (ppm) reported as <0.01–2 for Co–Ti, 0.4–1 for Fe–Al, 100–1000 for Fe–Co, below detection for Fe–Al–B solvent/catalysts. Note that addition of B in addition to N getter to solvent/catalyst allowed growth of blue Type IIb diamonds; higher concentrations in {1111} than in {100}. Colour depends on BN/GS at ≥1600°, SN at ≥1700°, 100% conversion at 1850°, decreasing to <1% at 1700°. N up to ~3300 ppm
Borzov et al. (2002)	Fe ₃ N + Gr	7	1550–1850	20 h	Y	Gr	
Pal'yanov et al. (1998b)	Ni–Fe + Gr	5.5–6.5	1500–1600	100–150 h	Y	?	
Kanda et al. (1999)	Na ₂ SO ₄ + Gr	7.7	2000	30 min	N	Gr, surrounded by NaCl–ZnO ₂ or BN	Grew diamond with 1200–1900 ppm N with BN container, ~200 ppm N with NaCl–ZrO ₂
Kanda (2000)							Review paper; discusses B and N in HPHT synthetic diamonds grown in metallic systems
Pal'yanov et al. (2001a)	S + Gr	7	1750–1850	3–7 h	Y	Gr	Up to 700 ppm N
Pal'yanov et al. (2002b)	MgCO ₃ + SiO ₂ , MgCO ₃ + Na ₂ CO ₃ + SiO ₂ , No Gr. High <i>H</i> ₂ from TiH _{1.9} in sample assembly	6–7	1350–1800	10–43 h	Y (in most) from TiH _{1.9} in sample assembly	Pt, high/ <i>H</i> ₂ ceramic	300–800 ppm N in diamonds from 1750–1800° expmts at 7 GPa, both starting materials
Liang et al. (2005)	Fe–Ni + NaN ₃ + Gr	5–5.8	1230–1480	15 min	N	ceramic	N conc varied from 500 to ~2000–2500 ppm with increasing NaN ₃ from 0–0.5 wt.%
Liang et al. (2006)	Fe–Ni + NaN ₃ + Gr	5–5.8	1230–1480	15 min	N	ceramic	N conc varied from 350–500 to 1700–2000 ppm w/ increasing NaN ₃ from 0–0.5 wt.%

Study	System	P (GPa)	T (C)	Duration	Seeds	Capsule/ buffering	Results
Palyanov et al. (2006)	(Fe,Ni) ₉ Si ₆ + Gr	7	1900	16, 40 h	Y Gr		~1000 ppm N
Chepurov et al. (2007)	Fe–Ni–C, Fe–Co–C + Ti + B ₂ O ₃	5.5–6	1350–1450	80–120 h	N Pt?		Growth of Type IIb boron-bearing monocrystalline diamonds. Almost no N
Palyanov et al. (2007b)	MgCO ₃ –SiO ₂ –Al ₂ O ₃ –FeS	6.3	1650, 1700	23.5 h 8 h	Y MgO+ Gr		Measured diamonds formed in two expts, both with ~1500 ppm N
Zhang et al. (2007)	Gr + Fe _{0.9} Ni _{0.1} + boron	5.4–5.6	1550–1700 K		N		Growth of large monocrystals of Type IIb diamonds
Reutsky et al. (2008b)	Fe–Ni + Gr	5.5	1450	90 h			SIMS study. Observed zoning in N across diamond. Also measured N isotopes Reported up to 850 ppm N in diamonds from carbonate-bearing expts
Spivak et al. (2008)	Fe–Ni + Ba(N ₃) ₂ + Gr	5–5.7	1230–1430	13 min	?		Report N conc varied from 200–400 to 1600–2400 ppm as Ba(N ₃) ₂ increased from 0 to 0.5 wt.%
Yu et al. (2008)	Fe–Co–Ni + NaN ₃ + Gr	5.4	1200	2–20 h	N pyrophyllite		Reported up to 1520 ppm N
Zhang et al. (2008)	Fe–Co–Ti + NaN ₃ + Gr						N contents: 133 ppm in Fe–Co, 121 ppm in Fe–Co–Ti
Chepurov et al. (2009b)	Fe–Co + Gr, Fe–Co–TiO ₂ + Gr, Fe–Co–Ti + Gr	5.5	1400	46–69 h	Y ?		9 ppm in Fe–Co–Ti
Palyanov et al. (2009)	S + Gr	6.3–7.5	1550–2000	3–40 h	Y Gr		≤ 10–1500 ppm N found
Shatskiy et al. (2009)	B + graphite mixture	20	1600		MAP		Growth of B-doped diamond to use them as heaters at HT (>3000°)
Palyanov et al. (2010b)	Fe–Ni + Gr, Fe ₃ N and CaCN ₂ N sources	5.5	1400	65 h	Y MgO	127–1077 ppm N with varying amounts of Fe ₃ N; 124–850 ppm N with varying CaCN ₂	
Huang et al. (2010a)	Ni–Mn–Co + NaN ₃ + Gr	~5.5	1240–1300	?	Y pyrophyllite	N conc ~200 to ~1250 ppm w/ increasing NaN ₃ from 0 to 0.8 wt.%	
Huang et al. (2010b)	Fe–Ni–Co + NaN ₃ + Gr	~5.5	~1230–1280	11 h	Y ceramic material	Report range of N conc from 700–750 ppm to 1671–1742 ppm N w/ increasing NaN ₃ from 0.3 to 0.6 wt.%	
Liu et al. (2011)	Carbonyl iron powder + Gr	5.2–6.8	1200–1800	10–20 min	?		Report 1100–1500 ppm N in diamond grown in carbonyl iron + Gr system
Palyanov et al. (2012)	Ni ₇ Fe ₃ + Mg(OH) ₂ + SiO ₂ + Gr	6	1370	15 h	Y MgO	Observed decrease in N from 220–230 ppm to 40–50 ppm with increasing H ₂ O in melt	
Zhang et al. (2012)	Fe–Ni + P ₃ N ₅ + Gr	5–6.3	1250–1550	15 min	N ?	Report N conc varied from 200–400 ppm to 1300–1600 ppm as P ₃ N ₅ increased from 0 to 0.4 wt.%	

Study	System	P (GPa)	T (C)	Duration	Seeds	Capsule/buffering	Results
Palyanov et al. (2013b)	Fe-(Mg,Ca)CO ₃	6.5, 7.5	1000–1400	8–60 h	Y	Pt	Diamonds grown in metal-carbon melt contained 100–200 ppm N, diamonds formed in carbonate melt had 1000–1500 ppm N
Liu et al. (2016)	Fe–Ni + Gr, Fe–Ni–Co + Gr. P ₃ N ₅ or C ₃ H ₆ N ₆ as N source	5–6.3	1300–1650	15 min–30 h	Y	MgO	N cone up to ~2300 ppm in FeNi-C + P ₃ N ₅ , up to ~3400 ppm in FeNiCo-C + C ₃ H ₆ N ₆
Khokhraykov et al. (2016)	Na ₂ C ₂ O ₄ + CaCN ₂	6.3	1500	2, 30 h	Y	Pt	No nucleation in 2 h expt. SN in 30 h expt. Found variable N content (100–1100 ppm) depending on growth direction
Palyanov et al. (2016)	Na ₂ C ₂ O ₄	6.3, 7.5	1300–1700	10–66 h	Y	Pt	50–150 ppm N in Na ₂ C ₂ O ₄ expts compared to 100–200 ppm N in Na ₂ CO ₃ + Gr expts
Reusky et al. (2017)	Na ₂ C ₂ O ₄	6	1400			Pt	SIMS study of carbonate-grown diamonds observed difference in conc of N between {111} and {100} of ~20x
Chen et al. (2018)	Fe–Ni + Al + NaN ₃ + Gr	5.8	1380–1400	?	Y	ZrO ₂ –MgO	Found N decreased with Al content: 80 ppm w/o Al, 28 ppm w/10% Al, <1 ppm N w/ 20% Al. Found N linearly increases from 372–1573 ppm w/ increasing NaN ₃ from 0.1–0.5%
Sokol et al. (2019)	Fe ₃ N + FeS	7.8	1600–1800	30–60 min	?	BN + Gr	Report 2100–2600 ppm N and 130–150 ppm B in diamond in equilibrium w/ BN
Palyanov et al. (2020b)	Ni ₇ Fe ₃ + Fe ₂ O ₃ + Gr	6	1400	40 h	Y	MgO	Found N increases from 200–250 ppm w/ no O additive to 1100–1200 ppm w/ 10 wt.% O

Notes: GS – diamond growth on seeds, SN – spontaneous nucleation and growth of diamond MAP – Multi-anvil press. Temperatures in *Results* column in °C.

Future directions

The growth of diamonds with or without impurities is of great importance for understanding the mechanisms at depth in the Earth. For example, experiments performed by Palyanov et al. (2013b) show that simultaneous diamond growth in metal-rich and in carbonate-rich parts of the same capsule would form diamonds containing only 100–200 ppm N when in contact with metallic Fe, whereas those formed in the carbonate melt zone contain 1000–1500 ppm N. This difference is explained by the siderophilic affinity of N to metallic liquids at high P, T conditions. The occurrence of Type II diamonds may be explained by growth in the presence of metallic melts (Smith and Kopylova 2013). Further experimental studies are necessary to confirm such a hypothesis.

CARBON ISOTOPE STUDIES

In general, the bulk carbon isotope composition of HPHT diamonds solely depends upon the initial carbon isotope composition of the diamond-forming system. All the diamonds from HPHT experiments have $\delta^{13}\text{C}$ in a range from –20 to –30‰ PDB, which is inherited from the initial graphite sources used for synthesis (Hoering 1961; Laptev et al. 1978; Ivanovskaya et al. 1981; Taniguchi et al. 1996; Reutsky et al. 2008a, 2015a) (Table 14). In the film-growth (FG) experiments, no significant isotope inhomogeneity is reported for produced diamond material (Hoering 1961; Laptev et al. 1978; Ivanovskaya et al. 1981). When the temperature gradient growth (TGG) method is used, carbon isotope fractionation, which accompanied the diamond crystallization from carbon solution in metal melt, produces a certain isotope profile in the direction of crystal growth (Reutsky et al. 2008a,b). In Fe-Co+Gr, Fe-Ni+Gr and Fe+Gr systems, the carbon isotope fractionation coefficients at 5.5 GPa and 1400–1500°C are the same and vary from about 2.0 to 4.5‰ (Reutsky et al. 2008b). Therefore, within the distance of 1.5 mm from the seed these diamond crystals show gradual decrease of $\delta^{13}\text{C}$ on a scale of 2–4‰, followed by slight fluctuation around carbon isotope composition of initial graphite (Reutsky et al. 2008a). In the metal–carbon systems the $\delta^{13}\text{C}$ of diamond always equal or higher than $\delta^{13}\text{C}$ of the initial graphite. The carbon isotope fractionation coefficients associated with diamond growth are strongly depends on the linear growth rate and may vary from 0 to 4.5‰ (Reutsky et al. 2012).

Carbon isotope fractionation was also studied in the $\text{NaCO}_3+\text{CO}_2+\text{C}$ model system with a single carbon source also studied (Reutsky et al. 2015a). The carbon isotope fractionation in those experiments show opposite direction, compared to metal–carbon systems, and the diamond here is always depleted in heavy (^{13}C) isotope in comparison with carbonate– CO_2 fluid, exactly as expected from calculations of isotope equilibrium (e.g., Richet et al. 1977). At 7.5 GPa temperature-dependence of carbon isotope fractionation coefficient was determined as the function: $\Delta_{\text{Carbonate fluid-Diamond}} = 7.38 \times 10^6 \times T^{-2}$ and established to be dependent on carbonate: CO_2 ratio in the fluid (Reutsky et al. 2015a). The scale of this depletion is comparable to that documented for metal–carbon systems and reaches 4‰. Later work on diamond experimental crystallization from carbonate–silicate–water fluid reveal a similar estimate of fluid/diamond carbon isotope fractionation at 7 GPa and 1400°C (Bureau et al. 2018).

Detailed investigation of different crystallographic sectors of HPHT diamonds reveal surface-controlled carbon isotope distribution within diamond crystals showing higher isotope fractionation on faces {100} in comparison with face {111} (Reutsky et al. 2017). This is supported by ab-initio calculations and provide explanation of systematic isotope lightening of growth sectors {100} relative to {111}.

Useful information on diamond growth can be obtained from investigation of paired carbon and nitrogen isotope fractionation during diamond growth in certain crystallographic directions using high spatial resolution technique such as secondary ion mass spectrometry.

Table 14. Studies of carbon isotope fractionation at HPHT diamond crystallization.

Study	System	P (GPa)	T (°C)	Duration	Seeds	IRMS technique	Results
Hoering (1961)	Metal melt + Gr	7	1700		N	Bulk combustion	Presumably FG. No difference of carbon isotope composition between starting graphite and bulk diamond is observed
Laptev et al. (1978)	Fe + Gr	4,5	1100–1200		N	Bulk combustion	Same result
Ivanovskaya et al. (1981)	Fe–Mn + Gr	10	1500			Bulk combustion	Same result
Boyd et al. (1988)	6,5	1800			G	Bulk combustion	Slight but analytically significant 0.6‰ heterogeneity across the crystal
Taniguchi et al. (1996)	Metal melt + Gr	?	?			Bulk combustion	Bulk diamond inherits $\delta^{13}\text{C}$ of initial graphite.
Arima et al. (2002)	K ₂ Mg(CO ₃) ₂ + Si	9–10				Bulk combustion	No influence of carbonate carbon was recognized
Reutsky et al. (2008a)	CaMg(CO ₃) ₂ + Si	7,7	1800	60 m	N	Bulk combustion	Broad correspondence of the resulting diamond composition to initial carbonate $\delta^{13}\text{C}$.
Reutsky et al. (2008b)	Fe–Ni + Gr; Fe–Co + Gr	5,5	1450	17.5 h	N	Bulk combustion	Used for carbon source verification
Reutsky et al. (2008b)	Fe–Ni + Gr	5,5	1450	90 h	G	SIMS	TGG: 3.2‰ difference between very last portion of diamond and residual carbon in quenched metal melt was documented
Satish-Kumar et al. (2011)	Fe + Gr	5,0	1200–2100	0.5–15 h	N	Bulk combustion	Detailed carbon isotope profiles along growth sectors of different crystal faces documented for the first time. Partition coefficients for carbon isotopes were obtained for {100} and {111} sectors of growth. Influence of diamond growth rate for particular crystal faces was recognized
Reutsky et al. (2012)	Fe–Ni + Gr	5,5	1450	17.5–160 h	N	Bulk combustion	C isotope fractionation between diamond and carbon solution in metal melt is determined
Palyanov et al. (2013b)	Mg _{0,9} Ca _{0,1} CO ₃ + Fe ⁰	6,5	1350–1550	8–60 h	N	Bulk combustion	Influence of linear growth rate to the carbon isotope partition coefficient in the metal–carbon system at HPHT was documented. Correspondence of observed relation to Burton–Prim–Slichter model was established
Reutsky et al. (2015b)	Fe–Ni + Gr	6,3	1600–1400	5 h	N	Bulk combustion	Up to 6.5‰ carbon isotope fractionation at diamond-producing redux interaction of carbonate and metal iron
Reutsky et al. (2015a)	Na ₂ C ₂ O ₄	6,3, 7,5	1300–1500, 1400–1700	10–40 h	N	Bulk combustion	Distribution of carbon isotopes between metal melt, crystalline Fe ₃ C and diamond near the peritectic point was established
Reutsky et al. (2017)	Na ₂ C ₂ O ₄	6	1400		G	SIMS	C isotope effect for carbonate–CO ₂ interaction in a sodium carbonate fluid at experimental P/T is close to 3‰. The carbon isotope fractionation at diamond crystallization from a carbonate fluid at 7.5 GPa decreases with increasing T based on the function: $\Delta_{\text{Carbonate fluid-Diamond}} = 7.38 \times 10^6 \times T^2$
Reutsky et al. (2018)	(Mg,Ca)CO ₃ + Fe	6,5	1550	10 h	N	SIMS	Surface induced C isotope fractionation during diamond crystallization was established from observed difference between {111} and {100} supported by ab-initio calculations
							A set of diamond crystals ranges in $\delta^{13}\text{C}$ from -0.5 to -17.1‰ was collected from a single experiment of carbonate–metal iron interaction with the single carbon source (initial carbonate $\delta^{13}\text{C} = +0.2\text{\textperthousand}$), establishing huge kinetic carbon isotope fractionation at redux interaction at P/T conditions of diamond stability

DIAMOND DISSOLUTION EXPERIMENTS

Overview

Natural diamonds exhibit various surface textures, acquired during their history and corresponding to growth and dissolution events. For a long time, the dissolution textures were attributed to the effect of the kimberlite melts while diamonds were brought up to the surface (Robinson 1979), and eventually to later secondary processes mostly due to transport and erosion.

Experimental studies evidenced that resorption features are also acquired from mantle-stable corrosive fluids when diamonds are residing at depth (Table 15). In the studies of Chepurov et al. (1985) and Khokhryakov and Pal'yanov (1990), it was experimentally demonstrated for the first time that dissolution of flat-faced diamonds in water-bearing melts results in the formation of rounded crystals, with morphology identical to natural dodecahedroids and octahedroids. The reader is invited to read the detailed review of Fedortchouk (2019), which combines the observation of the morphology of natural diamonds with the description of dissolution and etching experiments, and demonstrates the usefulness of the experimental approach. It is shown that the shape and size of the etch pits on diamond surface depends on the temperature and H₂O/CO₂ ratio in the fluid, whereas pressure affects the efficiency of diamond crystal shape transformation from octahedral into rounded resorbed forms. Thanks to experiments, the identification of resorption produced in the mantle source from that in the kimberlite magma is possible.

Resorption processes possibly occur in between multiple growth events, such as observed in fibrous diamonds (Klein-BenDavid et al. 2007), recently it was proposed that such corrosive mantle fluids would likely be of "melt" nature (Fedortchouk et al. 2019). Surprisingly, it is also observed that both dissolution and growth may occur in very similar fluids/melts, such as in the system carbonate–silicate enriched in H₂O–CO₂ (Khokhryakov and Pal'yanov 2007a). Growth and dissolution events may alternate during diamond formation, possibly depending on carbon saturation, water versus CO₂ proportions, or redox conditions.

Future directions

More experiments are necessary to decrypt the complexity of diamond's histories and to understand the sequence of growth and dissolution events that may occur to diamonds from their birth in the mantle to the exposure to the near surface.

CONCLUSIONS

As can be seen from the preceding sections, there has been an impressive body of experimental work related to diamond formation over the past decades. The widespread adoption of experimental apparatus such as the belt, the multi-anvil, and the laser-heated diamond-anvil systems have allowed researchers to access the necessary *P, T* space to address a variety of questions with respect to diamonds. It should be noted that the experimental data reviewed here are not always in unambiguous agreement with each other. This is largely resulting from the use in different scientific groups of different equipment and methods for preparing and conducting experiments.

Building on the work done in industrial laboratories growing diamonds in a variety of metal melts, the ability of a rich variety of fluids and melts, including those possibly stable in the Earth's mantle, to mediate crystallization of diamond has been firmly established. Actually, growing diamonds in these melts or fluids allows researchers to address questions such as isotopic fractionation during diamond growth and the incorporation of impurities into a growing diamond, which will provide valuable constraints to understanding the formation of diamonds in nature.

Table 15. Studies of diamond resorption.

Study	System		P (GPa)	T (C)	Duration	Seeds	Capsule/ buffering	Results
Evans and Sauter (1961)	Air and gas mixtures (O_2 , N or Ar, H_2O)		RP	800–1400	5 min–16 h	Y	Tubes	Diamond etching and graphitization
Evans and Phaal (1962)	O_2		RP	650–1350	?	Y	Silica and alumina	Diamond oxidation (dissolution) and etching
Davies and Evans (1972)	Air		RP and 4.8 and	1850–2000	Up to 200 min	Y	Pt	Diamond graphitization
Harris and Vance (1974)	Natural Kimberlites		RP and 0.1	1950–2200	30 min–24 h	Y	G, Pt and Ag/Pd	Vacuum graphitization and etching by degassing volatiles from natural kimberlite powder
Kanda et al. (1977)	H_2O		RP and 5	900–1600	5–30 min	Y	Pt	Etching of natural diamond octahedron
Yamaoka et al. (1980)	$Fe-O, Mn-O+ SiO_2$		1.5–4	1100–1500	5 min–5 h	Y	Pt, Mn and Fe oxide-based oxygen buffers	Shape of etching pits from redox conditions
Chepurov et al. (1985)	Alkaline basalt melt $\pm H_2O$		2.5	1300–1500	0.5–4 h	Y	Pt	Influence of H_2O on the shape of diamond dissolution
Cull and Meyer (1986)	$CO-CO_2$		RP	900–1000	12–48 h	Y	Pt/O_2 QFM–NNO	Diamond oxidation
Khokhryakov and Palyanov (1990)	Alkaline basalt melt $\pm H_2O$ $\pm CO_2$, lamprite melt		2.5–5.5	1100–1450	5–180 min	Y	Pt	Different resorption morphologies
Arima (1998)	Kimberlite melts		2.5	1300–1500	10–240 min	Y	Pt	Diamond resorption
Khokhryakov and Palyanov (2000)	$CaCO_3$		7.0	1700–1750	5 h	Y	Pt	Diamond dissolution
Sonin et al. (2000)	Air		RP	700–1200	5–120 min	Y	Pt crucible, HM, NNO, CCO buffers	Diamond oxidation and etching at temperature and for various oxygen fugacities
Khokhryakov et al. (2001)	$Na_2CO_3, CaCO_3, MgCO_3, CaMgSi_2O_6 + H_2O$		5.7	1400	10 min–40 h	Y	Pt	Diamond dissolution, evolution of crystal morphology

Study	System	P (GPa)	T (C)	Duration	Seeds	Capsule/ buffering	Results
Sonin et al. (2001)	Alkaline basalt melt	3	1300	30–90 min	Y	Pt	Diamond etching
Khokhryakov et al. (2002)	$\text{Na}_2\text{CO}_3 + \text{Fe}_2\text{O}_3$, $\text{Ag}_2\text{CO}_3, \text{H}_2\text{O}$, $\text{Ti}, \text{MgO} + \text{Ti}$	5.7	1400	1–20 h	Y	Pt, various $\text{O}_2/\text{H}_2\text{O}$ buffer	Diamond dissolution, effect of redox
Sonin et al. (2003)	Silicate melt–C–O–H–S	3	1300	15–30 min	Y	Pt (MAP)	Etching
Zhimulev et al. (2004)	Mantle xenoliths (dunite, eclogite, herzolite) + C–O–H fluid	5.5–6	1450–1500	1 h	Y	Pt (MAP)	Diamond etching
Kozai and Arima (2005)	Kimberlite, lamproite melts+ $\text{CaMg}(\text{CO}_3)_2$	1	1300–1420	20–600 min	Y	Pt/IW, MW, HM buffers	Dissolution
Khokhryakov and Palyanov (2006)	KNO_3 and NaNO_3 melts	RP	600–900	5–60 min	Y	alundum crucible	Dislocation etching
Sonin et al. (2006)	Basaltic melt	RP	1130	30–60 min	Y	HM NNO buffers	Etching at various oxygen fugacities
Fedoritchouk et al. (2007)	Kimberlite melt, Carbonate melt, Alkaline basalt+brucite and CaCO_3 and SiO_2	1	1150–1500	6 min	Y	Pt	Graphitization or resorption, depending on the fluid phase: H_2O and CO_2 (no reaction with the melt)
Khokhryakov and Palyanov (2007a)	$\text{CaMg}(\text{CO}_3)_2, \text{CaCO}_3$, $\text{CaMgSi}_2\text{O}_6$, kimberlite + H_2O	5.7	1400	0.17–37 h	Y	Pt	Diamond dissolution, evolution of crystal morphology
Khokhryakov and Palyanov (2007b)	NaNO_3 and KNO_3 melts	RP	750–800	5–60 min	Y	alundum crucible	Etching to detect planar defects
Arima and Kozai (2008)	Natural and synthetic kimberlite and MgCO_3	1–2.5	1300–1500	3–600 min	Y	Pt + H_2O IW buffer	Dissolution
Sonin et al. (2008)	NaCl and NaF melts	RP	1300–1350	30–120 min	Y	Pt	Etching
Sonin et al. (2009)	Alkali basalt + NaCl , NaF	3	1350	30 min	Y	Pt	Etching
Fedoritchouk and Canil (2009)	Gas mixtures: $\text{CO}-\text{CO}_2$	RP	1000–1100	10 min–17 h	Y	Pt	Variable $/\text{O}_2$ from –9.5 to –16.1 Diamond oxidation, morphology depending on the fluid

Study	System	P (GPa)	T (C)	Duration	Seeds	Capsule/ buffering	Results
Khokhryakov and Palyanov (2010)	$\text{Na}_2\text{CO}_3, \text{CaCO}_3, \text{CaMg(CO}_3\text{)} \pm \text{H}_2\text{O} \pm \text{CO}_2$	5.7–7.5	1400–1750	1–37 h	Y	Pt	Influence of fluid composition on the form of diamond dissolution
Sonin et al. (2010)	NaCl, Ca(OH)_2	3	1350	30–120 min	Y	Pt	Diamond etching
Khokhryakov et al. (2014)	KNO_3	RP	700	5–60 min	Y	alundum crucible	Effect of N impurity on etching
Khokhryakov and Palyanov (2015b)	KNO_3	RP	700	15–60 min	Y	alundum crucible	Effect of N impurity on etching
Fedoritchouk (2015)	H ₂ O-rich CO ₂ -rich	1	1150–1350	2240–2880 min	Y	Pt	Diamond resorption
Khokhryakov and Palyanov (2015a)	H ₂ O-carbonate melts (CaCO_3)	5.7	1300	30–45 h	Y	Pt	Dissolution of block diamond crystals
Sokol et al. (2015)	Kimberlite and carbonatite melts $\pm \text{H}_2\text{O}$	6.3	1400	0.5–10 h	Y	Pt \pm Re foil, Re-ReO ₂ and HM buffers	Dissolution and resorption of diamond as indicators for redox of resorption
Zhang et al. (2015)	$\text{H}_2\text{O} \pm \text{MgO} \pm \text{SiO}_2$	1–3	1150–1400	60–4320 min	Y	Pt	Shape and size of the etching pits depends on temperature and fluid composition
Zhimilev et al. (2016)	$\text{Fe}_{0.7}\text{S}_{0.3}$ melt	4	1400	1 h	Y	ZrO_2, CaO , and MgO	Diamond resorption
Sonin et al. (2018b)	$\text{Fe}_{0.7}\text{S}_{0.3}$ melt	4	1400	1 h	Y	ZrO_2, CaO , and MgO	Diamond resorption
Sonin et al. (2018a)	Fe melt + S in various amounts	3.5	1400	1 h	Y	MgO	Diamond dissolution
Chepurov et al. (2018)	Fe–S melt + kimberlite	4	1400	1 h	Y	MgO	Resorption in metal-sulfide-silicate melt
Khokhryakov et al. (2018)	Mg–Si–C	7–7.5 RP	1800, 700	30 min 5 min	Y	alundum crucible	Growth and selective dislocation etching
Khokhryakov and Palyanov (2018)	Carbonate melts H ₂ O-carbonate-silicate melts Sulfide melts	5.7–7.5	1100–2000	0.5–5 h	Y	Pt and G	Dissolution and graphitization as indicators of the sectorial structure of crystals

Study	System	P (GPa)	T (C)	Duration	Seeds	Capsule/ buffering	Results
Fedoritchouk et al. (2019)	MgO-H ₂ O(-CO ₂) MgO-SiO ₂ -H ₂ O(-CO ₂) CaO-MgO-SiO ₂ -CO ₂ (-H ₂ O) CaO-MgO-CO ₂ (-H ₂ O)	6	1200-1500	0.5-6 h	Y	Pt	Different resorption morphologies Only metasomatism by melts is destructive
Gryaznov et al. (2019)	Fe-Ni-S melts	3.5	1400		Y	MgO	Dissolution features due to metallic melts in the mantle
Khokhryakov et al. (2020)	Kimberlite melt + H ₂ O	6.3	1400	10 h	Y	Pt + Re foil, Etching and dissolution, used as indicators for redox of resorption Re-ReO ₂ and HM buffers	

Notes: RP – room pressure, MAP – Multi-anvil press, min – minutes, h – hours, G – graphite.

Where to from here?

Despite all our collective efforts, some fundamental questions remain. For example, what triggers diamond formation? What is the carbon source, what is the nature of the diamond's parents: fluids, melts, supercritical fluids? Is it depending on tectonic setting, or only on depth? How can we use the incorporation of impurities in diamonds to identify their growth mechanisms?

The experimental studies modeling slab-mantle reactions, whereby carbonate-bearing lithologies—representing subducted slab material—interact with reduced, metal-bearing mantle collectively are an excellent example of addressing a process question. But is this how all diamonds form? Classic models of diamond formation by, for example, oxidized fluids or melts interacting with reduced (but metal-free) mantle, or vice-versa, remain elusive to test experimentally. Other models, such as diamond formation by decompression or cooling of fluids (Stachel and Luth 2015), by partial melting in the presence of a hydrous, carbon-bearing fluid (Luth 2017; Smit et al. 2019), by pH changes in a fluid interacting with different mantle lithologies (Sverjensky and Huang 2015), under the influence of an electric field (Palyanov et al. 2021b), or by mixing of different fluids or melts (e.g., Huang and Sverjensky 2020) await experimental testing as well. There are still many experiments to perform to understand the growth of super deep diamonds in the transition zone and lower mantle. Another challenge for the future is the use of diamond growth to understand the mechanism of inclusions trapping: protogenetic versus syngenetic, or synchronous (Nestola et al. 2017) and thereby to provide information to properly decipher the complex messages delivered by inclusions about the deep Earth mineralogy and chemistry.

To conclude, there is still work to do! We need the experimental approach, in constant interactions with the study of natural diamonds and with models, to map the cartography of diamond growth at any depth into the Earth.

ACKNOWLEDGMENTS

The authors gratefully acknowledge support for their research from their respective funding agencies: NSERC Discovery Grants (RWL), Russian Science Foundation under grant no. 19-17-00075 and state assignment of IGM SB RAS (YNP), and the program Emergences 2019 Sorbonne-Université, CNRS, contract 193256 Hydrodiam (HB). Thorough and constructive reviews by Yana Fedortchouk and an anonymous reviewer significantly improved the manuscript. Finally, the patience of the editors was much appreciated.

REFERENCES

- Akaishi M, Yamaoka S (2000) Crystallization of diamond from C–O–H fluids under high-pressure and high-temperature conditions. *J Cryst Growth* 209:999–1003
- Akaishi M, Kanda H, Yamaoka S (1990a) Synthesis of diamond from graphite–carbonate system under very high temperature and pressure. *J Cryst Growth* 104:578–581
- Akaishi M, Kanda H, Yamaoka S (1990b) High pressure synthesis of diamond in the systems of graphite-sulfate and graphite-hydroxide. *Jpn J Appl Phys* 2 29:L1172–L1174
- Akaishi M, Yamaoka S, Ueda F, Ohashi T (1996) Synthesis of polycrystalline diamond compact with magnesium carbonate and its physical properties. *Diamond Relat Mater* 5:2–7
- Akaishi M, Shaji Kumar MD, Kanda H, Yamaoka S (2000) Formation process of diamond from supercritical H₂O–CO₂ fluid under high pressure and high temperature conditions. *Diamond Relat Mater* 9:1945–1950
- Akaishi M, Shaji Kumar MD, Kanda H, Yamaoka S (2001) Reactions between carbon and a reduced C–O–H fluid under diamond-stable HP-HT condition. *Diamond Relat Mater* 10:2125–2130
- Arefiev AV, Shatskiy A, Podborodnikov IV, Litasov KD (2019) The K₂CO₃–CaCO₃–MgCO₃ system at 6 GPa: Implications for diamond forming carbonatitic melts. *Minerals* 9:558
- Arima M (1998) Experimental study of growth and resorption of diamond in kimberlitic melts at high pressures and temperatures. *Int Kimberlite Confer: Extended Abstr* 7:32–34

- Arima M, Kozai Y (2008) Diamond dissolution rates in kimberlitic melts at 1300–1500 °C in the graphite stability field. *Eur J Mineral* 20:357–364
- Arima M, Kozai Y, Akaishi M (2002) Diamond nucleation and growth by reduction of carbonate melts under high-pressure and high-temperature conditions. *Geology* 30:691–694
- Arima M, Nakayama K, Akaishi M, Yamaoka S, Kanda H (1993) Crystallization of diamond from a silicate melt of kimberlite composition in high-pressure and high-temperature experiments. *Geology* 21:968–970
- Bataleva YV, Palyanov YN, Sokol AG, Borzdov YM, Palyanova GA (2012) Conditions for the origin of oxidized carbonate–silicate melts: Implications for mantle metasomatism and diamond formation. *Lithos* 128–131:113–125
- Bataleva YV, Palyanov YN, Sokol AG, Borzdov YM, Bayukov OA (2015a) The role of rocks saturated with metallic iron in the formation of ferric carbonate–silicate melts: Experimental modeling under *P-T*-conditions of lithospheric mantle. *Russ Geol Geophys* 56:143–154
- Bataleva YV, Palyanov YN, Borzdov YM, Bayukov OA, Sobolev NV (2015b) Interaction of iron carbide and sulfur under *P-T* conditions of the lithospheric mantle. *Dokl Earth Sci* 463:707–711
- Bataleva YV, Palyanov YN, Borzdov YM, Sobolev NV (2016a) Graphite and diamond formation via the interaction of iron carbide and Fe,Ni-sulfide under mantle *P-T* parameters. *Dokl Earth Sci* 471:1144–1148
- Bataleva YV, Palyanov YN, Borzdov YM, Bayukov OA, Sobolev NV (2016b) The formation of graphite upon the interaction of subducted carbonates and sulfur with metal-bearing rocks of the lithospheric mantle. *Dokl Earth Sci* 466:88–91
- Bataleva YV, Palyanov YN, Borzdov YM, Kupriyanov IN, Sokol AG (2016c) Synthesis of diamonds with mineral, fluid and melt inclusions. *Lithos* 265:292–303
- Bataleva YV, Palyanov YN, Sokol AG, Borzdov YM, Bayukov OA (2016d) Wüstite stability in the presence of a CO₂–fluid and a carbonate–silicate melt: Implications for the graphite/diamond formation and generation of Fe-rich mantle metasomatic agents. *Lithos* 244:20–29
- Bataleva YV, Palyanov YN, Borzdov YM, Bayukov OA, Sobolev NV (2016e) Conditions for diamond and graphite formation from iron carbide at the *P-T* parameters of lithospheric mantle. *Russian Geol Geophys* 57:176–189
- Bataleva YV, Palyanov YN, Borzdov YM, Bayukov OA, Zdrokov EV (2017) Iron carbide as a source of carbon for graphite and diamond formation under lithospheric mantle *P-T* parameters. *Lithos* 286–287:151–161
- Bataleva Y, Palyanov Y, Borzdov Y, Novoselov I, Bayukov O (2018a) Graphite and diamond formation in the carbide–oxide–carbonate interactions (Experimental modeling under mantle *P-T*-conditions). *Minerals* 8:522
- Bataleva YV, Palyanov YN, Borzdov YM, Bayukov OA, Sobolev NV (2018b) Experimental modeling of C⁰-forming processes involving cohenite and CO₂–fluid in a silicate mantle. *Dokl Earth Sci* 483:1427–1430
- Bataleva YV, Palyanov YN, Borzdov YM, Novoselov ID, Bayukov OA, Sobolev NV (2018c) Conditions of formation of iron–carbon melt inclusions in garnet and orthopyroxene under *P-T* conditions of lithospheric mantle. *Petrology* 26:565–574
- Bataleva YV, Palyanov YN, Borzdov YM, Zdrokov EV, Novoselov ID, Sobolev NV (2018d) Formation of the Fe,Mg-silicates, Fe⁰, and graphite (diamond) assemblage as a result of cohenite oxidation under lithospheric mantle conditions. *Dokl Earth Sci* 479:335–338
- Bataleva YV, Palyanov YN, Borzdov YM, Novoselov ID, Bayukov OA (2019) An effect of reduced S-rich fluids on diamond formation under mantle–slab interaction. *Lithos* 336–337:27–39
- Bayarjargal L, Shumilova TG, Friedrich A, Winkler B (2010) Diamond formation from CaCO₃ at high pressure and temperature. *Eur J Mineral* 22:29–34
- Bobrov AV, Litvin YA (2009) Peridotite–eclogite–carbonatite systems at 7.0–8.5 GPa: Concentration barrier of diamond nucleation and syngenesis of its silicate and carbonate inclusions. *Russian Geol Geophys* 50:1221–1233
- Bobrov AV, Litvin YA (2011) Mineral equilibria of diamond-forming carbonate–silicate systems. *Geochem Int* 49:1267–1363
- Bobrov AV, Litvin YA, Divaev FK (2004) Phase relations and diamond synthesis in the carbonate–silicate rocks of the Chagatai Complex, Western Uzbekistan: Results of experiments at *P*=4–7 GPa and *T*=1200–1700 °C. *Geochem Int* 42:39–48
- Boettcher AL, Mysen BO, Allen JC (1973) Techniques for the control of water fugacity and oxygen fugacity for experimentation in solid-media high-pressure apparatus. *J Geophys Res* 78:5898–5901
- Borzdov YM, Sokol AG, Pal'yanov YN, Kalinin AA, Sobolev NV (1999) Studies of diamond crystallization in alkaline silicate, carbonate and carbonate–silicate melts. *Doklady Akademii Nauk* 366:530–533
- Borzdov Y, Pal'yanov Y, Kupriyanov I, Gusev V, Khokhryakov A, Sokol A, Efremov A (2002) HPHT synthesis of diamond with high nitrogen content from an Fe₃N–C system. *Diamond Relat Mater* 11:1863–1870
- Boulard E, Gloter A, Corgne A, Antonangeli D, Auzende AL, Perrillat JP, Guyot F, Fiquet G (2011) New host for carbon in the deep Earth. *PNAS* 108:5184–5187
- Boulard E, Menguy N, Auzende AL, Benzerara K, Bureau H, Antonangeli D, Corgne A, Morard G, Siebert J, Perrillat JP, Guyot F (2012) Experimental investigation of the stability of Fe-rich carbonates in the lower mantle. *J Geophys Res: Solid Earth* 117
- Bovenkerk HP (1961) Some observations on the morphology and crystal characteristics of synthetic diamonds. *Am Mineral* 46:952–963
- Boyd SR, Pillinger CT, Milledge HJ, Mendelssohn MJ, Seal M (1988) Fractionation of nitrogen isotopes in a synthetic diamond of mixed crystal habit. *Nature* 331:604–607

- Boyd SR, Pineau F, Javoy M (1994) Modeling the growth of natural diamonds. *Chem Geol* 116:29–42
- Brey GP, Kogarko LN, Ryabchikov ID (1991) Carbon dioxide in kimberlitic melts. *Neues Jahrb Mineral Monatsh* 4:159–168
- Brey GP, Girmis AV, Bulatov VK, Höfer HE, Gerdés A, Woodland AB (2015) Reduced sediment melting at 7.5–12 GPa: phase relations, geochemical signals and diamond nucleation. *Contrib Mineral Petrol* 170:1–25
- Bureau H, Langenhorst F, Auzende AL, Frost DJ, Esteve I, Siebert J (2012) The growth of fibrous, cloudy and polycrystalline diamonds. *Geochim Cosmochim Acta* 77:202–214
- Bureau H, Frost DJ, Bolfan-Casanova N, Leroy C, Esteve I, Cordier P (2016) Diamond growth in mantle fluids. *Lithos* 265:4–15
- Bureau H, Remusat L, Esteve M, Pinti DL, Cartigny P (2018) The growth of lithospheric diamonds. *Sci Adv* 4: eaat1602
- Burns RC, Hansen JO, Spits RA, Sibanda M, Welbourn CM, Welch DL (1999) Growth of high purity large synthetic diamond crystals. *Diamond Relat Mater* 8:1433–1437
- Cartigny P (2005) Stable isotopes and the origin of diamond. *Elements* 1:79–84
- Chen L, Miao X, Ma H, Guo L, Wang Z, Yang Z, Fang C, Jia X (2018) Synthesis and characterization of diamonds with different nitrogen concentrations under high pressure and high temperature conditions. *CrystEngComm* 20:7164–7169
- Chepurov AI, Khokhriakov AF, Sonin VM, Palianov IN, Sobolev NV (1985) The shapes of diamond crystal dissolution in silicate melts under high-pressure. *Doklady Akademii Nauk* 285:212–216
- Chepurov AI, Zhimulev EI, Fedorov, II, Sonin VM (2007) Inclusions of metal solvent and color of boron-bearing monocrystals of synthetic diamond. *Geol Ore Deposits* 49:648–651
- Chepurov AI, Zhimulev EI, Sonin VM, Chepurov AA, Pokhilko NP (2009a) Crystallization of diamond in metal-sulfide melts. *Dokl Earth Sci* 428:1139–1141
- Chepurov AI, Zhimulev EI, Eliseev AP, Sonin VM, Fedorov, II (2009b) The genesis of low-N diamonds. *Geochem Int* 47:522–525
- Chepurov AI, Sonin VM, Zhimulev EI, Chepurov AA, Tomilenko AA (2011) On the formation of element carbon during decomposition of CaCO₃ at high *P-T* parameters under reducing conditions. *Dokl Earth Sci* 441:1738–1741
- Chepurov AI, Sonin VM, Zhimulev EI, Chepurov AA, Pomazansky BS, Zemnukhov AL (2018) Dissolution of diamond crystals in a heterogeneous (metal-sulfide-silicate) medium at 4 GPa and 1400 degrees C. *J Mineral Petrol Sci* 113:59–67
- Chrenko RM, McDonald RS, Darrow KA (1967) Infra-red spectrum of diamond coat. *Nature* 213:474–476
- Cull FA, Meyer HOA (1986) Oxidation of diamond at high temperature and 1 atm total pressure with controlled oxygen fugacity. *Int Kimberlite Confer: Extended Abstracts* 4:377–379
- Dasgupta R, Grewal DS (2019) Origin and early differentiation of carbon and associated life-essential volatile elements on Earth. *In: Deep Carbon: Past to Present.* Orcutt BN, Daniel I, Dasgupta R, (eds). Cambridge University Press, Cambridge, p 4–39
- Davies G, Evans T (1972) Graphitization of diamond at zero pressure and at a high pressure. *Proc R Soc London Ser A* 328:413–427
- Day HW (2012) A revised diamond-graphite transition curve. *Am Mineral* 97:52–62
- Dobrzhinetskaya LF, Green HW (2007) Diamond synthesis from graphite in the presence of water and SiO₂: Implications for diamond formation in quartzites from Kazakhstan. *International Geology Review* 49:389–400
- Dobrzhinetskaya LF, Renfro AP, Green HW (2004) Synthesis of skeletal diamonds: Implications for microdiamond formation in orogenic belts. *Geology* 32:869–872
- Dobrzhinetskaya LF, Wirth R, Green HW (2007) A look inside of diamond-forming media in deep subduction zones. *PNAS* 104:9128–9132
- Dorfman SM, Badro J, Nabiei F, Prakapenka VB, Cantoni M, Gillet P (2018) Carbonate stability in the reduced lower mantle. *Earth Planet Sci Lett* 489:84–91
- Drewitt JWE, Walter MJ, Zhang H, McMahon SC, Edwards D, Heinen BJ, Lord OT, Anzellini S, Kleppe AK (2019) The fate of carbonate in oceanic crust subducted into earth's lower mantle. *Earth Planet Sci Lett* 511:213–222
- Eggler DH, Baker DR (1982) Reduced volatiles in the system C–O–H: Implications to mantle melting, fluid formation, and diamond genesis. *In: High-pressure research in geophysics. Vol 12.* Akimoto S, Manghnani MH, (eds). Center for Academic Publications, Tokyo, p 237–250
- Evans T, Phaal C (1962) The kinetics of the diamond–oxygen reaction. *In: Proceedings of the Fifth Conference on Carbon.* Pergamon, p 147–153
- Evans T, Sauter DH (1961) Etching of diamond surfaces with gases. *Philos Mag* 6:429–440
- Fagan AJ, Luth RW (2011) Growth of diamond in hydrous silicate melts. *Contrib Mineral Petrol* 161:229–236
- Farré-de-Pablo J, Proenza JA, González-Jiménez JM, García-Casco A, Colás V, Roqué-Rossell J, Camprubí A, Sánchez-Navas A (2018) A shallow origin for diamonds in ophiolitic chromitites. *Geology* 47:75–78
- Farré-de-Pablo J, Proenza JA, González-Jiménez JM, García-Casco A, Colás V, Roqué-Rossell J, Camprubí A, Sánchez-Navas A (2019) A shallow origin for diamonds in ophiolitic chromitites Reply. *Geology* 47:E477–E478
- Fedortchouk Y (2015) Diamond resorption features as a new method for examining conditions of kimberlite emplacement. *Contrib Mineral Petrol* 170:1–19
- Fedortchouk Y (2019) A new approach to understanding diamond surface features based on a review of experimental and natural diamond studies. *Earth Sci Rev* 193:45–65

- Fedortchouk Y, Canil D (2009) Diamond oxidation at atmospheric pressure: development of surface features and the effect of oxygen fugacity. *Eur J Mineral* 21:623–635
- Fedortchouk Y, Canil D, Semenets E (2007) Mechanisms of diamond oxidation and their bearing on the fluid composition in kimberlite magmas. *Am Mineral* 92:1200–1212
- Fedortchouk Y, Liebske C, McCammon C (2019) Diamond destruction and growth during mantle metasomatism: An experimental study of diamond resorption features. *Earth Planet Sci Lett* 506:493–506
- Fisher D, Lawson SC (1998) The effect of nickel and cobalt on the aggregation of nitrogen in diamond. *Diamond Relat Mater* 7:299–304
- Frezzotti M-L, Huizinga J-M, Compagnoni R, Selverstone J (2014) Diamond formation by carbon saturation in C–O–H fluids during cold subduction of oceanic lithosphere. *Geochim Cosmochim Acta* 143:68–86
- Gaillou E, Post JE, Rost D, Butler JE (2012) Boron in natural type IIb blue diamonds: Chemical and spectroscopic measurements. *Am Mineral* 97:1–18
- Galvez ME, Beyssac O, Martinez I, Benzerara K, Chaduteau C, Malvoisin B, Malavieille J (2013) Graphite formation by carbonate reduction during subduction. *Nat Geosci* 6:473–477
- Galvez ME, Pubellier M (2019) How do subduction zones regulate the carbon cycle? In: Deep Carbon: Past to Present. Orcutt BN, Daniel I, Dasgupta R, (eds). Cambridge University Press, Cambridge, p 276–312
- Girnis AV, Brey GP, Bulatov VK, Höfer HE, Woodland AB (2018) Graphite to diamond transformation during sediment–peridotite interaction at 7.5 and 10.5 GPa. *Lithos* 310–311:302–313
- Green BL, Collins AT, Breeding CM (2022) Diamond spectroscopy, defect centers, color, and treatments. *Rev Mineral Geochem* 88:637–688
- Gryaznov IA, Zhimulev EI, Sonin VM, Lindenblot ES, Chepurov AA, Sobolev NV (2019) Morphological features of diamond crystals resulting from dissolution in a Fe–Ni–S melt under high pressure. *Dokl Earth Sci* 489:1449–1452
- Gunn SC, Luth RW (2006) Carbonate reduction by Fe–S–O melts at high pressure and high temperature. *Am Mineral* 91:1110–1116
- Harris JW (1968) Recognition of diamond inclusions. 1. Syngenetic mineral inclusions. *Ind Diam Rev* 28:402–410
- Harris JW, Vance ER (1974) Studies of reaction between diamond and heated kimberlite. *Contrib Mineral Petro* 47:237–244
- Hoering TC (1961) The carbon isotope effect in the synthesis of diamond. Year Book–Carnegie Institution of Washington 60:204
- Holloway JR, Burnham CW, Millhollen GL (1968) Generation of H₂O–CO₂ mixtures for use in hydrothermal experimentation. *J Geophys Res* 73:6598–6600
- Hong SM, Akaishi M, Yamaoka S (1999) Nucleation of diamond in the system of carbon and water under very high pressure and temperature. *J Cryst Growth* 200:326–328
- Huang F, Sverjensky DA (2020) Mixing of carbonatitic into saline fluid during panda diamond formation. *Geochim Cosmochim Acta* 284:1–20
- Huang WL, Wyllie PJ (1976) Melting relationships in the systems CaO–CO₂ and MgO–CO₂ to 33 kilobars. *Geochim Cosmochim Acta* 40:129–132
- Huang GF, Jia XP, Li SS, Zhang YF, Li Y, Zhao M, Ma HA (2010a) Synthesis of large diamond crystals containing high-nitrogen concentration at high pressure and high temperature using Ni-based solvent by temperature gradient method. *Chin Phys B* 19
- Huang GF, Jia XP, Li SS, Hu MH, Li Y, Zhao M, Yan BM, Ma HA (2010b) Effects of additive NaN₃ on the HPHT synthesis of large single crystal diamond grown by TGM. *Sci China Phys Mech Astronom* 53:1831–1835
- Irfune T, Kurio A, Sakamoto S, Inoue T, Sumiya H, Funakoshi K (2004) Formation of pure polycrystalline diamond by direct conversion of graphite at high pressure and high temperature. *Phys Earth Planet Inter* 143–44:593–600
- Ivanovskaya IN, Shterenberg LY, Makhov SF, Musina AR, Filonenko VP (1981) On carbon isotope fractionation in solid-phase synthesis of diamond. *Geokhimiya* 9:1415–1417
- Izraeli ES, Harris JW, Navon O (2001) Brine inclusions in diamonds: a new upper mantle fluid. *Earth Planet Sci Lett* 187:323–332
- Jablon BM, Navon O (2016) Most diamonds were created equal. *Earth Planet Sci Lett* 443:41–47
- Jones AP, Genge M, Carmody L (2013) Carbonate melts and carbonatites. In: Carbon in Earth. Vol 75. Hazen RM, Jones AP, Baross JA, (eds). p 289–322
- Kaminsky FW, Wirth R (2011) Iron carbide inclusions in lower-mantle diamond from Juina, Brazil. *Can Mineral* 49:555–572
- Kanda H (2000) Large diamonds grown at high pressure conditions. *Braz J Phys* 30:482–489
- Kanda H, Yamaoka S (1993) Inhomogeneous distribution of nitrogen impurities in {111} growth sectors of high-pressure synthetic diamond. *Diamond Relat Mater* 2:1420–1423
- Kanda H, Yamaoka S, Setaka N, Komatsu H (1977) Etching of diamond octahedrons by high-pressure water. *J Cryst Growth* 38:1–7
- Kanda H, Akaishi M, Yamaoka S (1999) Synthesis of diamond with the highest nitrogen concentration. *Diamond Relat Mater* 8:1441–1443
- Kelemen PB, Manning CE (2015) Reevaluating carbon fluxes in subduction zones, what goes down, mostly comes up. *PNAS* 112:E3997–E4006

- Kennedy CS, Kennedy GC (1976) The equilibrium boundary between graphite and diamond. *J Geophys Res* 81:2467–2470
- Keppler H (2003) Water solubility in carbonatite melts. *Am Mineral* 88:1822–1824
- Khokhryakov AF, Pal'yanov YN (1990) Morphology of diamond crystals dissolved in hydrous silicate melts. *Mineralogischeskiy Zhurnal* 12:14–23
- Khokhryakov AF, Pal'yanov YN (2000) The dissolution forms of diamond crystals in CaCO_3 melt at 7 GPa. *Russian Geol Geophys* 41:682–687
- Khokhryakov AF, Palyanov YN (2006) Revealing of dislocations in diamond crystals by the selective etching method. *J Cryst Growth* 293:469–474
- Khokhryakov AF, Pal'yanov YN (2007a) The evolution of diamond morphology in the process of dissolution: Experimental data. *Am Mineral* 92:909–917
- Khokhryakov AF, Palyanov YN (2007b) Revealing of planar defects and partial dislocations in large synthetic diamond crystals by the selective etching. *J Cryst Growth* 306:458–464
- Khokhryakov AF, Pal'yanov YN (2010) Influence of the fluid composition on diamond dissolution forms in carbonate melts. *Am Mineral* 95:1508–1514
- Khokhryakov AF, Palyanov YN (2015a) Effect of crystal defects on diamond morphology during dissolution in the mantle. *Am Mineral* 100:1528–1532
- Khokhryakov AF, Palyanov YN (2015b) Effect of nitrogen impurity on etching of synthetic diamond crystals. *J Cryst Growth* 430:71–74
- Khokhryakov AF, Palyanov YN (2018) Manifestation of diamond sectoriality during dissolution and graphitization. *J Cryst Growth* 502:1–6
- Khokhryakov AF, Pal'yanov YN, Sobolev NV (2001) Evolution of crystal morphology of natural diamond in dissolution processes: Experimental data. *Dokl Earth Sci* 381:884–888
- Khokhryakov AF, Pal'yanov YN, Sobolev NV (2002) Crystal morphology as an indicator of redox conditions of natural diamond dissolution at the mantle PT parameters. *Dokl Earth Sci* 385:534–537
- Khokhryakov AF, Nechaev DV, Sokol AG, Palyanov YN (2009) Formation of various types of graphite inclusions in diamond: Experimental data. *Lithos* 112:683–689
- Khokhryakov AF, Palyanov YN, Kupriyanov IN, Borzdov YM, Sokol AG (2014) Effect of nitrogen impurity on the dislocation structure of large HPHT synthetic diamond crystals. *J Cryst Growth* 386:162–167
- Khokhryakov AF, Palyanov YN, Kupriyanov IN, Nechaev DV (2016) Diamond crystallization in a CO_2 -rich alkaline carbonate melt with a nitrogen additive. *J Cryst Growth* 449:119–128
- Khokhryakov AF, Palyanov YN, Borzdov YM, Kozhukhov AS, Sheglov DV (2018) Dislocation etching of diamond crystals grown in Mg–C system with the addition of silicon. *Diamond Relat Mater* 88:67–73
- Khokhryakov AF, Nechaev DV, Sokol AG (2020) Microrelief of rounded diamond crystals as an indicator of the redox conditions of their resorption in a kimberlite melt. *Crystals* 10
- Kiseeva ES, Litasov KD, Yaxley GM, Ohtani E, Kamenetsky VS (2013) Melting and phase relations of carbonated eclogite at 9–21 GPa and the petrogenesis of alkali-rich melts in the deep mantle. *J Petrol* 54:1555–1583
- Klein-BenDavid O, Izraeli ES, Hauri E, Navon O (2004) Mantle fluid evolution—A tale of one diamond. *Lithos* 77:243–253
- Klein-BenDavid O, Izraeli ES, Hauri E, Navon O (2007) Fluid inclusions in diamonds from the Diavik mine, Canada and the evolution of diamond-forming fluids. *Geochim Cosmochim Acta* 71:723–744
- Kozai Y, Arima M (2005) Experimental study on diamond dissolution in kimberlitic and lamproitic melts at 1300–1420°C and 1 GPa with controlled oxygen partial pressure. *Am Mineral* 90:1759–1766
- Kraus D, Vorberger J, Pak A, Hartley NJ, Fletcher LB, Frydrych S, Galtier E, Gamboa EJ, Gericke DO, Glenzer SH, Granados E (2017) Formation of diamonds in laser-compressed hydrocarbons at planetary interior conditions. *Nat Astron* 1:606–611
- Laptev VA, Ivanovskaya IN, Galimov EM (1978) A study of carbon isotope fractionation in the process of diamond synthesis. VII All-union symposium on stable isotopes in geochemistry:95
- Latourette T, Holloway JR (1994) Oxygen fugacity of the diamond plus C–O fluid assemblage and CO_2 fugacity at 8-GPa. *Earth Planet Sci Lett* 128:439–451
- Lee C-TA, Jiang H, Dasgupta R, Torres M (2019) A framework for understanding whole-Earth carbon cycling. In: Deep carbon: Past to present. Orcutt BN, Daniel I, Dasgupta R, (eds). Cambridge University Press, Cambridge, p 313–357
- Li K, Li L, Pearson DG, Stachel T (2019) Diamond isotope compositions indicate altered igneous oceanic crust dominates deep carbon recycling. *Earth Planet Sci Lett* 516:190–201
- Liang ZZ, Jia X, Ma HA, Zang CY, Zhu PW, Guan QF, Kanda H (2005) Synthesis of HPHT diamond containing high concentrations of nitrogen impurities using NaN_3 as dopant in metal–carbon system. *Diamond Relat Mater* 14:1932–1935
- Liang ZZ, Kanda H, Jia X, Ma HA, Zhu PW, Guan QF, Zang CY (2006) Synthesis of diamond with high nitrogen concentration from powder catalyst-C-additive NaN_3 by HPHT. *Carbon* 44:913–917
- Litasov KD, Goncharov AF, Hemley RJ (2011) Crossover from melting to dissociation of CO_2 under pressure: Implications for the lower mantle. *Earth Planet Sci Lett* 309:318–323

- Litasov KD, Shatskiy A, Ohtani E (2014) Melting and subsolidus phase relations in peridotite and eclogite systems with reduced COH fluid at 3–16 GPa. *Earth Planet Sci Lett* 391:87–99
- Litasov KD, Kagi H, Bekker TB, Hirata T, Makino Y (2019a) Cubooctahedral type Ib diamonds in ophiolitic chromitites and peridotites: the evidence for anthropogenic contamination. *High Press Res* 39:480–488
- Litasov KD, Kagi H, Voropaev SA, Hirata T, Ohfuji H, Ishibashi H, Makino Y, Bekker TB, Sevastyanov VS, Afanasiev VP, Pokhilenco NP (2019b) Comparison of enigmatic diamonds from the Tolbachik arc volcano (Kamchatka) and Tibetan ophiolites: Assessing the role of contamination by synthetic materials. *Gondwana Res* 75:16–27
- Litvin YA (2003) Alkaline-chloride components in processes of diamond growth in the mantle and high-pressure experimental conditions. *Dokl Earth Sci* 389:388–391
- Litvin YA, Butvina VG (2004) Diamond-forming media in the system eclogite-carbonatite-sulfide-carbon: Experiments at 6.0–8.5 GPa. *Petrology* 12:377–387
- Litvin YA, Bobrov A (2008) Experimental study of diamond crystallization in carbonate-peridotite melts at 8.5 GPa. *Dokl Earth Sci* 422:1167–1171
- Litvin YA, Spivak AV (2003) Rapid growth of diamondite at the contact between graphite and carbonate melt: Experiments at 7.5–8.5 GPa. *Dokl Earth Sci* 391A:888–891
- Litvin YA, Zharikov VA (1999) Primary fluid-carbonatitic inclusions in diamond: Experimental modeling in the system $K_2O-Na_2O-CaO-MgO-FeO-CO_2$ as a diamond formation medium in experiment at 7–9 GPa. *Dokl Earth Sci* 367A:801–805
- Litvin YA, Chudinovskikh LT, Zharikov VA (1997) Crystallization of diamond and graphite from alkaline-carbonate melts at 7–11 GPa. *Doklady Akademii Nauk* 355:669–672
- Litvin YA, Chudinovskikh LT, Zharikov VA (1998a) Seed growth of diamond in the system $Na_2Mg(CO_3)_2-K_2Mg(CO_3)_2-C$ at 8–10 GPa. *Doklady Akademii Nauk* 359:818–820
- Litvin YA, Chudinovskikh LT, Zharikov VA (1998b) Crystallization of diamond in the system $Na_2Mg(CO_3)_2-K_2Mg(CO_3)_2-C$ at 8–10 GPa. *Doklady Akademii Nauk* 359:668–670
- Litvin YA, Chudinovskikh LT, Saparin GV, Obyden SK, Chukichev MV, Vavilov VS (1998c) Peculiarities of diamonds formed in alkaline carbonate-carbon melts at pressures of 8–10 GPa: Scanning electron microscopy and cathodoluminescence data. *Scanning* 20:380–388
- Litvin YA, Aldushin KA, Zharikov VA (1999a) Synthesis of diamond at 8.5–9.5 GPa in the system $K_2Ca(CO_3)_2-Na_2Ca(CO_3)_2-C$ modeling compositions of fluid-carbonatitic inclusions in kimberlitic diamonds. *Dokl Earth Sci* 367A:813–816
- Litvin YA, Chudinovskikh LT, Saparin GV, Obyden SK, Chukichev MV, Vavilov VS (1999b) Diamonds of new alkaline carbonate-graphite HP syntheses: SEM morphology, CCL-SEM and CL spectroscopy studies. *Diamond Relat Mater* 8:267–272
- Litvin YA, Spivak AV, Matveev YA (2003) Experimental study of diamond formation in the molten carbonate–silicate rocks of the Kokchetav metamorphic complex at 5.5–7.5 GPa. *Geochem Int* 41:1090–1098
- Litvin YA, Jones AP, Beard AD, Divaev FK, Zharikov VA (2001) Crystallization of diamond and syngenetic minerals in melts of diamondiferous carbonatites of the Chagatai Massif, Uzbekistan: Experiment at 7.0 GPa. *Dokl Earth Sci* 381:1066–1069
- Litvin YA, Butvina VG, Bobrov AV, Zharikov VA (2002) The first synthesis of diamond in sulfide-carbon systems: The role of sulfides in diamond genesis. *Dokl Earth Sci* 382:40–43
- Litvin YA, Kurat G, Dobosi G (2005a) Experimental study of diamondite formation in carbonate–silicate melts; a model approach to natural processes. *Russ Geol Geophys* 46:1285–1299
- Litvin YA, Shushkanova AV, Zharikov VA (2005b) Immiscibility of sulfide-silicate melts in the mantle: Role in the syngensis of diamond and inclusions (based on experiments at 7.0 GPa). *Dokl Earth Sci* 403:719–722
- Litvin YA, Litvin VY, Kadik AA (2008a) Experimental characterization of diamond crystallization in melts of mantle silicate-carbonate-carbon systems at 7.0–8.5 GPa. *Geochem Int* 46:531–553
- Litvin YA, Litvin V, Kadik A (2008b) Study of diamond and graphite crystallization from eclogite-carbonatite melts at 8.5 GPa: The role of silicates in diamond genesis. *Dokl Earth Sci* 419:486–491
- Litvin Y, Spivak A, Solopova N, Dubrovinsky L (2014) On origin of lower-mantle diamonds and their primary inclusions. *Phys Earth Planet Inter* 228:176–185
- Litvin YA, Spivak AV, Simonova DA, Dubrovinsky LS (2017) On origin and evolution of diamond-forming lower-mantle systems: physicochemical studies in experiments at 24 and 26 GPa. *J Phys Conf Ser* 950:042045
- Liu LG, Lin CC, Yang YJ (2001) Formation of diamond by decarbonation of $MnCO_3$. *Solid State Commun* 118:195–198
- Liu X, Jia X, Zhang Z, Li Y, Hu M, Zhou Z, Ma H-a (2011) Crystal growth and characterization of diamond from carbonyl iron catalyst under high pressure and high temperature conditions. *Cryst Growth Des* 11:3844–3849
- Liu X, Jia X, Fang C, Ma H-A (2016) Diamond crystallization and growth in N–H enriched environment under HPHT conditions. *CrystEngComm* 18:8506–8515
- Lonsdale K, Milledge HJ, Nave E (1959) X-ray studies of synthetic diamonds. *Mineral Mag* 32:185–201
- Luth R (2017) Diamond formation during partial melting in the Earth's mantle. *GSA Annual Meeting* in Seattle, Washington, USA-2017. *Geol Soc Am* 49:Abstr #20–26

- Maeda F, Ohtani E, Kamada S, Sakamaki T, Hirao N, Ohishi Y (2017) Diamond formation in the deep lower mantle: a high-pressure reaction of $MgCO_3$ and SiO_2 . *Sci Rep* 7:40602
- Martin AM, Hammouda T (2011) Role of iron and reducing conditions on the stability of dolomite + coesite between 4.25 and 6 GPa—a potential mechanism for diamond formation during subduction. *Eur J Mineral* 23:5–16
- Martirosyan NS, Litasov KD, Lobanov SS, Goncharov AF, Shatskiy A, Ohfuji H, Prakapenka V (2019) The Mg -carbonate– Fe interaction: Implication for the fate of subducted carbonates and formation of diamond in the lower mantle. *Geosci Front* 10:1449–1458
- Massonne H-J (2019) A shallow origin for diamonds in ophiolitic chromitites: Comment. *Geology* 47:e476–e476
- Matjuschkina V, Woodland AB, Frost DJ, Yaxley GM (2020) Reduced methane-bearing fluids as a source for diamond. *Sci Rep* 10:6961
- McCubbin FM, Sverjensky DA, Steele A, Mysen BO (2014) In-situ characterization of oxalic acid breakdown at elevated P and T: Implications for organic C–O–H fluid sources in petrologic experiments. *Am Mineral* 99:2258–2271
- McDonough WF, Sun SS (1995) The composition of the Earth. *Chem Geol* 120:223–253
- Milledge HJ (1961) Coesite as an inclusion in G.E.C. synthetic diamonds. *Nature* 190:1181–1181
- Mysen B (2018) Mass transfer in the Earth's interior: fluid–melt interaction in aluminosilicate–C–O–H–N systems at high pressure and temperature under oxidizing conditions. *Prog Earth Planet Science* 5:6
- Navon O, Hutchison ID, Rossman GR, Wasserburg GJ (1988) Mantle-derived fluids in diamond micro-inclusions. *Nature* 335:784–789
- Nestola F, Jung H, Taylor LA (2017) Mineral inclusions in diamonds may be synchronous but not syngenetic. *Nat Commun* 8:14168
- Newton RC, Sharp WE (1975) Stability of forsterite + CO_2 and its bearing on the role of CO_2 in the mantle. *Earth Planet Sci Lett* 26:239–244
- Nimis P (2022) Pressure and temperature data for diamonds. *Rev Mineral Geochem* 88:533–566
- Nimis P, Alvaro M, Nestola F, Angel RJ, Marquardt K, Rustioni G, Harris JW, Marone F (2016) First evidence of hydrous silicic fluid films around solid inclusions in gem-quality diamonds. *Lithos* 260:384–389
- Okada T, Utsumi W, Shimomura O (2002a) In situ x-ray observations of the diamond formation process in the $C-H_2O-MgO$ system. *J Phys Condens Matter* 14:11331–11335
- Okada T, Utsumi W, Kaneko H, Yamakata M, Shimomura O (2002b) In situ X-ray observations of the decomposition of brucite and the graphite–diamond conversion in aqueous fluid at high pressure and temperature. *Physi Chem Minerals* 29:439–445
- Okada T, Utsumi W, Kaneko H, Turkevich V, Hamaya N, Shimomura O (2004) Kinetics of the graphite–diamond transformation in aqueous fluid determined by in-situ X-ray diffractions at high pressures and temperatures. *Phys Chem Minerals* 31:261–268
- Onodera A, Suito K, Morigami Y (1992) High-pressure synthesis of diamond from organic compounds. *Proceedings of the Japan Academy Series B-Physical and Biological Sciences* 68:167–171
- Osorgin NI, Palianov IN, Sobolev NV, Khokhriakova IP, Chepurov AI, Shugurova NA (1987) Inclusions of liquefied gases in diamond crystals. *Doklady Akademii Nauk Sssr* 293:1214–1217
- Palyanov YN, Sokol AG (2009) The effect of composition of mantle fluids/melts on diamond formation processes. *Lithos* 112:690–700
- Pal'yanov YN, Khokhryakov AF, Borzdov YM, Doroshev AM, Tomilenko AA, Sobolev NV (1994) Inclusions in synthetic diamonds. *Doklady Akademii Nauk* 338:78–80
- Pal'yanov YN, Khokhryakov AF, Borzdov YM, Sokol AG, Gusev VA, Rylov GM, Sobolev NV (1997) Growth conditions and real structure of synthetic diamond crystals. *Russian Geol Geophys* 38:920–945
- Pal'yanov YN, Sokol AG, Borzdov YM, Sobolev NV (1998a) Experimental study of diamond crystallization in carbonate–carbon systems in connection with the problem of diamond genesis in magmatic and metamorphic rocks. *Geologiya I Geofizika* 39:1780–1792
- Pal'yanov YN, Borzdov YM, Sokol AG, Khokhriakov AF, Gusev VA, Rylov GM, Sobolev NV (1998b) High-pressure synthesis of high-quality diamond single crystals. *Diamond Relat Mater* 7:916–918
- Pal'yanov YN, Sokol AG, Borzdov YM, Khokhryakov AF, Sobolev NV (1999a) Diamond formation from mantle carbonate fluids. *Nature* 400:417–418
- Pal'yanov YN, Sokol AG, Borzdov YM, Khokhryakov AF, Sobolev NV (1999b) The diamond growth from Li_2CO_3 , Na_2CO_3 , K_2CO_3 and Cs_2CO_3 solvent-catalysts at $P = 7$ GPa and $T = 1700–1750^\circ C$. *Diamond Relat Mater* 8:1118–1124
- Pal'yanov YN, Sokol AG, Khokhryakov AF, Pal'yanova GA, Borzdov YM, Sobolev NV (2000) Diamond and graphite crystallization in COH fluid at PT parameters of the natural diamond formation. *Dokl Earth Sci* 375:1395–1398
- Pal'yanov Y, Borzdov Y, Kupriyanov I, Gusev V, Khokhryakov A, Sokol A (2001a) High-pressure synthesis and characterization of diamond from a sulfur–carbon system. *Diamond Relat Mater* 10:2145–2152
- Palyanov YN, Shatsky VS, Sokol AG, Tomilenko AA, Sobolev NV (2001b) Crystallization of metamorphic diamond: An experimental modeling. *Dokl Earth Sci* 381:935–938

- Pal'yanov YN, Sokol AG, Borzdov YM, Khokhryakov AF (2002a) Fluid-bearing alkaline carbonate melts as the medium for the formation of diamonds in the Earth's mantle: an experimental study. *Lithos* 60:145–159
- Pal'yanov YN, Sokol AG, Borzdov YM, Khokhryakov AF, Sobolev NV (2002b) Diamond formation through carbonate–silicate interaction. *Am Mineral* 87:1009–1013
- Pal'yanov YN, Borzdov YM, Ovchinnikov IY (2003) Experimental study of the interaction between pentlandite melt and carbon at mantle *PT* parameters: Condition of diamond and graphite crystallization. *Dokl Earth Sci* 392:1026–1029
- Pal'yanov YN, Sokol AG, Sobolev NV (2005a) Experimental modeling of mantle diamond-forming processes. *Russian Geol Geophys* 46:1271–1284
- Pal'yanov YN, Sokol AG, Tomilenco AA, Sobolev NV (2005b) Conditions of diamond formation through carbonate–silicate interaction. *Eur J Mineral* 17:207–214
- Palyanov YN, Borzdov YM, Khokhryakov AF, Kupriyanov IN, Sobolev NV (2006) Sulfide melts–graphite interaction at HPHT conditions: Implications for diamond genesis. *Earth Planet Sci Lett* 250:269–280
- Palyanov YN, Shatsky VS, Sobolev NV, Sokol AG (2007a) The role of mantle ultrapotassic fluids in diamond formation. *PNAS* 104:9122–9127
- Palyanov YN, Borzdov YM, Bataleva YV, Sokol AG, Palyanova GA, Kupriyanov IN (2007b) Reducing role of sulfides and diamond formation in the Earth's mantle. *Earth Planet Sci Lett* 260:242–256
- Palyanov YN, Kupriyanov IN, Borzdov YM, Sokol AG, Khokhryakov AF (2009) Diamond crystallization from a sulfur–carbon system at HPHT conditions. *Cryst Growth Des* 9:2922–2926
- Palyanov YN, Sokol AG, Khokhryakov AF, Sobolev NV (2010a) Experimental study of interaction in the CO₂-C system at mantle *PT* parameters. *Dokl Earth Sci* 435:1492–1495
- Palyanov YN, Borzdov YM, Khokhryakov AF, Kupriyanov IN, Sokol AG (2010b) Effect of nitrogen impurity on diamond crystal growth processes. *Cryst Growth Des* 10:3169–3175
- Palyanov YN, Borzdov YM, Kupriyanov IN, Khokhryakov AF (2012) Effect of H₂O on diamond crystal growth in metal–carbon systems. *Cryst Growth Des* 12:5571–5578
- Palyanov YN, Khokhryakov AF, Borzdov YM, Kupriyanov IN (2013a) Diamond growth and morphology under the influence of impurity adsorption. *Cryst Growth Des* 13:5411–5419
- Palyanov YN, Bataleva YV, Sokol AG, Borzdov YM, Kupriyanov IN, Reutsky VN, Sobolev NV (2013b) Mantle–slab interaction and redox mechanism of diamond formation. *PNAS* 110:20408–20413
- Palyanov YN, Sokol AG, Khokhryakov AF, Kruk AN (2015) Conditions of diamond crystallization in kimberlite melt: experimental data. *Russian Geol Geophys* 56:196–210
- Palyanov YN, Kupriyanov IN, Sokol AG, Borzdov YM, Khokhryakov AF (2016) Effect of CO₂ on crystallization and properties of diamond from ultra-alkaline carbonate melt. *Lithos* 265:339–350
- Palyanov YN, Borzdov YM, Khokhryakov AF, Bataleva YV, Kupriyanov IN (2020a) Effect of sulfur on diamond growth and morphology in metal–carbon systems. *Crystengcomm* 22:5497–5508
- Palyanov YN, Borzdov YM, Kupriyanov IN, Bataleva YV, Nechaev DV (2020b) Effect of oxygen on diamond crystallization in metal–carbon systems. *ACS Omega*
- Palyanov YN, Khokhryakov AF, Kupriyanov IN (2021a) Crystallomorphological and crystallochemical indicators of diamond formation conditions. *Crystal Rep* 66:142–155
- Palyanov YN, Borzdov YM, Sokol AG, Bataleva YV, Kupriyanov IN, Reutsky VN, Wiedenbeck M, Sobolev NV (2021b) Diamond formation in an electric field under deep Earth conditions. *Sci Adv* 7:eabb4644
- Podborodnikov IV, Shatskiy A, Arefiev AV, Bekhtenova A, Litasov KD (2019) New data on the system Na₂CO₃–CaCO₃–MgCO₃ at 6 GPa with implications to the composition and stability of carbonatite melts at the base of continental lithosphere. *Chem Geol* 515:50–60
- Polyakov VI, Rukovichnikov AI, Rossukanyi NM, Ralchenko VG (2001) Electrical properties of thick boron and nitrogen contained CVD diamond films. *Diamond Relat Mater* 10:593–600
- Ree S, Griffin WL, Pearson NJ, Araujo D, Zedgenizov D, O'Reilly SY (2010) Trace-element patterns of fibrous and monocrystalline diamonds: Insights into mantle fluids. *Lithos* 118:313–337
- Reutsky VN, Borzdov YM, Palyanov YN (2008a) Carbon isotope fractionation associated with HPHT crystallization of diamond. *Diamond Relat Mater* 17:1986–1989
- Reutsky VN, Harte B, Eimf, Borzdov YM, Palyanov YN (2008b) Monitoring diamond crystal growth, a combined experimental and SIMS study. *Eur J Mineral* 20:365–374
- Reutsky VN, Borzdov YM, Palyanov YN (2012) Effect of diamond growth rate on carbon isotope fractionation in Fe–Ni–C system. *Diamond Relat Mater* 21:7–10
- Reutsky V, Borzdov Y, Palyanov Y, Sokol A, Izokh O (2015a) Carbon isotope fractionation during experimental crystallisation of diamond from carbonate fluid at mantle conditions. *Contrib Mineral Petrol* 170
- Reutsky VN, Borzdov YM, Palyanov YN (2015b) Carbon isotope fractionation during high pressure and high temperature crystallization of Fe-C melt. *Chem Geol* 406:18–24
- Reutsky VN, Palyanov YN, Borzdov YM, Sokol AG (2015c) Isotope fractionation of carbon during diamond crystallization in model systems. *Russian Geol Geophys* 56:239–244

- Reutsky VN, Kowalski PM, Palyanov YN, Wiedenbeck M, Eimf (2017) Experimental and theoretical evidence for surface-induced carbon and nitrogen fractionation during diamond crystallization at high temperatures and high pressures. *Crystals* 7:190
- Reutsky VN, Palyanov YN, Wiedenbeck M (2018) Carbon isotope composition of diamond crystals grown via redox mechanism. *Geochem Int* 56:1398–1404
- Richert P, Bottinga Y, Javoy M (1977) A review of hydrogen, carbon, nitrogen, oxygen, sulphur, and chlorine stable isotope fractionation among gaseous molecules. *Annu Rev Earth Planet Sci* 5:65–110
- Robinson DN (1979) Surface textures and other features of diamonds. PhD University of Cape Town, Cape Town
- Roedder E (ed) (1984) Fluid Inclusions. Reviews in Mineralogy, Vol. 12, Mineralogical Society of America, Chantilly, Virginia
- Rubie DC (1999) Characterising the sample environment in multianvil high-pressure experiments. *Phase Transitions* 68:431–451
- Satish-Kumar M, So H, Yoshino T, Kato M, Hiroi Y (2011) Experimental determination of carbon isotope fractionation between iron carbide melt and carbon: ^{12}C -enriched carbon in the Earth's core? *Earth Planet Sci Lett* 310:340–348
- Sato K, Akaishi M, Yamaoka S (1999) Spontaneous nucleation of diamond in the system $\text{MgCO}_3\text{-CaCO}_3\text{-C}$ at 7.7 GPa. *Diamond Relat Mater* 8:1900–1905
- Schrauder M, Navon O (1993) Solid carbon dioxide in a natural diamond. *Nature* 365:42–44
- Seto Y, Hamane D, Nagai T, Fujino K (2008) Fate of carbonates within oceanic plates subducted to the lower mantle, and a possible mechanism of diamond formation. *Physi Chem Minerals* 35:223–229
- Shaji Kumar MD, Akaishi M, Yamaoka S (2000) Formation of diamond from supercritical $\text{H}_2\text{O-CO}_2$ fluid at high pressure and high temperature. *J Cryst Growth* 213:203–206
- Shaji Kumar MD, Akaishi M, Yamaoka S (2001) Effect of fluid concentration on the formation of diamond in the $\text{CO}_2\text{-H}_2\text{O}$ -graphite system under HP-HT conditions. *J Cryst Growth* 222:9–13
- Shatskiy A, Borzakov YM, Litasov KD, Sharygin IS, Palyanov YN, Ohtani E (2015a) Phase relationships in the system $\text{K}_2\text{CO}_3\text{-CaCO}_3$ at 6 GPa and 900–1450°C. *Am Mineral* 100:223–232
- Shatskiy A, Yamazaki D, Morard G, Cooray T, Matsuzaki T, Higo Y, Funakoshi K, Sumiya H, Ito E, Katsura T (2009) Boron-doped diamond heater and its application to large-volume, high-pressure, and high-temperature experiments. *Rev Sci Instrum* 80:023907
- Shatskiy AF, Litasov KD, Palyanov YN (2015b) Phase relations in carbonate systems at pressures and temperatures of lithospheric mantle: review of experimental data. *Russian Geol Geophys* 56:113–142
- Shatsky AF, Borzakov YM, Sokol AG, Pal'yanov YN (2002) Phase formation and diamond crystallization in carbon-bearing ultrapotassic carbonate-silicate systems. *Geologiya I Geofizika* 43:940–950
- Shushkanova AV, Litvin YA (2006) Formation of diamond polycrystals in pyrrhotite-carbonic melt: Experiments at 6.7 GPa. *Dokl Earth Sci* 409:916–920
- Shushkanova AV, Litvin YA (2008a) Diamond nucleation and growth in sulfide-carbon melts: An experimental study at 6.0–7.1 GPa. *Eur J Mineral* 20:349–355
- Shushkanova AV, Litvin YA (2008b) Diamond formation in sulfide pyrrhotite-carbon melts: Experiments at 6.0–7.1 GPa and application to natural conditions. *Geochem Int* 46:37–47
- Siebert J, Guyot F, Malavergne V (2005) Diamond formation in metal–carbonate interactions. *Earth Planet Sci Lett* 229:205–216
- Smit KV, Stachel T, Luth RW, Stern RA (2019) Evaluating mechanisms for eclogitic diamond growth: An example from Zimmi Neoproterozoic diamonds (West African craton). *Chem Geol* 520:21–32
- Smit KV, Shirey SB, Stern RA, Steele A, Wang W (2016) Diamond growth from C–H–N–O recycled fluids in the lithosphere: Evidence from CH_4 micro-inclusions and $\delta^{13}\text{C}-\delta^{15}\text{N}$ content in Marange mixed-habit diamonds. *Lithos* 265:68–81
- Smith EM, Kopylova MG (2013) Implications of metallic iron for diamonds and nitrogen in the sublithospheric mantle. *Can J Earth Sci* 51:510–516
- Smith EM, Wang W (2016) Fluid CH_4 and H_2 trapped around metallic inclusions in HPHT synthetic diamond. *Diamond Relat Mater* 68:10–12
- Smith EM, Shirey SB, Nestola F, Bullock ES, Wang J, Richardson SH, Wang W (2016) Large gem diamonds from metallic liquid in Earth's deep mantle. *Science* 354:1403–1405
- Sokol AG, Pal'yanov YN (2004) Diamond crystallization in fluid and carbonate-fluid systems under mantle P-T conditions: 2. An analytical review of experimental data. *Geochem Int* 42:1018–1032
- Sokol AG, Pal'yanov YN (2008) Diamond formation in the system $\text{MgO-SiO}_2\text{-H}_2\text{O-C}$ at 7.5 GPa and 1,600°C. *Contrib Mineral Petrol* 155:33–43
- Sokol AG, Pal'yanov YN, Borzakov YM, Khokhryakov AF, Sobolev NV (1998) Crystallization of diamond from Na_2CO_3 melt. *Dokl Earth Sci* 361:388–391
- Sokol AG, Borzakov YM, Khokhryakov AF, Pal'yanov YN, Sobolev NV (1999) Diamond crystallization in silicate-fluid systems at $P = 7.0$ GPa and $T = 1700\text{--}1750^\circ\text{C}$. *Doklady Akademii Nauk* 368:99–102
- Sokol AG, Tomilenko AA, Pal'yanov YN, Borzakov YM, Pal'yanova GA, Khokhryakov AF (2000) Fluid regime of diamond crystallisation in carbonate-carbon systems. *Eur J Mineral* 12:367–375

- Sokol AG, Pal'yanov YN, Pal'yanova GA, Khokhryakov AF, Borzdov YM (2001a) Diamond and graphite crystallization from C–O–H fluids under high pressure and high temperature conditions. *Diamond Relat Mater* 10:2131–2136
- Sokol AG, Borzdov YM, Pal'yanov YN, Khokhryakov AF, Sobolev NV (2001b) An experimental demonstration of diamond formation in the dolomite–carbon and dolomite–fluid–carbon systems. *Eur J Mineral* 13:893–900
- Sokol AG, Pal'yanov YN, Pal'yanova GA, Tomilenco AA (2004) Diamond crystallization in fluid and carbonate–fluid systems under mantle P–T conditions: 1. Fluid composition. *Geochim Int* 42:830–838
- Sokol AG, Palyanova GA, Palyanov YN, Tomilenco AA, Melenovsky VN (2009) Fluid regime and diamond formation in the reduced mantle: Experimental constraints. *Geochim Cosmochim Acta* 73:5820–5834
- Sokol AG, Palyanov YN, Litasov KD (2010) Effect of oxygen fugacity on the H₂O storage capacity of forsterite in the carbon-saturated systems. *Geochim Cosmochim Acta* 74:4793–4806
- Sokol AG, Khokhryakov AF, Palyanov YN (2015) Composition of primary kimberlite magma: constraints from melting and diamond dissolution experiments. *Contrib Mineral Petrol* 170:1–18
- Sokol AG, Palyanov YN, Tomilenco AA, Bul'bak TA, Palyanova GA (2017) Carbon and nitrogen speciation in nitrogen-rich C–O–H–N fluids at 5.5–7.8 GPa. *Earth Planet Sci Lett* 460:234–243
- Sokol AG, Khokhryakov AF, Borzdov YM, Kupriyanov IN, Palyanov YN (2019) Solubility of carbon and nitrogen in a sulfur-bearing iron melt: Constraints for siderophile behavior at upper mantle conditions. *Am Mineral* 104:1857–1865
- Solopova NA, Spivak AV, Litvin YA, Shiryayev AA, Tsel'movich VA, Nekrasov AN (2013) Kinetic peculiarities of diamond crystallization in K–Na–Mg–Ca–carbonate–carbon melt–solution. *Phys Solid State* 55:373–376
- Solopova NA, Dubrovinsky L, Spivak AV, Litvin YA, Dubrovinskaia N (2015) Melting and decomposition of MgCO₃ at pressures up to 84 GPa. *Physi Chem Minerals* 42:73–81
- Sonin VM, Fedorov, II, Pokhilenko LN, Pokhilenko NP (2000) Diamond oxidation rate as related to oxygen fugacity. *Geol Ore Deposits* 42:496–502
- Sonin VM, Zhimulev EI, Fedorov, II, Tomilenco AA, Chepurov AI (2001) Etching of diamond crystals in a dry silicate melt at high P–T parameters. *Geochem Int* 39:268–274
- Sonin VM, Zhimulev EI, Chepurov AI, Afanas'ev VP, Tomilenco AA (2003) Etching of diamond crystals in the system silicate melt–C–O–H–S fluid under a high pressure. *Geochem Int* 41:688–693
- Sonin VM, Zhimulev EI, Fedorov, II, Chepurov AI (2006) Effect of oxygen fugacity on the etching rate of diamond crystals in silicate melt. *Geol Ore Deposits* 48:499–501
- Sonin VM, Zhimulev EI, Chepurov AI, Fedorov II (2008) Diamond stability in NaCl and NaF melts at high pressure. *Dokl Earth Sci* 420:641–643
- Sonin VM, Zhimulev EI, Chepurov AI, Pokhilenko NP (2009) Diamond stability in silicate–halogenide melts at high pressure. *Dokl Earth Sci* 425:441–443
- Sonin VM, Zhimulev EI, Chepurov AI, Afanas'ev VP, Pokhilenko NP (2010) High-pressure etching of diamond in chloride melt in the presence of aqueous fluid. *Dokl Earth Sci* 434:1359–1361
- Sonin VM, Zhimulev EI, Chepurov AA, Chepurov AI, Pokhilenko NP (2018a) Influence of the sulfur concentration in a Fe–S melt on diamond preservation under P–T conditions of the Earth's mantle. *Dokl Earth Sci* 481:922–924
- Sonin VM, Zhimulev EI, Pomazanskiy BS, Zemnukhov AL, Chepurov AA, Afanasiev VP, Chepurov AI (2018b) Morphological features of diamond crystals dissolved in Fe_{0.7}S_{0.3} melt at 4 GPa and 1400°C. *Geol Ore Deposits* 60:82–92
- Spivak AV, Litvin YA (2004) Diamond syntheses in multicomponent carbonate–carbon melts of natural chemistry: Elementary processes and properties. *Diamond Relat Mater* 13:482–487
- Spivak AV, Litvin YA (2012) Paragenetic relations of diamond with silicate and carbonate minerals in the carbonatite–diamond system: Experiments at 8.5 GPa. *Geochem Int* 50:217–226
- Spivak AV, Litvin YA, Shushkanova AV, Litvin VY, Shiryayev AA (2008) Diamond formation in carbonate–silicate–sulfide–carbon melts: Raman- and IR-microspectroscopy. *Eur J Mineral* 20:341–347
- Spivak AV, Litvin YA, Ovsyannikov SV, Dubrovinskaya NA, Dubrovinsky LS (2012) Stability and breakdown of Ca¹³CO₃ melt associated with formation of ¹³C-diamond in static high pressure experiments up to 43 GPa and 3900 K. *J Solid State Chem* 191:102–106
- Srikanth V, Akaishi M, Yamaoka S, Yamada H, Taniguchi T (1997) Diamond synthesis from graphite in the presence of MnCO₃. *Journal of the American Ceramic Society* 80:786–790
- Stachel T, Harris JW (2008) The origin of cratonic diamonds—Constraints from mineral inclusions. *Ore Geol Rev* 34:5–32
- Stachel T, Luth RW (2015) Diamond formation — Where, when and how? *Lithos* 220–223:200–220
- Stachel T, Aulbach S, Harris JW (2022a) Mineral inclusions in lithospheric diamonds. *Rev Mineral Geochem* 88:307–392
- Stachel T, Cartigny P, Chacko T, Pearson DG (2022) Carbon and nitrogen in mantle-derived diamonds. *Rev Mineral Geochem* 88:809–876
- Stagno V (2019) Carbon, carbides, carbonates and carbonatitic melts in the Earth's interior. *J Geol Soc* 176:375–387
- Stagno V, Frost DJ (2010) Carbon speciation in the asthenosphere: Experimental measurements of the redox conditions at which carbonate-bearing melts coexist with graphite or diamond in peridotite assemblages. *Earth Planet Sci Lett* 300:72–84
- Stöckhert B, Duyster J, Trepmann C, Massonne H-J (2001) Microdiamond daughter crystals precipitated from supercritical COH + silicate fluids included in garnet, Erzgebirge, Germany. *Geology* 29:391–394

- Sumiya H, Satoh S (1996) High-pressure synthesis of high-purity diamond crystal. *Diamond Relat Mater* 5:1359–1365
- Sumiya H, Satoh S (1999) Synthesis of polycrystalline diamond with new non-metallic catalyst under high pressure and high temperature. *Inter J Refractory Metals Hard Mater* 17:345–350
- Sumiya H, Toda N, Satoh S (2002) Growth rate of high-quality large diamond crystals. *J Cryst Growth* 237:1281–1285
- Sun LL, Akaishi M, Yamaoka S (2000) Formation of diamond in the system of Ag_2CO_3 and graphite at high pressure and high temperatures. *J Cryst Growth* 213:411–414
- Sun LL, Wu Q, Wang WK (2001) Bulk diamond formation from graphite in the presence of C–O–H fluid under high pressure. *High Press Res* 21:159–173
- Sverjensky DA, Huang F (2015) Diamond formation due to a pH drop during fluid–rock interactions. *Nat Commun* 6:8702
- Taniguchi T, Dobson D, Jones AP, Rabe R, Milledge HJ (1996) Synthesis of cubic diamond in the graphite–magnesium carbonate and graphite– $\text{K}_2\text{Mg}(\text{CO}_3)_2$ systems at high pressure of 9–10 GPa region. *J Mater Res* 11:2622–2632
- Thomassot E, Cartigny P, Harris JW, Viljoen KS (2007) Methane-related diamond crystallization in the Earth's mantle: Stable isotope evidences from a single diamond-bearing xenolith. *Earth Planet Sci Lett* 257:362–371
- Thomson AR, Walter MJ, Kohn SC, Brooker RA (2016) Slab melting as a barrier to deep carbon subduction. *Nature* 529:76–79
- Tiraboschi C, Tumiati S, Recchia S, Miozzi F, Poli S (2016) Quantitative analysis of COH fluids synthesized at HP-HT conditions: an optimized methodology to measure volatiles in experimental capsules. *Geofluids* 16:841–855
- Tomilenco AA, Chepurov AI, Pal'yanov YN, Shebanin AP, Sobolev NV (1998) Hydrocarbon inclusions in synthetic diamonds. *Eur J Mineral* 10:1135–1141
- Tomlinson E, Jones A, Milledge J (2004) High-pressure experimental growth of diamond using C– K_2CO_3 –KCl as an analogue for Cl-bearing carbonate fluid. *Lithos* 77:287–294
- Tomlinson EL, Howell D, Jones AP, Frost DJ (2011) Characteristics of HPHT diamond grown at sub-lithosphere conditions (10–20 GPa). *Diamond Relat Mater* 20:11–17
- Tschauner O, Mao HK, Hemley RJ (2001) New transformations of CO_2 at high pressures and temperatures. *Physical Review Letters* 87:075701
- Tschauner O, Huang S, Greenberg E, Prakapenka VB, Ma C, Rossman GR, Shen AH, Zhang D, Newville M, Lanzirotti A, Tait K (2018) Ice-VII inclusions in diamonds: Evidence for aqueous fluid in Earth's deep mantle. *Science* 359:1136
- Wang Y, Kanda H (1998) Growth of HPHT diamonds in alkali halides: possible effects of oxygen contamination. *Diamond Relat Mater* 7:57–63
- Weiss Y, Cazs J, Navon O (2022) Fluid inclusions in fibrous diamonds. *Rev Mineral Geochem* 88:475–532
- Weiss Y, Kessel R, Griffin WL, Kiflawi I, Klein-BenDavid O, Bell DR, Harris JW, Navon O (2009) A new model for the evolution of diamond-forming fluids: Evidence from microinclusion-bearing diamonds from Kankan, Guinea. *Lithos* 112:660–674
- Weiss Y, Kiflawi I, Davies N, Navon O (2014) High-density fluids and the growth of monocrystalline diamonds. *Geochim Cosmochim Acta* 141:145–159
- Whitney JA (1972) The effect of reduced H_2O fugacity on the buffering of oxygen fugacity in hydrothermal experiments. *Am Mineral* 57:1902–1908
- Wilding M, Bingham PA, Wilson M, Kono Y, Drewitt JWE, Brooker RA, Parise JB (2019) CO_{3+1} network formation in ultra-high pressure carbonate liquids. *Sci Rep* 9:15416
- Yamaoka S, Kanda H, Setaka N (1980) Etching of diamond octahedrons at high-temperatures and pressure with controlled oxygen partial-pressure. *J Mater Sci* 15:332–336
- Yamaoka S, Akaishi M, Kanda H, Osawa T (1992) Crystal growth of diamond in the system of carbon and water under very high pressure and temperature. *J Cryst Growth* 125:375–377
- Yamaoka S, Shaji Kumar MD, Akaishi M, Kanda H (2000) Reaction between carbon and water under diamond-stable high pressure and high temperature conditions. *Diamond Relat Mater* 9:1480–1486
- Yamaoka S, Shaji Kumar MD, Kanda H, Akaishi M (2002a) Formation of diamond from CaCO_3 in a reduced C–O–H fluid at HP-HT. *Diamond Relat Mater* 11:1496–1504
- Yamaoka S, Shaji Kumar MD, Kanda H, Akaishi M (2002b) Thermal decomposition of glucose and diamond formation under diamond-stable high pressure-high temperature conditions. *Diamond Relat Mater* 11:118–124
- Yamaoka S, Shaji Kumar MD, Kanda H, Akaishi M (2002c) Crystallization of diamond from CO_2 fluid at high pressure and high temperature. *J Cryst Growth* 234:5–8
- Yang JS, Lian DY, Robinson PT, Qiu T, Xiong FH, Wu WW (2019) A shallow origin for diamonds in ophiolitic chromitites. *Geology* 47:E475–E475
- Yin LW, Li MS, Gong ZG, Xu B, Song YJ, Hao ZY (2002) Analysis of nanometer inclusions in high pressure synthesized diamond single crystals. *Chem Phys Lett* 355:490–496
- Yu RZ, Ma HA, Liang ZZ, Liu WQ, Zheng YJ, Jia X (2008) HPHT synthesis of diamond with high concentration nitrogen using powder catalyst with additive $\text{Ba}(\text{N}_3)_2$. *Diamond Relat Mater* 17:180–184
- Zdrokow E, Novoselov I, Bataleva Y, Borzdov Y, Palyanov Y (2019) Experimental modeling of silicate and carbonate sulfidation under lithospheric mantle P,T-parameters. *Minerals* 9

- Zhang C, Duan Z (2010) GFluid: An Excel spreadsheet for investigating C–O–H fluid composition under high temperatures and pressures. Computers and Geosciences 36:569–572
- Zhang J, Prakapenka V, Kubo A, Kavner A, Green HW, Dobrzhinetskaya LF (2011) Diamond formation from amorphous carbon and graphite in the presence of COH fluids: An *in situ* high-pressure and -temperature laser-heated diamond anvil cell experimental study. In: Ultrahigh-pressure metamorphism: 25 years after the discovery of coesite and diamond. Dobrzhinetskaya LF, Faryad SW, Wallis S, Cuthbert S (eds). Elsevier, London, p 113–124
- Zhang JQ, Ma HA, Jiang YP, Liang ZZ, Tian Y, Jia X (2007) Effects of the additive boron on diamond crystals synthesized in the system of Fe-based alloy and carbon at HPHT. Diamond Relat Mater 16:283–287
- Zhang YF, Zang CY, Ma HG, Zhongzhu LZ, Lin Z, Li SS, Jia XP (2008) HPHT synthesis of large single crystal diamond doped with high nitrogen concentration. Diamond Relat Mater 17:209–211
- Zhang Z, Fedortchouk Y, Hanley JJ (2015) Evolution of diamond resorption in a silicic aqueous fluid at 1–3 GPa: Application to kimberlite emplacement and mantle metasomatism. Lithos 227:179–193
- Zhang ZF, Jia XP, Liu XB, Hu MH, Li Y, Yan BM, Ma HA (2012) Synthesis and characterization of a single diamond crystal with a high nitrogen concentration. Chin Phys B 21
- Zhimulev EI, Shein MA, Pokhilenko NP (2013) Diamond crystallization in the Fe–S–C system. Dokl Earth Sci 451:729–731
- Zhimulev EI, Sonin VM, Mironov AM, Chepurov AI (2016a) Effect of sulfur concentration on diamond crystallization in the Fe–C–S system at 5.3–5.5 GPa and 1300–1370 °C. Geochem Int 54:415–422
- Zhimulev EI, Sonin VM, Afanasiev VP, Chepurov AI, Pokhilenko NP (2016b) Fe–S melt as a likely solvent of diamond under mantle conditions. Dokl Earth Sci 471:1277–1279
- Zhimulev EI, Sonin VM, Fedorov, II, Tomilenco AA, Pokhilenko LN, Chepurov AI (2004) Diamond stability with respect to oxidation in experiments with minerals from mantle xenoliths at high *P*–*T* parameters. Geochem Int 42:520–525
- Zhimulev EI, Chepurov AI, Sinyakova EF, Sonin VM, Chepurov AA, Pokhilenko NP (2012) Diamond crystallization in the Fe–Co–S–C and Fe–Ni–S–C systems and the role of sulfide–metal melts in the genesis of diamond. Geochem Int 50:205–216